Passivity based stability analysis of the power control of interconnected droop-based grid-forming inverters

Control and Automation Report

Jan Peter Mortensen Christiansen
Jonas Lillelund Jørgensen

Aalborg University
4th Semester Control and Automation Master Programme
Date of Completion: May 31, 2023

Study Board of Electronics and IT
Aalborg University
http://www.aau.dk

AALBORG UNIVERSITY
STUDENT REPORT

Title:
Passivity based stability analysis of the power control of interconnected droop based grid-forming inverters

Theme:
Grid-forming inverter control and passivity

Project Period:
February 2023 - June 2023

Project Group:
CA1032

Participant(s):
Jan Peter Mortensen Christiansen
Jonas Lillelund Jørgensen

Supervisor(s):
Jan Dimon Bendtsen

Copies: 0

Page Numbers: 74

Date of Completion:
May 31, 2023

Abstract:

Grid-forming inverters are becoming increasingly relevant due to an increase of inverter based energy resources. The stability of grids with high penetration of inverter based resources is therefore of great interest. This report aims to show stability of such grids using passivity analysis. An approach that was used to show passivity of grids dominated by synchronous generators by Spanias *et al.* [1], where the bus dynamics and interconnection of buses are viewed as two separate systems in an interconnection is investigated.

A time varying phasor model is used and generators are replaced by inverters. It is shown that such a system cannot be passive. Viewing the complex power as the input to the inverter dynamics and the voltage magnitude and phase angle as the output, passivity of the inverter dynamics can be shown. However, to show stability of the interconnection of inverters using the circle criterion, the interconnection needs to be strictly passive, which it is not. However, using a feedback passivization could in theory remedy this at the cost of accurate time synchronization. Using the invariance principle it is shown that the stability of the system is guaranteed under the assumptions that the system is lossless and the phase angle differences between inverters are small. Simulation models of the Two Area Network from Kundur *et al.* [2] and the IEEE Reliability Test System [3] are used to investigate the stability of the system without the strict assumptions.

Contents

1 Introduction **1**

2 The power grid and passivity **4**
2.1 Transmission lines 5
2.2 Transformers 5
2.3 Synchronous generators 5
2.4 Inverters 6
2.5 Loads 6
2.6 Passivity 6

3 Grid forming inverters **9**
3.1 Inner voltage and current control 9
3.2 Droop-based control 10

4 Passivity analysis of a droop controlled inverter **12**
4.1 Phasor approximation 12
4.2 Bus dynamics of a droop controlled inverter 13
4.3 Network dynamics 17
4.4 Steady state simulation 18
4.5 Linearization of the bus dynamics and network 19
4.6 Passivity of a droop controlled inverter 23
4.7 Network as impedance 25

5 Passivity in polar coordinates **27**
5.1 Stability of droop control in polar coordinates 27
5.2 Passivity of example network 32
5.3 Stability of interconnected inverters using the invariance principle 35
5.4 Effects of the feed forward damper 38
5.5 N interconnected inverters 41
5.6 Stability of the reactive power regulation 43

6 The effects of loads and losses **46**
6.1 Two Area Network 46
6.2 Model parameters 49
6.3 Network behavior 52
6.4 Load step and parameter ranges 56
6.5 IEEE 24 Bus Network 60

7 Discussion **64**
7.1 Feedback passivation with coordinated control 64
7.2 Current limiting 66
7.3 Capacity for virtual inertia 66
7.4 Disturbances and noise 66

8 Conclusion **67**

Bibliography **68**

Appendix **70**

A Comparison of simulation to the linearization **71**

B Positive realness of a first order low pass filter **74**

Preface

This report is written on the 4th semester of the Control and Automation Master Programme at AAU. The authors would like to thank Vestas and especially their representatives for the collaboration.

Thanks to user *seagul* at Pixabay for making available the front page image.

Aalborg University, May 31, 2023

Jan Peter Mortensen Christiansen
<jpmc18@student.aau.dk>

Jonas Lillelund Jørgensen
<jlja18@student.aau.dk>

1 Introduction

In recent years more ambitious climate goals and innovations in renewable energy resources have changed the situation on the electric grid as more electricity is generated from renewable sources. As shown in Figure 1.1 the capacity of solar and wind electricity in the European Union has almost doubled in the last 10 years and it is expected to increase even further as member states attempt to fulfill the goals stated in the climate legislation. That goal is a 55% reduction of greenhouse gas emissions before the year 2030 as compared to the levels of the year 1990 [4].

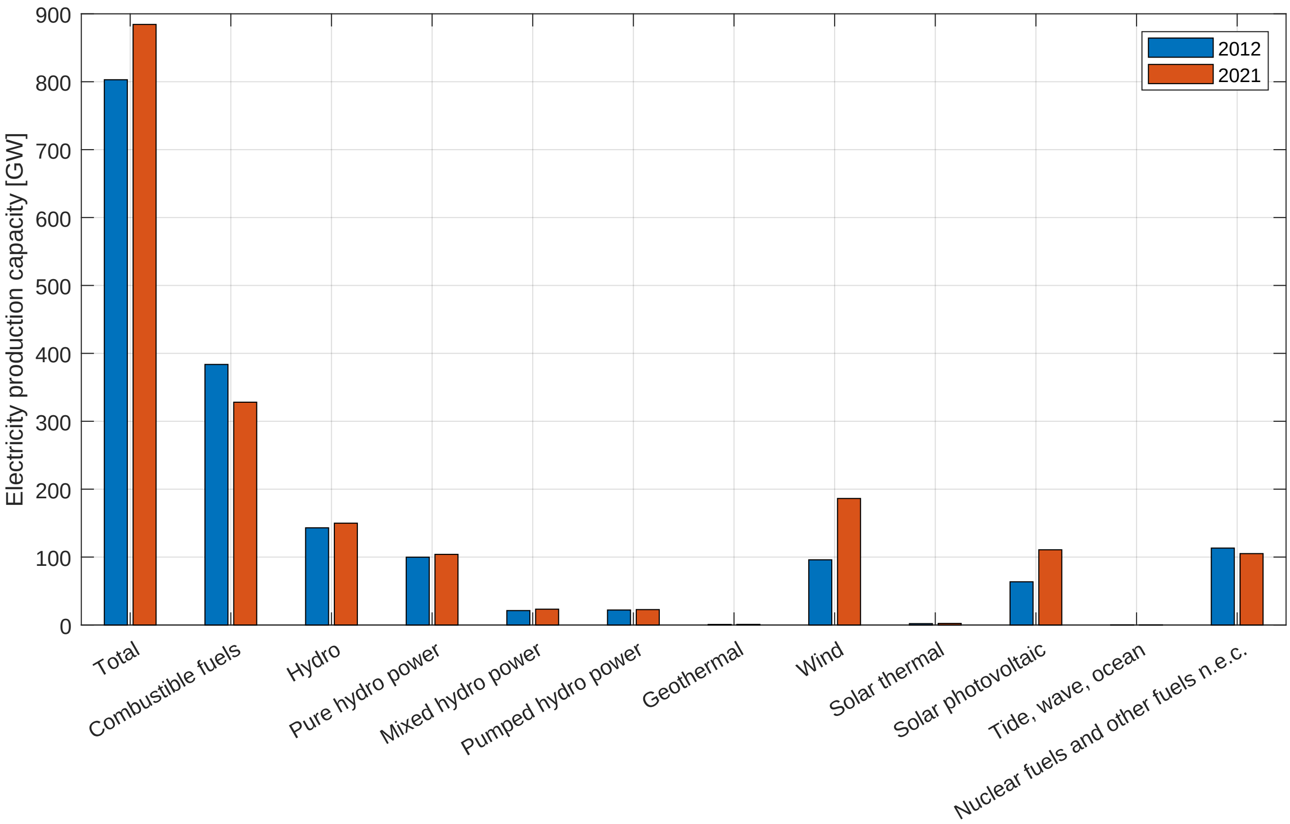

Figure 1.1: Electricity capacity by source (Standard International Energy product Classification) in the European Union [5]. n.e.c. means *not elsewhere classified*.

The shift towards renewable energy resources has brought with it a reduction in classic synchronous generator based power, since inverter-based power conversion is common in both wind turbines and photovoltaics. However, depending on how these inverters are controlled they can both be a burden and an asset to the electrical grid [6].

The power grid is divided into three layers: The transmission, distribution, and substation grid. As the name suggests, the transmission grid is where most long range transmission of power takes place. Big synchronous generators that produce the majority of the power that is needed by the consumers are connected directly to the transmission grid. At the distribution grid, the power is distributed to larger substations and also some larger consumers, like industrial and commercial customers. The substation grids are typically small grids that are fed by a single substation and consist of a few residential buildings [7]. The described structure of the electrical grid is shown in simplified form in 1.2.

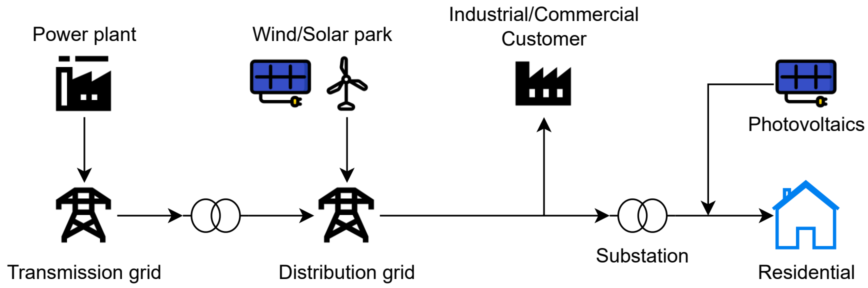

Figure 1.2: Simplified diagram of the electrical grid structure [8]. [1]

Large synchronous generators like those found in coal, gas, or nuclear power plants, generate power via an alternator that is driven by a engine shaft. This, combined with the fact that the rotation is directly coupled to the synchronous frequency which forms the grid, means that the inertia of the rotor assembly prohibits the frequency of the power grid to change too rapidly [2]. Most distributed energy resources like photovoltaics and wind turbines are connected at the distribution or even substation layer of the power grid. This has the effect of creating a lot of interconnected micro grids, which is different from the structure of the classical power grid.

Wind turbines, which still use alternators to produce electrical power, benefit from not running at synchronous speeds [9]. Other sources, like photovoltaics, do not use alternators and thus posses no inherent inertia to stabilize the local grid. These renewable energy sources instead use inverters, which produce a synchronous AC current by switching transistors and filtering the current. Because semiconductor electronics typically do not tolerate much over current, these inverters are operated like current sources that can easily be limited to protect the hardware from failing. They also need to be synchronized with the power grid in some way. Typically, this is done via a *Phase Locked Loop* (PLL) which can estimate the grids frequency and phase. These inverters are called Grid Following Inverters (GFLIs).

For the devices connected to the electric grid to function correctly, the grid must run within spec, which includes that the voltage and frequency must be correct. The guidelines for the different areas of Europe are defined by the European Commission [10]. The grid is divided in multiple synchronous areas where continental Europe is one of them. In this area the maximum permitted instantaneous frequency deviation is 800 mHz and the maximum steady-state deviation is 200 mHz. In order to facilitate the requirements of different synchronous areas, requirements for different types of generators are defined as well [11]. Generating units must be able to change their active and reactive power in response to frequency and voltage changes in order to keep the frequency stable and share load variations. While grid following inverters are capable of meeting these regulations, following the grid works best for strong grids with a lot of power coming from synchronous machines. For weaker grids, which have few to no synchronous machines to guide the grid frequency, the GFLIs amplify frequency oscillations [12] and for grids with only inverters there would not be a frequency to follow. Therefore, GFLIs are potentially problematic for the grid and the use of *Grid Forming inverters* (GFMIs) that can be made to behave more like generators is becoming an interesting alternative for distributed energy resources. GFMIs are potentially capable of functioning independently and have better stability properties in weaker grids [13].

[1]This image is derivative of [8] and is under the Creative-Commons license. The assets used in the figure are provided by Diagrams.net.

GFMIs differ from GFLIs in the way they are controlled. GFLIs are controlled as current sources that can deliver active power by injecting in-phase current to the grid, while GFMIs function as voltage sources where the phase and amplitude is controlled. More generally GFMIs are capable of independently forming a frequency and voltage on a grid. Another type of grid forming device is the synchronous generator, which is very well understood and has been in use for well over a century now. Since inverters have the potential to emulate the behaviors of these, many of the same control methods can be used for GFMIs. However, the distributed nature of many inverter based resources means that the amount of units that needs to be controlled increases. Especially important is the concept of power sharing between distributed units, which is achieved by changing the frequency of the generator based on the generated power. This can be emulated in the control of inverters, giving them the opportunity to produce virtual inertia, as long as current limitations and energy storage capabilities allow it. A major advantage of the GFMI is that it does not measure the frequency and phase of the grid via a PLL. Rather, it changes its own frequency based on power measurements according to the given droop characteristics, allowing for power based frequency synchronization. The delay associated with this mechanism is much smaller than first having to estimate the frequency of the grid via a PLL and respond to it [13]. This eliminates the need for a strong grid to follow and can even be used to start or maintain a grid without any synchronous generators.

One method of dealing with the increased complexity when investigating the stability of the grid is the use of the concept of passivity, which can be viewed as an extension to stability. Broadly speaking, a system is passive if the energy absorbed by the system is always greater than or equal to the change in energy stored in the system. Note that energy in this context is not necessarily physical energy but rather defined from input-output relationships of components [14]. The idea is that interconnections of passive systems yield passive systems which means they are at least Lyapunov stable. Furthermore, when interconnecting systems with excess of passivity they can compensate for a lack of passivity in other parts of the system [15]. Some authors have proposed the use of passivity as a tool for tuning generators. Spanias *et al.* [1] has shown that the electrical grid under a central phasor approximation is a passive system, and that if the busses are designed to be input strictly passive the entire electrical grid is asymptotically stable given a set of criteria. Passivity of the entire grid is not a necessary condition for stability and they show using simulation models that even though they only passivate a selection of busses on a grid it still improves the transient performance. It therefore seems that passivity is a promising tool for alleviating unwanted instability in an increasingly complex electrical grid. Especially their use in inverter based systems is of interest with the current increase in inverter based power and the growing concerns for the stability of the grid. This leads to the initial problem statement:

> *What is the working principle of droop-based grid forming inverter control? Can the stability of the power grid be guaranteed using passivity analysis and how do the control parameters affect the passivity of the system?*

2 The power grid and passivity

As mentioned in the introduction the passivity properties have previously been investigated by dividing the electrical grid into transmission lines and buses [1]. This chapter aims to define which parts of the grid constitute the buses, and how these can be viewed as interconnected systems for the purpose of ensuring passivity of the frequency and voltage control.

In general terms, a bus is a point of connection for which the voltage of all connected devices is the same and for which can be associated reactive and active power [2]. Buses are points in which the generators, inverters, transmission lines etc. intersect. The dynamics of a bus itself is independent of all other buses. They can therefore be viewed as a block diagonal system consisting of all buses. It is important to note that not all nodes in the network are buses. Only the nodes where the voltage is given from a dynamic system. Thus, nodes where inverters, generators, and/or motors are directly connected are considered buses in this report. The buses are connected through the network, which consists of transmission lines and transformers. The network forms an interconnection between the inputs and outputs of the buses. Each inverter on the grid is connected to a bus in the network. Given all bus voltages, the current out of the inverter into the bus node can be calculated. Figure 2.1 shows an example of a grid with three voltage source inverters and two loads, connected through transmission lines and transformers. The buses in this case are the node between the inverters and the transformers, since the voltage at these nodes is given from the dynamics of the inverters. Everything in between the inverters is considered the network.

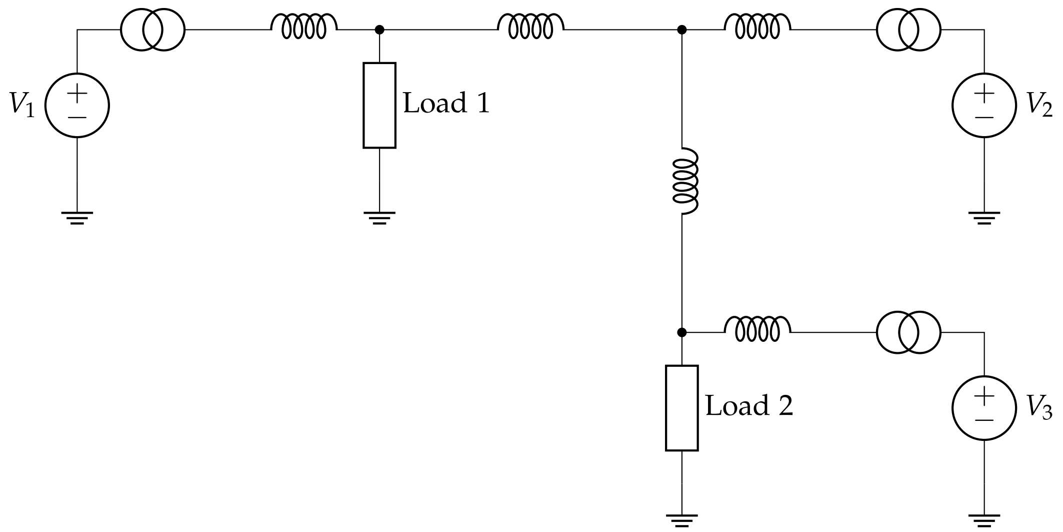

Figure 2.1: Interconnection of three voltage source inverters and two loads. The transmission lines are shown as inductances and the transformers are shown as two overlapping circles.

In some cases, the loads can also be considered buses, since they might have dynamics. An example of such a load would be an electrical motor. Note that, while the grid is a three phase system, for many purposes it can be viewed as a balanced system, meaning that the behavior of each phase is the same, but separated by an angle 120°. In these cases single phase diagrams are used. In the following, the typical components found on the grid are described.

2.1 Transmission lines

Transmission lines allow power transfer between the different buses. The behavior of voltage and current across the length of the transmission line takes the form of a wave equation [2]. For many purposes only the terminal behavior is of interest and these are usually modeled using an equivalent π-model consisting of series impedance and shunt admittance, depending on the length and properties of the transmission line. An illustration of this model is shown in Figure 2.2.

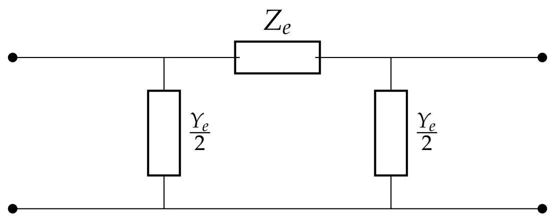

Figure 2.2: Equivalent π-model of a transmission line [2]. Z_e is the equivalent impedance and Y_e is the equivalent admittance

The equivalent π-model only works for short transmission lines, usually up to between 80 and 200 km. This model does not include any fast transients of the inductance or capacitance as it is a phasor model. However, if the transients of the transmission lines happen much faster than those of the voltage and frequency control employed in the inverters, then it is not necessary to use a more complicated model of the transmission lines.

2.2 Transformers

Transformers are used to transform the voltage up to voltage of the transmission lines and down again. When the ratio of nominal voltages is equal to the ratio of primary and secondary windings and neglecting the magnetizing reactance, the transformer can be viewed as a series impedance if the unit system is chosen correctly. A typical set of base units could be the nominal voltages and the rated power of the transformer [2]. However, most transformers have the capability to change the turn ratio for the purposes of voltage control. In this case the transformer can be modeled with a π-equivalent model [2].

2.3 Synchronous generators

Another component that can be found in a typical grid network is the synchronous generator. These generators typically generate and maintain the electrical voltage and frequency of the grid. Synchronous generators are special in the sense that the electrical frequency is coupled with the rotation of the mechanical system inside the generator. This gives the grid an inertia that restricts the rate of change of frequency. The power load is shared among the generators on the grid by utilizing droop control, which adjusts the power output of a generator based on the frequency of the grid. At the synchronous frequency, the electrical power, which is determined by the load, is balanced with the mechanical torque of the turbine driving the rotor of the generator. If the load on the grid increases, the rotation of the synchronous generators will slow down because the electrical torque becomes larger. To match the new load requirement, the generators power output is increased to match the new electrical torque, speed up the rotor to match the synchronous frequency once more. The rate at which the power is increased depends on the rated power output of the generator. Therefore its is common practice to adjust the power output such that a 2.5 % drop in frequency corresponds to half of the rated power output. That way each generator responds to the load increase proportional to their rated power output [2]. Frequency droop allows a small change in electrical frequency, in order to match the required power generation. Usually, a few larger generators then increase their rated power output to lift the frequency back up to the nominal frequency of the grid [2].

2.4 Inverters

Another form of power supply on the grid are inverters. Inverter based power sources are different because they do not necessarily have a mechanical subsystem directly coupled to the electrical frequency. Inverters have therefore been controlled as current sources that inject power, following the voltage magnitude and frequency on the grid. The advantage of current controlled inverters is that the current can easily be limited in order to protect the hardware from over current. Inverter operating in grid following mode, where the current is injected in-phase with the grid, work well in strong grids, meaning grids with a lot of inertia from synchronous generators. Another advantage for grid following inverters is that they do not need an energy storage, since they do not need to produce virtual inertia. A problem arises when the grid is weak, meaning the frequency and voltage is less stable. Changes in frequency are amplified by grid following inverters and the grid can become unstable at high penetration levels of inverter based power [12]. Therefore, another method of controlling inverters is of increasing interest: The grid forming inverter control [13]. Grid forming inverters do not measure the phase of the grid directly. They function more like generators on the sense that they inject power into the grid and synchronize to the grid frequency by themselves. Rather than a current source, grid forming inverters are viewed as voltage sources [13]. Because of this, they also need current limiting capabilities in order to protect the hardware. Grid forming inverters are able to function in islanded grids that have little to no inertia because they themselves produce virtual inertia. In order to produce virtual inertia flexibility in the power delivery, typically in the form of energy storage, is necessary. Another option is to have an over capacity in energy production that can be used provide additional power during spikes.

2.5 Loads

Finally, there are also loads on the grid consuming all the power produced by the generators and inverters. Most loads require purely active or real power. But some loads, for example some industrial motors, require some reactive power as well. This has the effect of changing the phase angle between the voltage and current in the network. Reactive power is a concept that describes power that is not consumed at the load, but flows back and forth between the consumer and the producer. Even though the energy is not consumed, the current still flows through the transmission line leading to heat losses and wear in the hardware.

2.6 Passivity

In broad terms, passivity is a property of any system with equal number of inputs and outputs, that indicates that the system is dissipative in nature. A passive system will never accumulate more signal energy than it is supplied. Mathematically, this means that there exists a storage function, that is a positive definite function of the state trajectories of the system, and the time derivative of which is always less than the signal power supplied to the system. For passivity specifically the supply rate $s(u, y)$ is defined as the inner product between the input and the output of the system:

$$s(u, y) = u^T y \tag{2.1}$$

Passivity means that the rate of change of energy in the system is always less than this supply rate. Equivalently, the energy stored in the system is always less than or equal to the energy supplied to it. The necessary definitions as defined by Khalil [14] are stated in the following. Let the dynamic system S be defined as:

$$S: \quad \begin{aligned} \dot{x} &= f(x, u) \\ y &= h(x, u) \end{aligned} \tag{2.2}$$

Khalil [14] defines passivity of a dynamic system like S as the following:

Definition 2.1 *The system S is passive if there exists a continuously differentiable positive semi-definite function $V(x)$ (called the storage function) such that*

$$u^T y \geq \dot{V} = \frac{\partial V(x)}{\partial x} f(x, u), \qquad \forall (x, u) \tag{2.3}$$

Moreover, it is

- *lossless if $u^T y = \dot{V}$.*
- *input strictly passive if $u^T y \geq \dot{V} + u^T \phi(u)$ and $u^T \phi(u) > 0$, $\forall\, u \neq 0$.*
- *output strictly passive if $u^T y \geq \dot{V} + y^T \rho(y)$ and $y^T \rho(y) > 0$, $\forall\, y \neq 0$.*
- *strictly passive if $u^T y \geq \dot{V} + \psi(x)$ for som positive definite function $\psi(s)$.*

In all cases, the inequality should hold for all (x, u).

Memoryless systems are systems with an output that is directly defined from the input to the system, meaning that they have no dynamics. Khalil [14] defines the passivity of memoryless functions as:

Definition 2.2 *The system $y = h(t, u)$ is*

- *passive if $u^T y \geq 0$*
- *lossless if $u^T y = 0$*
- *input strictly passive if $u^T y \geq u^T \phi(u) > 0$, $\forall u \neq 0$*
- *output strictly passive if $u^T y \geq y^T \rho(y) > 0$, $\forall y \neq 0$*

In all cases, the inequalities should hold for all (t, u).

Passive systems are stable in the sense of Lyapunov. This means that the systems energy will never increase without input and the states will always either stay in place ore move closer to the origin. Usually, the coordinates of the system are chosen such that the equilibrium point is at the origin $x = 0$. Strict passivity on the other hand implies that the system states will asymptotically approach the origin in a finite time. Storage functions and Lyapunov functions are very similar. Consider the storage function of a passive system as a Lyapunov function candidate. Note that storage functions fulfill all the requirements to be viewed as such. Setting the input to the system to zero yields the following:

$$\dot{V} \leq 0 \tag{2.4}$$

Therefore, the storage function for a passive system can also be viewed as a Lyapunov function for zero input. Thus the system is stable while no input is applied.

Spanias *et al.* [1] showed that the network of transmission lines is passive when viewed as a impedance matrix transforming voltages into currents. The individual buses then take the currents as input in order to produce a bus voltage corresponding to the requested injected power. This model is shown in Figure 2.3.

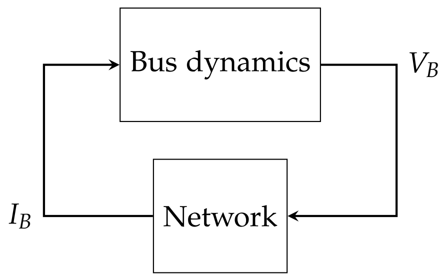

Figure 2.3: Interconnection of a bus on the power grid with the rest of the network according to Spanias *et al.* [1].

According to Spanias *et al.* [1] as long as all bus dynamics are passive, the interconnection with the network will also be passive. This follows directly from Theorem 7.1 in Khalil [14]:

Theorem 2.1 *The feedback connection of two passive systems is passive.*

Now that the basic components of the grid have been defined and the approach for using passivity to investigate the stability of the power grid is outlined, the control algorithms for the grid forming inverters are investigated.

3 Grid forming inverters

There are many different grid forming methods already described in the literature. Rathnayake *et al.* [13] places the existing methodologies into three major groups: The Droop-based control, Synchronous machine-based control, and "other" types of control. These are all outer controllers in the sense that they provide the voltage amplitude and phase reference that needs to be generated by the inverter. The inverter is thus controlled like a voltage source. In this chapter the basic concept of a droop controlled inverter is investigated. Droop-based grid forming inverter control is one of the most straight forward control methods for grid forming inverters. It shares a lot of similarities with the *Virtual Synchronous Machine* based control as well [13]. The simplest control scheme is chosen as there is no reason to add complexity if it is not necessary for the purposes of studying passivity. First, a typical inner control structure of grid forming inverters is described. Next a droop controlled inverter is described in more detail.

3.1 Inner voltage and current control

In this section it is detailed how the inverter can to some extent be viewed as a simple voltage source with regards to the slower power control and synchronization loops. The control structure of the inner control loop of a conventional grid forming inverter is shown in Figure 3.1.

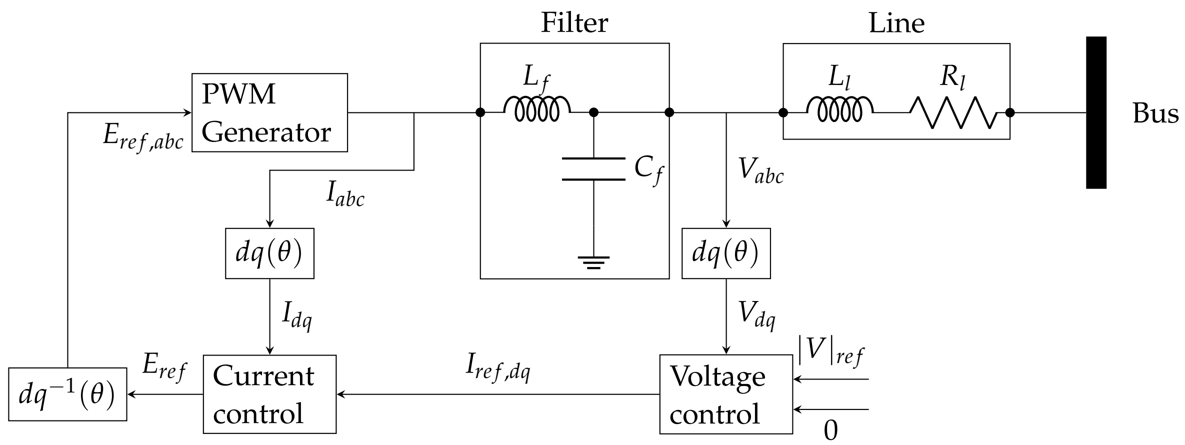

Figure 3.1: The inner control of a conventional grid forming inverter without current limiting [6] [16]. In this depiction, the output voltage is controlled to be aligned with that of the DQ-transformation hence the zero reference to the voltage control q-axis. Note θ is to be generated by the power control.

The purpose of the inner control is to control the output voltage of the inverter, i.e. the voltage after the filter, and also to limit the current to protect the inverter. The voltage control is typically achieved by the use of a cascaded control where the voltage across the LC filter is controlled by PI controllers. Due to the series inductor in the filter, the current is proportional to the average voltage of the PWM generator. Likewise the voltage of the capacitor is proportional to the current. In the dq coordinate frame this basic relation is still true, however there is some known cross coupling terms that must be removed. The bandwidth of this inner control is typically relatively large and for the purposes of power control the inverter can be viewed as controlled voltage behind a line impedance which is usually mainly inductive.

3.2 Droop-based control

Droop control is an outer control loop that provides the set point for the voltage control as well as the phase angle used for the dq-transformation. It takes inspiration from the traditional control employed when controlling multiple synchronous generators in parallel. In order for generators to respond to a load change proportionally to their individual power rating, the synchronous frequency is drooped. This means that the generator produces the rated power as longs as the synchronous frequency is at the rated frequency. Should the frequency drop due to an increase in load on the grid, the power of the generator is increased linearly and proportionally with the change in frequency [2]. This is illustrated in Figure 3.2.

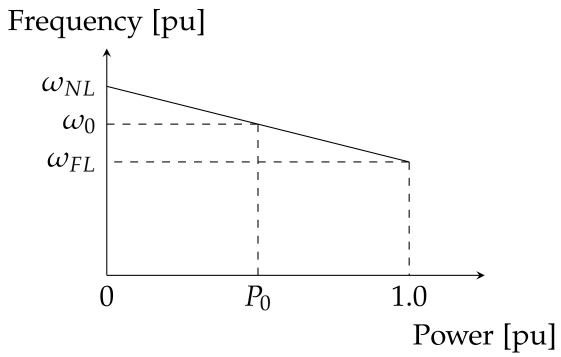

Figure 3.2: Typical frequency droop-characteristic. When the frequency is at the operating point ω_0 the power output is P_0. The maximum rated power output of the generator is reached at the *full load* frequency ω_{FL}. The generator produces no power at the *no load* frequency ω_{NL}.

The droop characteristic shown in 3.2 is basically a proportional controller of the form

$$\frac{\Delta\omega}{\Delta P} = K_P \tag{3.1}$$

where:

$\Delta\omega$ is the change in frequency
ΔP is the change in active power
K_P is a constant

Sometimes, a low-pass filter (LPF) is included in the droop-control as well to reduce unwanted harmonic oscillations [13]. The resulting transfer function becomes:

$$\frac{\Delta\omega}{\Delta P} = K_P \frac{\omega_P}{s+\omega_P} = \frac{K_P}{\tau_P s + 1}, \qquad \tau_P = \frac{1}{\omega_P} \tag{3.2}$$

where:

ω_P is the cut-off frequency of the LPF for the P-ω droop
τ_P is the time constant of the LPF for the P-ω droop

Designers might also be interested in providing a virtual inertia to the network to replace the inertia of generators. One way to do this is to model the swing equation of the rotation shaft in a synchronous generator. Typically this design is called a *Virtual Synchronous Generator* (VSG). In general there are multiple ways to implement the VSG, however a low-pass filter is mathematically equivalent to a basic VSG implementation [13]. Therefore it is not investigated separately.

The voltage amplitude can be controlled based on the reactive power:

$$\frac{\Delta V}{\Delta Q} = K_Q \frac{\omega_Q}{s+\omega_Q} = \frac{K_Q}{\tau_Q s+1}, \qquad \tau_Q = \frac{1}{\omega_Q} \tag{3.3}$$

where:

ΔV	is the change in voltage magnitude
ΔQ	is the change in reactive power
K_Q	is a constant
ω_Q	is the cut-off frequency of the LPF for the Q-V droop
τ_Q	is the time constant of the LPF for the Q-V droop

The voltage magnitude set point is provided by the Q-V droop directly. The phase angle can be obtained by integrating the frequency obtained by the P-ω droop. The control structure is summarized in Figure 3.3.

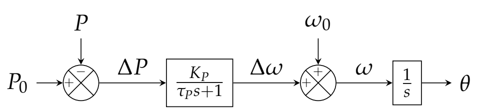

Figure 3.3: Block diagram of the $P-\omega$- and $Q-V$ droop control law [13]. The active and reactive power set points are called P_0 and Q_0 respectively and the frequency and voltage set points are called ω_0 and V_0 respectively.

In this report the focus is on the control shown in Figure 3.3. The inner voltage, current, and PWM control shown in Figure 3.1 is assumed to be fast enough that its dynamics can be ignored. Note that the line impedance in the figure is still relevant. Figure 3.4 shows the resulting inverter control.

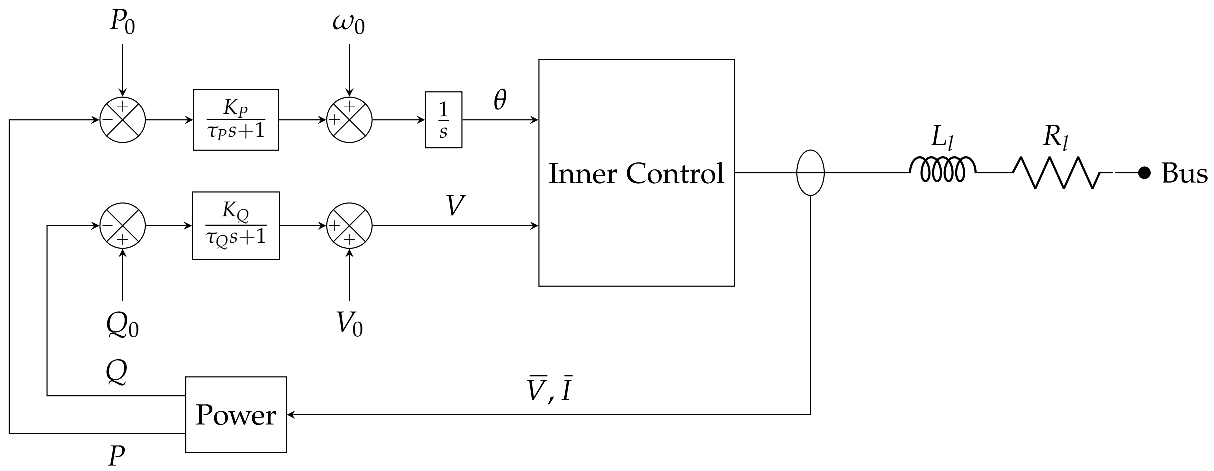

Figure 3.4: Overview of the control structure.

As indicated by the circle around the output of the inner control, the voltage and current are measured after the inner control and before the line impedance connecting the inverter to the bus. The inner control is fast and its dynamics are assumed to be insignificant for the droop control. The passivity of this droop-based voltage source inverter control is investigated in the following chapters.

4 Passivity analysis of a droop controlled inverter

This chapter explores the passivity of a droop controlled inverter connected to an infinite bus through a line impedance. This is done in order to investigate the passivity of droop controlled inverters viewed with a bus voltage as output and injected current as the input as is proposed by Spanias *et al.* [1]. First off, the dynamic phasor approximation of the dqz-coordinate transformation is described. The phasor approximation is then used to model the dynamics of the bus, including the droop control. The dynamic equations are simulated to find a steady state that can be used to linearize the dynamic model. The passivity of the linear model is then analyzed using the positive realness of the corresponding transfer matrix. Finally the results of the passivity analysis are discussed and a change in coordinates is proposed in order to alleviate some of the problems with viewing the network as an admittance.

4.1 Phasor approximation

Some assumptions are made about the system in order to simplify the analysis. First off, it is assumed that all systems are balanced and symmetrical. In a balanced three-phase system the currents and voltages each sum to zero. For the electrical system to be symmetric all component values must be the same between the three phases. Using these assumptions, the three phase signal can be reduced to a two dimensional signal via the dqz-transform. Let a three phase voltage signal be given as:

$$\begin{bmatrix} v_a \\ v_b \\ v_c \end{bmatrix} = \begin{bmatrix} V(t)\cos(\omega t + \phi(t)) \\ V(t)\cos(\omega t + \phi(t) - \frac{2\pi}{3}) \\ V(t)\cos(\omega t + \phi(t) + \frac{2\pi}{3}) \end{bmatrix} \tag{4.1}$$

where:

$V(t)$	is the time varying magnitude of the voltage signal
ω	is the frequency of the signal
$\phi(t)$	is the time varying phase of the voltage signal

Assuming that the angle used for the dqz-transform is $\theta(t) = \omega t$, where ω is a constant frequency, it is shown in Levron *et al.* [17] that the dqz-coordinates for such a balanced system are given as:

$$\begin{bmatrix} v_d \\ v_q \\ v_z \end{bmatrix} = \begin{bmatrix} V(t)\cos\phi(t) \\ V(t)\sin\phi(t) \\ 0 \end{bmatrix} \tag{4.2}$$

In reality, the frequency is not constant, but as long as it is changing slowly, the deviation can be seen as a time varying phase instead of a change in frequency. Thus, when keeping the dqz-transformation synchronized with the synchronous frequency, the three-phase signal reduces to a slowly varying phasor:

$$\overline{V} = V(t)e^{j\phi(t)} = V(t)\cos\phi(t) + jV(t)\sin\phi(t) = V_d + jV_q \tag{4.3}$$

This representation is only subtly different from dqz-coordinates. A bigger difference comes when viewing electrical components like inductors in this phasor representation. This will be described further in the next section.

4.2 Bus dynamics of a droop controlled inverter

This section establishes the relationship between the injected bus current and the bus voltage of a droop controlled inverter. As mentioned in Section 3.1 the inverter with inner control is viewed as a controlled voltage source behind a series impedance. For simplicity it is assumed that the line has no series resistance. Furthermore, this analysis utilities a constant grid frequency which should be chosen to be an equilibrium point of the inverter frequency control. The idea is to investigate if there exist some frequency at all that attracts every inverter. As a first approach the other bus is an infinite bus, and if the inverters is not attracted to the frequency of this bus it de-synchronizes. The resulting setup is shown in Figure 4.1.

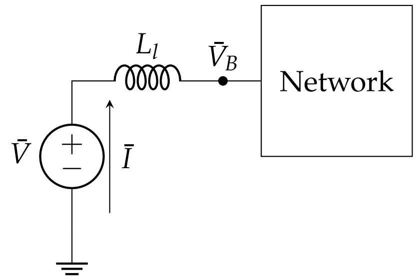

Figure 4.1: An inverter viewed as a controlled voltage source connected to an electrical network through an inductor.

When viewed as phasors, the relationship between the voltages and current in Figure 4.1 can be expressed using Ohm's law. The current through the inductor is given as the difference in voltages divided by the impedance:

$$\bar{I} = \frac{\bar{V} - \bar{V}_B}{jX_L} \tag{4.4}$$

$$\bar{V}_B = \bar{V} - jX_L\bar{I} \tag{4.5}$$

where:

$\bar{V}$	is the voltage phasor produced by the inverter
$\bar{V}_B$	is the bus voltage phasor
$\bar{I}$	is the current phasor produced by the inverter
X_L	is the reactance of the line inductance

The phasors can also be written in vector form where the components are the real and imaginary part of the phasor:

$$\bar{V} = V_a + jV_b = \begin{bmatrix} V_a \\ V_b \end{bmatrix} \tag{4.6}$$

Equation (4.5) can be written with this vector form by first expanding the phasor terms into real and imaginary parts:

$$V_{B,a} + jV_{B,b} = V_a + jV_b - jX_L(I_a + jI_b) = (V_a + X_L I_b) + j(V_b - X_L I_a) \tag{4.7}$$

From this, Equation (4.7) can be consolidated into matrix-vector notation:

$$\begin{bmatrix} V_{B,a} \\ V_{B,b} \end{bmatrix} = \begin{bmatrix} V_a \\ V_b \end{bmatrix} - \begin{bmatrix} 0 & -X_L \\ X_L & 0 \end{bmatrix} \begin{bmatrix} I_a \\ I_b \end{bmatrix} \tag{4.8}$$

Until now, the phasors have all been written in the buses reference frame which was denoted with the subscripts a and b. Instead, the phasors can be expressed in the reference frame of the inverter. Furthermore, the reference frame is chosen in a such a way, that the internal voltage $\overline{V}$ aligns with the real axis. This new reference frame is denoted with a d for the real part and a q for the imaginary part. Let the phase angle of the bus frame be denoted ϕ and the phase angle of the inverter frame be denoted θ. The difference in phase angles is denoted δ.

$$\delta = \phi - \theta \tag{4.9}$$

Figure 4.2 shows how the two coordinate systems are related to each other.

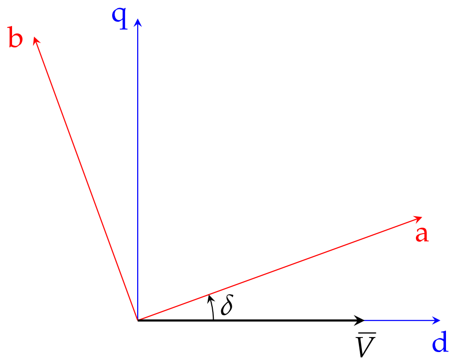

Figure 4.2: Relationship between the bus reference frame (red) and the internal inverter reference frame. The bus frame is rotated counter-clockwise with the angle δ with respect to the inverter frame. The internal voltage of the inverter $\overline{V}$ aligns with the real axis of the inverter frame.

To express the internal voltage in the buses reference frame, the voltage phasors needs to be rotated clockwise by δ. For this purpose the coordinate transformation T is defined as:

$$T(\delta): \quad (a,b) \rightarrow (d,q) \tag{4.10}$$

Since $T(\delta)$ is a simple counter-clockwise rotation, the phasor and matrix representations are easily found.

$$T(\delta) = e^{j\delta} \quad \text{or} \quad T(\delta) = \begin{bmatrix} \cos\delta & -\sin\delta \\ \sin\delta & \cos\delta \end{bmatrix} \tag{4.11}$$

Thus, the internal voltage can be written in the inverter reference frame as:

$$\overline{V}_{dq} = T(\delta)\overline{V}_{ab} \tag{4.12}$$

The relationship in Equation (4.5) can now be transformed into the inverter frame, by applying a clockwise rotation to both sides of the equation:

$$T(\delta)\overline{V}_{B,ab} = T(\delta)\overline{V}_{ab} - jX_L T(\delta)\bar{I}_{ab} \tag{4.13a}$$
$$\overline{V}_{B,dq} = \overline{V}_{dq} - jX_L\bar{I}_{dq} \tag{4.13b}$$

This can also be expressed in vector form:

$$\begin{bmatrix} V_{B,d} \\ V_{B,q} \end{bmatrix} = \begin{bmatrix} V_d \\ 0 \end{bmatrix} - \begin{bmatrix} 0 & -X_L \\ X_L & 0 \end{bmatrix} \begin{bmatrix} I_d \\ I_q \end{bmatrix} \tag{4.14}$$

Note that the voltage in the q-direction is always zero, because the coordinate frame was chosen for this specific purpose. Next, the dynamic states of the controller are investigated.

Firstly, the states, inputs, and outputs of the system need to be defined, in order to determine the dynamics of the system. The input to the system u is the currents that are measured at the bus in the reference frame of the bus. ie. the current phasor $\bar{I}_{a,b}$:

$$u = \begin{bmatrix} I_a \\ I_b \end{bmatrix} \tag{4.15}$$

The output of the system y is the bus voltage phasor in the buses reference frame $\overline{V}_{B,ab}$:

$$y = \begin{bmatrix} V_{B,a} \\ V_{B,b} \end{bmatrix} \tag{4.16}$$

The output map h is Equation (4.8), as it links the input and output. The output map also requires knowledge about the internal voltage $\overline{V}_{ab}$. This voltage is therefore identified as a state. In order to simplify the dynamic equations, the state is chosen to be the internal voltage in the inverter reference frame. Because the transformation between reference frames requires the phase angle difference, δ is also chosen as a state. Finally, it is assumed, that the bus phase angle is determined by integrating the grid frequency, which is constant. The dynamics of the phase angle difference is therefore determined exclusively by the dynamics of the inverters internal phase angle θ, which is the integral of the inverters internal frequency ω. Thus the states x of the system are identified as:

$$x = \begin{bmatrix} \omega \\ V_d \\ \delta \end{bmatrix} \tag{4.17}$$

Next, the dynamics of the individual states are determined starting with the frequency and voltage. From Equation (3.2) the differential equation for the frequency droop controller can be derived:

$$\Delta\omega = \frac{K_P}{\tau_P s + 1}\Delta P \tag{4.18a}$$

$$s\Delta\omega = \frac{1}{\tau_P}\left(K_P \Delta P - \Delta\omega\right) \tag{4.18b}$$

In time domain this becomes:

$$\Delta\dot{\omega} = \frac{1}{\tau_p}\left(K_P \Delta P - \Delta\omega\right) \tag{4.19}$$

Similarly, from Equation (3.3) the dynamics of the $Q - V$ droop are:

$$\Delta\dot{V} = \frac{1}{\tau_Q}\left(K_Q \Delta Q - \Delta V\right) \tag{4.20}$$

The droop control is based on the changes in frequency and voltage:

$$\Delta\omega = \omega - \omega_0 \tag{4.21a}$$

$$\Delta V = V - V_0 \tag{4.21b}$$

Because of this, the time derivatives of the changes in frequency and voltage are the same as the derivatives of just the frequency and voltage:

$$\Delta\dot{\omega} = \dot{\omega} \tag{4.22a}$$

$$\Delta\dot{V} = \dot{V} \tag{4.22b}$$

Also, the changes in active and reactive power are given as:

$$\Delta P = P_0 - P \tag{4.23a}$$
$$\Delta Q = Q_0 - Q \tag{4.23b}$$

The dynamics of the frequency and voltage thus become:

$$\dot{\omega} = \frac{1}{\tau_P}(K_P(P_0 - P) - (\omega - \omega_0)) \tag{4.24}$$
$$\dot{V} = \frac{1}{\tau_Q}(K_Q(Q_0 - Q) - (V - V_0)) \tag{4.25}$$

From here, an expression of the active and reactive power as a function of bus voltage and current is needed. The three phase complex power S in phasor notation is written as [18]:

$$\bar{S} = \frac{3}{2}\overline{V}_{B,dq}\bar{I}^*_{dq} \tag{4.26}$$

where:

$\bar{I}^*_{dq}$ is the complex conjugate of the current phasor in the inverter reference frame

The choice of reference frame is arbitrary, but the inverter frame comes with the benefit of having $V_q = 0$, which will simplify the expression in the end. The active power is the real part of the complex power, while the reactive power equates to the imaginary part. When the complex power is written out as real and imaginary parts it becomes:

$$\bar{S} = P + jQ = \frac{3}{2}(V_{B,d} + jV_{B,q})(I_d - jI_q) = \frac{3}{2}(V_{B,d}I_d + V_{B,q}I_q) + j\frac{3}{2}(V_{B,q}I_d - V_{B,d}I_q) \tag{4.27}$$

The active and reactive power are therefore recognized as:

$$P = \frac{3}{2}(V_{B,d}I_d + V_{B,q}I_q) \tag{4.28a}$$
$$Q = \frac{3}{2}(V_{B,q}I_d - V_{B,d}I_q) \tag{4.28b}$$

Using these expressions for the power, the dynamics of the frequency and voltage can be expanded. The frequency dynamics in Equation (4.24) become:

$$\dot{\omega} = \frac{1}{\tau_P}\left(K_P\left(P_0 - \frac{3}{2}(V_{B,d}I_d + V_{B,q}I_q)\right) - (\omega - \omega_0)\right) \tag{4.29}$$

Using Equation (4.14) the frequency dynamics can be expressed without the bus voltages. Furthermore, the currents are expressed in the bus reference frame using the coordinate transformation in Equation (4.10):

$$\begin{aligned}
\dot{\omega} &= \frac{1}{\tau_P}\left(K_P\left(P_0 - \frac{3}{2}((V_d + X_L I_q)I_d - X_L I_d I_q)\right) - (\omega - \omega_0)\right) && (4.30a)\\
&= \frac{1}{\tau_P}\left(K_P\left(P_0 - \frac{3}{2}V_d I_d\right) - (\omega - \omega_0)\right) && (4.30b)\\
&= \frac{1}{\tau_P}\left(K_P\left(P_0 - \frac{3}{2}\begin{bmatrix} V_d & 0 \end{bmatrix}\begin{bmatrix} I_d \\ I_q \end{bmatrix}\right) - (\omega - \omega_0)\right) && (4.30c)\\
&= \frac{1}{\tau_P}\left(K_P\left(P_0 - \frac{3}{2}\begin{bmatrix} V_d & 0 \end{bmatrix}\begin{bmatrix} \cos\delta & -\sin\delta \\ \sin\delta & \cos\delta \end{bmatrix}\begin{bmatrix} I_a \\ I_b \end{bmatrix}\right) - (\omega - \omega_0)\right) && (4.30d)
\end{aligned}$$

Equivalently, the voltage dynamics can be expressed as the following:

$$\dot{V} = \frac{1}{\tau_Q}\left(k_Q\left(Q_0 - \frac{3}{2}(V_{B,q}I_d - V_{B,d}I_q)\right) - (V_d - V_0)\right) \tag{4.31a}$$

$$= \frac{1}{\tau_Q}\left(k_Q\left(Q_0 - \frac{3}{2}(-X_L I_d^2 - (V_d + I_q X_L)I_q)\right) - (V_d - V_0)\right) \tag{4.31b}$$

$$= \frac{1}{\tau_Q}\left(k_Q\left(Q_0 + \frac{3}{2}\left\{\begin{bmatrix} I_d & I_q \end{bmatrix}\begin{bmatrix} X_L & 0 \\ 0 & X_L \end{bmatrix}\begin{bmatrix} I_d \\ I_q \end{bmatrix} + \begin{bmatrix} 0 & V_d \end{bmatrix}\begin{bmatrix} I_d \\ I_q \end{bmatrix}\right\}\right) - (V_d - V_0)\right) \tag{4.31c}$$

$$= \frac{1}{\tau_Q}\left(k_Q\left(Q_0 + \frac{3}{2}\left\{\begin{bmatrix} I_d & I_q \end{bmatrix}\begin{bmatrix} X_L & 0 \\ 0 & X_L \end{bmatrix}\begin{bmatrix} I_d \\ I_q \end{bmatrix} + \begin{bmatrix} 0 & V_d \end{bmatrix}\begin{bmatrix} \cos\delta & -\sin\delta \\ \sin\delta & \cos\delta \end{bmatrix}\begin{bmatrix} I_a \\ I_b \end{bmatrix}\right\}\right) - (V_d - V_0)\right) \tag{4.31d}$$

Finally, the dynamics of the phase angle difference δ are needed. From the definition of the phase angle difference in Equation (4.9), the dynamics are found as:

$$\dot{\delta} = \dot{\phi} - \dot{\omega} = \omega_r - \omega \tag{4.32}$$

where:

ω_r is the reference frequency of the bus

The other half of the system is the network, which produces a current given the voltages in the network. The network is described in the next section.

4.3 Network dynamics

As a first approach the network is a transmission line modeled as a resistor in series with an inductor, which connects to an infinite bus. The network is shown on Figure 4.3.

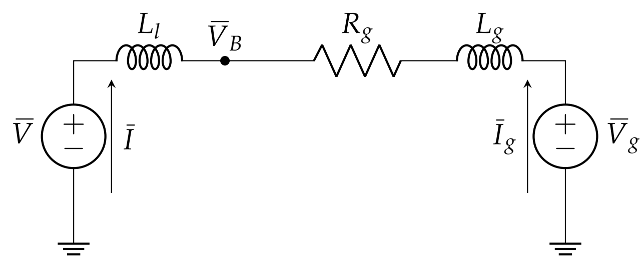

Figure 4.3: An inverter viewed as a controlled voltage source connected to an electrical network through an inductor.

The network takes the bus voltage as an input and produces the corresponding injected current, which is fed back into the inverter dynamics. Using Ohm's law, it can be seen from Figure 4.3 that:

$$\bar{I} = Y_L(\overline{V} - \overline{V}_B) \tag{4.33}$$

$$\bar{I}_g = Y_g(\overline{V}_g - \overline{V}_B) \tag{4.34}$$

where:

$\overline{V}_g$ is the infinite bus or grid voltage phasor
$Y_L = \frac{1}{jX_L}$ is the line admittance
$Y_g = \frac{1}{R_g + jX_g}$ is the grid admittance

Isolating $\overline{V}_B$ in Equation (4.34) yields:

$$\overline{V}_B = \overline{V_g} - \frac{1}{Y_g}\bar{I}_g \tag{4.35}$$

Substituting $\overline{V}_B$ in Equation (4.33) with Equation (4.35) gives an expression for the current:

$$\bar{I} = Y_L\left(\overline{V} - \left(\overline{V}_g - \frac{1}{Y_g}\bar{I}_g\right)\right) \tag{4.36}$$

Kirchhoff's current law gives $\bar{I}_g = -\bar{I}$, and thus:

$$\bar{I} = Y_L\left(\overline{V} - \left(\overline{V}_g + \frac{1}{Y_g}\bar{I}\right)\right) \tag{4.37}$$

Rearranging the expression for the current gives:

$$\bar{I} = \left(\frac{Y_L Y_g}{Y_L + Y_g}\right)(\overline{V} - \overline{V}_g) \tag{4.38}$$

With the bus dynamics and network equations in place the system can be set up as an ODE and simulated using Matlab.

4.4 Steady state simulation

In order to find a steady state solution the system is simulated using ode15s with the parameters shown in Table 4.1 and Table 4.2. The relative tolerance is set to 10^{-5}. Note that the frequency of the infinite bus is chosen as ω_0 and the voltage angle of the infinite bus also determines the network reference in this case.

Table 4.1: Droop control parameters.

Parameter	K_P	τ_P	K_Q	τ_Q	P_0	Q_0	V_0	ω_0
Value	15	0.05	10	0.1	0.5 W	0.1 VAR	1 V	$2\pi 50$

Table 4.2: Network parameters.

Parameter	L_l	L_g	R_g	V_g
Value	100 µH	1000 µH	0.05 Ω	1 V

The simulation is run with these parameters for 5 seconds to ensure the system reaches a stable steady state. The initial conditions for the states are:

$$x_0 = \begin{bmatrix} \omega_0 \\ V_{d,0} \\ \delta_0 \end{bmatrix} = \begin{bmatrix} 2\pi 50\ \frac{\text{rad}}{\text{s}} \\ 1\,\text{V} \\ 0\,\text{rad} \end{bmatrix} \tag{4.39}$$

Figure 4.4 shows the state trajectories of the bus dynamics.

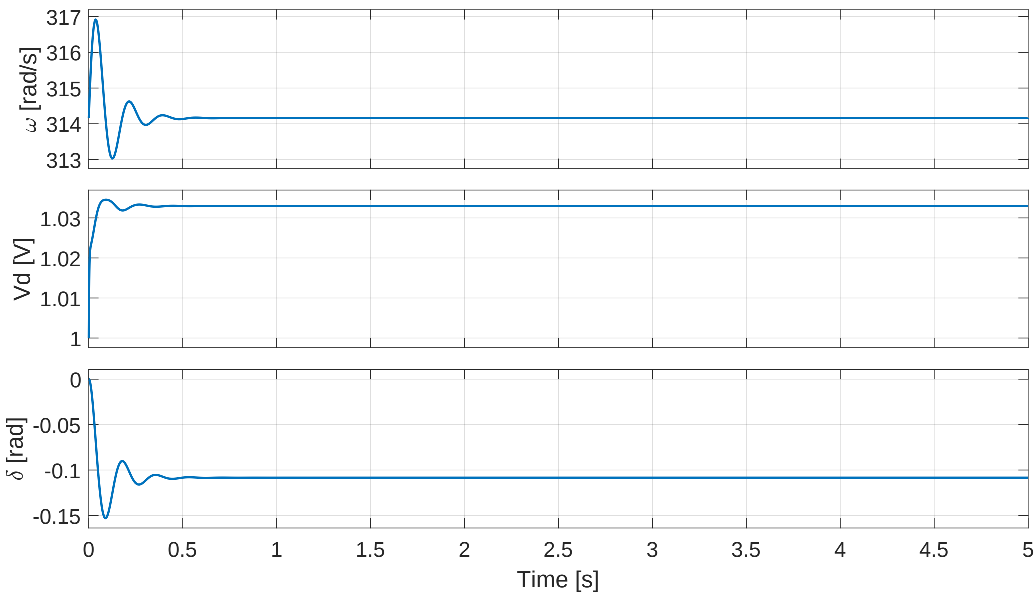

Figure 4.4: State trajectories of a droop controlled inverter connected to an infinite bus through an inductive transmission line.

The system does appear to be in steady state at the end of the 5 seconds. The states $\hat{x}$ and the inputs $\hat{u}$ at the steady state are shown in Table 4.3.

Table 4.3: System states and inputs in steady state.

Parameter	$\hat{\omega}$	$\hat{V}_d$	$\hat{\delta}$	$\hat{I}_a$	$\hat{I}_b$
Value	$314.1593\ \frac{\text{rad}}{\text{s}}$	1.0330 V	-0.1084 rad	0.3279 A	-0.0304 A

Now that a steady state is found, the inverter dynamics can be linearized in order to ease the passivity analysis.

4.5 Linearization of the bus dynamics and network

The dynamics derived in this chapter are non-linear. This makes analysis of the system difficult. Therefore, the system is linearized to make it easier to investigate passivity properties. For the purpose of linearization, a first order Taylor approximation is used. A first order Taylor approximation of the function $f(x)$ around the operating point a is given as:

$$f(x) \approx f(a) + f'(a)(x-a) \tag{4.40}$$

In this case the operating point is $(\hat{x}, \hat{u})$ and the function f denotes the dynamics of the system:

$$\dot{x} = f(x,u) = f(\omega, V_d, \delta, I_a, I_b) \tag{4.41}$$

Because the dynamics are a vector function, the derivative in Equation (4.40) is replaced by the Jacobian $J_f(\hat{x}, \hat{u})$ with respect to both the states and the inputs:

$$f(x,u) \approx f(\hat{x},\hat{u}) + J_f(\hat{x},\hat{u}) \left(\begin{bmatrix} x \\ u \end{bmatrix} - \begin{bmatrix} \hat{x} \\ \hat{u} \end{bmatrix} \right) = f(\hat{x},\hat{u}) + J_f(\hat{x},\hat{u}) \begin{bmatrix} \tilde{x} \\ \tilde{u} \end{bmatrix} \tag{4.42}$$

The small signal change in states and inputs are:

$$\widetilde{x} = x - \hat{x} \tag{4.43a}$$

$$\widetilde{u} = u - \hat{u} \tag{4.43b}$$

From the definition of the states, the Jacobian can be identified as:

$$J_f = \begin{bmatrix} J_\omega \\ J_{V_d} \\ J_\delta \end{bmatrix} \tag{4.44}$$

where:

J_ω is the Jacobian of the frequency dynamics
J_{V_d} is the Jacobian of the voltage dynamics
J_δ is the Jacobian of the phase angle difference dynamics

The frequency dynamics of the inverter are a function of the frequency ω itself, the inverter voltage V_d, the bus currents I_a and I_b, and the phase angle difference δ:

$$\begin{aligned}\dot{\omega} &= f_\omega(\omega, V_d, \delta, I_a, I_b) \\ &= \frac{K_P}{\tau_P}\left(P_0 - \frac{3}{2}\begin{bmatrix} V_d & 0 \end{bmatrix}\begin{bmatrix} \cos\delta & -\sin\delta \\ \sin\delta & \cos\delta \end{bmatrix}\begin{bmatrix} I_a \\ I_b \end{bmatrix}\right) - \frac{\omega - \omega_0}{\tau_P}\end{aligned} \tag{4.45}$$

The Jacobian of the frequency dynamics is therefore:

$$J_\omega = \begin{bmatrix} \frac{\partial f_\omega}{\partial \omega} & \frac{\partial f_\omega}{\partial V_d} & \frac{\partial f_\omega}{\partial \delta} & \frac{\partial f_\omega}{\partial I_a} & \frac{\partial f_\omega}{\partial I_b} \end{bmatrix} \tag{4.46a}$$

$$\frac{\partial f_\omega}{\partial \omega} = -\frac{1}{\tau_P} \tag{4.46b}$$

$$\frac{\partial f_\omega}{\partial V_d} = -\frac{3K_P}{2\tau_P}(I_a \cos\delta - I_b \sin\delta) \tag{4.46c}$$

$$\frac{\partial f_\omega}{\partial \delta} = -\frac{3K_P}{2\tau_P} V_d(-I_a \sin\delta - I_b \cos\delta) \tag{4.46d}$$

$$\frac{\partial f_\omega}{\partial I_a} = -\frac{3K_P}{2\tau_P} V_d \cos\delta \tag{4.46e}$$

$$\frac{\partial f_\omega}{\partial I_b} = +\frac{3K_P}{2\tau_P} V_d \sin\delta \tag{4.46f}$$

Similarly, the voltage dynamics are also a function of itself, the current and the phase angle difference, but not the frequency:

$$\begin{aligned}\dot{V}_d &= f_V(\omega, V_d, \delta, I_a, I_b) \\ &= \frac{K_Q}{\tau_Q}\left(Q_0 + \frac{3}{2}\left\{\begin{bmatrix} I_a & I_b \end{bmatrix}\begin{bmatrix} X_L & 0 \\ 0 & X_L \end{bmatrix}\begin{bmatrix} I_a \\ I_b \end{bmatrix} + \begin{bmatrix} 0 & V_d \end{bmatrix}\begin{bmatrix} \cos(\delta) & -\sin(\delta) \\ \sin(\delta) & \cos(\delta) \end{bmatrix}\begin{bmatrix} I_a \\ I_b \end{bmatrix}\right\}\right) - \frac{(V_d - V_0)}{\tau_Q}\end{aligned} \tag{4.47}$$

The Jacobian of the voltage dynamics is thus:

$$J_{V_d} = \begin{bmatrix} \frac{\partial f_{V_d}}{\partial \omega} & \frac{\partial f_{V_d}}{\partial V_d} & \frac{\partial f_{V_d}}{\partial \delta} & \frac{\partial f_{V_d}}{\partial I_a} & \frac{\partial f_{V_d}}{\partial I_b} \end{bmatrix} \tag{4.48a}$$

$$\frac{\partial f_{V_d}}{\partial \omega} = 0 \tag{4.48b}$$

$$\frac{\partial f_{V_d}}{\partial V_d} = \frac{3}{2}\frac{K_Q}{\tau_Q}(\sin(\delta)I_a + \cos(\delta)I_b) - \frac{1}{\tau_Q} \tag{4.48c}$$

$$\frac{\partial f_{V_d}}{\partial \delta} = \frac{3}{2}\frac{K_Q}{\tau_Q}(V_d\cos(\delta)I_a - V_d\sin(\delta)I_b) \tag{4.48d}$$

$$\frac{\partial f_{V_d}}{\partial I_a} = \frac{3}{2}\frac{K_Q}{\tau_Q}(2I_aX_L + V_d\sin(\delta)) \tag{4.48e}$$

$$\frac{\partial f_{V_d}}{\partial I_b} = \frac{3}{2}\frac{K_Q}{\tau_Q}(2I_bX_L + V_d\cos(\delta)) \tag{4.48f}$$

Furthermore, the dynamics of the phase angle difference are:

$$\dot{\delta} = f_\delta(\omega, V_d, \delta, I_a, I_b) = \dot{\phi} - \dot{\omega} = \omega_r - \omega \tag{4.49}$$

The Jacobian of f_δ becomes:

$$J_\delta = \begin{bmatrix} \frac{\partial f_\delta}{\partial \omega} & \frac{\partial f_\delta}{\partial V_d} & \frac{\partial f_\delta}{\partial \delta} & \frac{\partial f_\delta}{\partial I_a} & \frac{\partial f_\delta}{\partial I_b} \end{bmatrix} = \begin{bmatrix} -1 & 0 & 0 & 0 & 0 \end{bmatrix} \tag{4.50}$$

Additionally, the output map of the system needs to be linearized as well. The first order Taylor approximation of h is:

$$y = h(x,u) = h(\hat{x},\hat{u}) + J_h(\hat{x},\hat{u})\left(\begin{bmatrix} x \\ u \end{bmatrix} - \begin{bmatrix} \hat{x} \\ \hat{u} \end{bmatrix}\right) \tag{4.51}$$

The output map h in this case refers to Equation (4.8), but with the internal voltage transformed into the inverter frame, because the state is V_d:

$$\begin{bmatrix} V_{B,a} \\ V_{B,b} \end{bmatrix} = h(\omega, V_d, \delta, I_a, I_b) = \begin{bmatrix} \cos\delta & \sin\delta \\ -\sin\delta & \cos\delta \end{bmatrix}\begin{bmatrix} V_d \\ 0 \end{bmatrix} - \begin{bmatrix} 0 & -X_L \\ X_L & 0 \end{bmatrix}\begin{bmatrix} I_a \\ I_b \end{bmatrix} \tag{4.52}$$

The Jacobian of the output map is therefore:

$$J_h = \begin{bmatrix} \frac{\partial h}{\partial \omega} & \frac{\partial h}{\partial V_d} & \frac{\partial h}{\partial \delta} & \frac{\partial h}{\partial I_a} & \frac{\partial h}{\partial I_b} \end{bmatrix} = \begin{bmatrix} 0 & \cos(\delta) & -\sin(\delta)V_d & 0 & X_L \\ 0 & -\sin(\delta) & -\cos(\delta)V_d & -X_L & 0 \end{bmatrix} \tag{4.53}$$

With all the Jacobians obtained it is possible to write a linearization of the state space:

$$\frac{d}{dt}\begin{bmatrix} \omega \\ V_d \\ \delta \end{bmatrix} \approx f(\hat{x},\hat{u}) + \left.\begin{bmatrix} \frac{\partial f_\omega}{\partial \omega} & \frac{\partial f_\omega}{\partial V_d} & \frac{\partial f_\omega}{\partial \delta} \\ \frac{\partial f_{V_d}}{\partial \omega} & \frac{\partial f_{V_d}}{\partial V_d} & \frac{\partial f_{V_d}}{\partial \delta} \\ \frac{\partial f_\delta}{\partial \omega} & \frac{\partial f_\delta}{\partial V_d} & \frac{\partial f_\delta}{\partial \delta} \end{bmatrix}\right|_{\substack{x=\hat{x} \\ u=\hat{u}}} \begin{bmatrix} \widetilde{\omega} \\ \widetilde{V}_d \\ \widetilde{\delta} \end{bmatrix} + \left.\begin{bmatrix} \frac{\partial f_\omega}{\partial I_a} & \frac{\partial f_\omega}{\partial I_b} \\ \frac{\partial f_{V_d}}{\partial I_a} & \frac{\partial f_{V_d}}{\partial I_b} \\ \frac{\partial f_\delta}{\partial I_a} & \frac{\partial f_\delta}{\partial I_b} \end{bmatrix}\right|_{\substack{x=\hat{x} \\ u=\hat{u}}} \begin{bmatrix} \widetilde{I}_a \\ \widetilde{I}_b \end{bmatrix} \tag{4.54a}$$

$$\begin{bmatrix} V_{B,a} \\ V_{B,b} \end{bmatrix} \approx h(\hat{x},\hat{u}) + \left.\begin{bmatrix} \frac{\partial h}{\partial \omega} & \frac{\partial h}{\partial V_d} & \frac{\partial h}{\partial \delta} \end{bmatrix}\right|_{\substack{x=\hat{x} \\ u=\hat{u}}} \begin{bmatrix} \widetilde{\omega} \\ \widetilde{V}_d \\ \widetilde{\delta} \end{bmatrix} + \left.\begin{bmatrix} \frac{\partial h}{\partial I_a} & \frac{\partial h}{\partial I_b} \end{bmatrix}\right|_{\substack{x=\hat{x} \\ u=\hat{u}}} \begin{bmatrix} \widetilde{I}_a \\ \widetilde{I}_b \end{bmatrix} \tag{4.54b}$$

The constant terms in the linearization $f(\hat{x}, \hat{u})$ and $h(\hat{x}, \hat{u})$ are moved to the other side of the equality sign. The left side of the equations thus becomes the small signal state derivatives $\dot{\tilde{x}}$ and output $\tilde{y}$.

$$\dot{\tilde{x}} = \dot{x} - f(\hat{x}, \hat{u}) \tag{4.55a}$$

$$\tilde{y} = y - h(\hat{x}, \hat{u}) \tag{4.55b}$$

Using the steady state from Table 4.3, the linearization defines the linear system P:

$$P: \quad \begin{aligned} \dot{\tilde{x}} &= A\tilde{x} + B\tilde{u} \\ \tilde{y} &= C\tilde{x} + D\tilde{u} \end{aligned} \tag{4.56}$$

where:

$$\begin{aligned} A &= \begin{bmatrix} -20 & -145.2126 & -30.5441 \\ 0 & -19.8564 & 50 \\ -1 & 0 & 0 \end{bmatrix}, & B &= \begin{bmatrix} -462.1052 & -50.3091 \\ -13.6792 & 153.7486 \\ 0 & 0 \end{bmatrix} \\ C &= \begin{bmatrix} 0 & 0.9941 & 0.1118 \\ 0 & 0.1082 & -1.0269 \end{bmatrix}, & D &= \begin{bmatrix} 0 & 0.0314 \\ -0.0314 & 0 \end{bmatrix} \end{aligned} \tag{4.57}$$

The system P is in a feedback with the network K. This is illustrated in Figure 4.5.

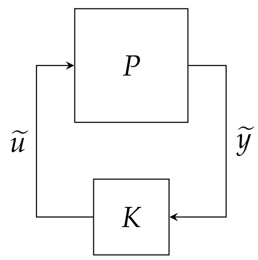

Figure 4.5: Illustration of the coupling of the network with the dynamics of the inverter.

The figure shows the feedback K that replaces the network. The system K relates the bus voltage $\overline{V}_B$ and the current $\bar{I}$. This relationship is known from Equation (4.34) and Kirchhoff's current law:

$$\bar{I} = -Y_g(\overline{V}_g - \overline{V}_B) \tag{4.58}$$

Equation (4.58) needs to be linearized in order to obtain the relationship between the small signal versions of the bus voltage and current. It is assumed that the bus is infinite and thus the voltage $\overline{V}_g$ is constant. A first order Taylor approximation of the current yields:

$$\bar{I} \approx \hat{\bar{I}} + J_{\bar{I}}\tilde{\overline{V}}_B \tag{4.59}$$

The small signal current is defined as:

$$\tilde{\bar{I}} = \bar{I} - \hat{\bar{I}} \tag{4.60}$$

Combining this with the Taylor approximation gives the network system K:

$$K: \qquad \tilde{\bar{I}} = Y_g\tilde{\overline{V}}_B \tag{4.61}$$

It is verified through a simulation, that the linearization is a good approximation of the non-linear system for small changes in the power set points. This is done in Appendix A. Next, the passivity of the droop controlled inverter is investigated

4.6 Passivity of a droop controlled inverter

According to Khalil [14] the passivity of an LTI system can be inferred from its positive realness. Let S be an LTI system of the form:

$$S: \quad \begin{aligned} \dot{x} &= Ax + Bu \\ y &= Cx + Du \end{aligned} \tag{4.62}$$

The transfer matrix G of the system is given as:

$$G(s) = C(sI - A)^{-1}B + D \tag{4.63}$$

According to Lemma 5.4 in Khalil [14] an LTI system is passive if $G(s)$ is positive real, and strictly passive if $G(s)$ is strictly positive real. Khalil [14] defines positive realness of a transfer matrix as follows:

Definition 4.1 *An $m \times m$ proper rational transfer function matrix $G(s)$ is positive real if*

- *poles of all elements of $G(s)$ are in the LHP,*
- *for all real ω for which $j\omega$ is not a pole of any element of $G(s)$, the matrix $G(j\omega) + G^T(-j\omega)$ is positive semidefinite, and*
- *any pure imaginary pole $j\omega$ of any element of $G(s)$ is a simple pole and the residue matrix $\lim_{s\to j\omega}(s - j\omega)G(s)$ is positive semidefinite Hermitian.*

It is strictly positive real if $G(s - \varepsilon)$ is positive real for some $\varepsilon > 0$.

For the passivity analysis the linear system P in Equation (4.56) is used. The state space matrices are given in Equation (4.57). The eigenvalues of the A-matrix are found to be:

$$\text{eig}(A) = \begin{bmatrix} 9.4498 \\ -24.6531 + 14.9914j \\ -24.6531 - 14.9914j \end{bmatrix} \tag{4.64}$$

Since A is not Hurwitz, the inverter system is not open loop stable. Since the system is not stable in the first place, it cannot be passive either. Open loop stability of the bus dynamics is necessary for passivity. It is infeasible to write an analytical expression for the eigenvalues of the open loop system and see exactly why the system is not open loop stable. Instead it is opted to plot the closed and open loop relationship between power, voltage, and angle to see what is happening.

The active and reactive power at the bus are the controlled variables, the phase and amplitude of the inverter voltage are the actuation variables. For the simplicity of this analysis it is assumed that there exists a mostly inductive connection between the internal inverter voltage and the grid voltage which is represented as an infinite bus. Thus the active and reactive power supplied by the inverter can be represented by the following equations [2]:

$$P = \frac{3|\overline{V}||\overline{V}_g|}{2X_L}\sin(\theta - \phi) \tag{4.65}$$

$$Q = \frac{3|\overline{V}|^2}{2X_L} - \frac{3|\overline{V}||\overline{V}_g|}{2X_L}\cos(\theta - \phi) \tag{4.66}$$

Droop control assumes that the cross coupling between the active power and voltage as well as the reactive power and the angle is small. It is also assumed that the angle $\theta - \phi$ is small in the operating point. With these assumptions the behavior of the control can be plotted. The active power as a function of the phase angle θ is shown in Figure 4.6a and the reactive power as a function of the voltage magnitude $|\overline{V}|$ is shown in Figure 4.6b.

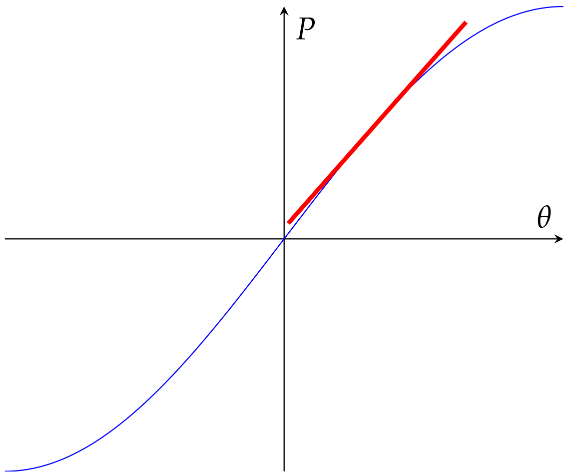

(a) Active power as a function of the phase angle (blue line). The red line shows the slope near a operating reasonable operating point.

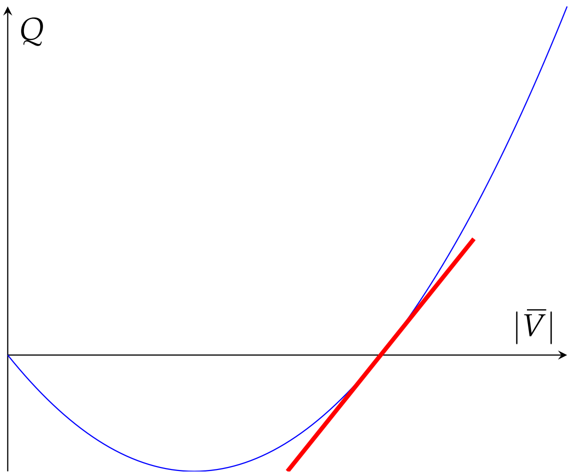

(b) Reactive power as a function of the voltage magnitude (blue line). The red line shows the slope near a reasonable operating point

Figure 4.6

It is seen that the relationship between active power and angle is sinusoidal, and assuming that the angle is small in the operating point this is a positive linear relationship. For the reactive power, assuming the operating points is around zero reactive power and a non zero voltage, while the angle difference is small, the relationship between reactive power and voltage is also positive. The open loop condition is that the input is held constant. This means that the injected current is constant, which leads to the following injected power:

$$S = \frac{3}{2}\overline{V}\overline{I}^* = \frac{3|\overline{V}||\overline{I}|}{2}\left[\cos(\theta - \theta_I) + j\sin(\theta - \theta_I)\right] \tag{4.67}$$

where:

θ_I is the phase angle of the current in the inverter reference frame

The difference in voltage and current phase angle is assumed to be small (i.e. the power factor is close to 1), since the power set point is mostly active power. Hence the cosine term in Equation (4.67) dominates. Using this expression for the complex power, and assuming that the current is constant, the following plots in Figure 4.7 can be inferred.

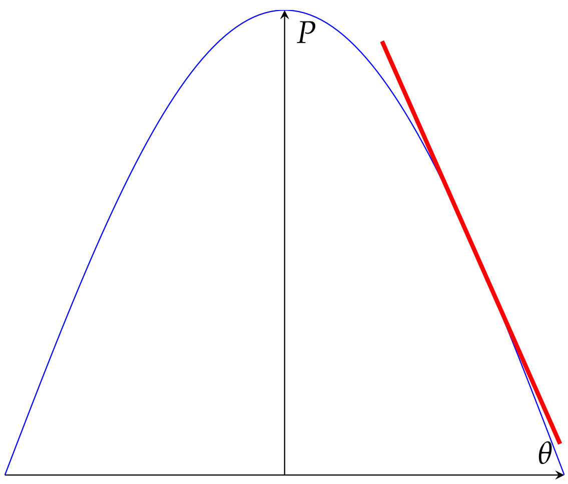

(a) Active power as a function of the phase angle with constant current (blue line). The red line shows the slope near a operating point where the current lags the voltage.

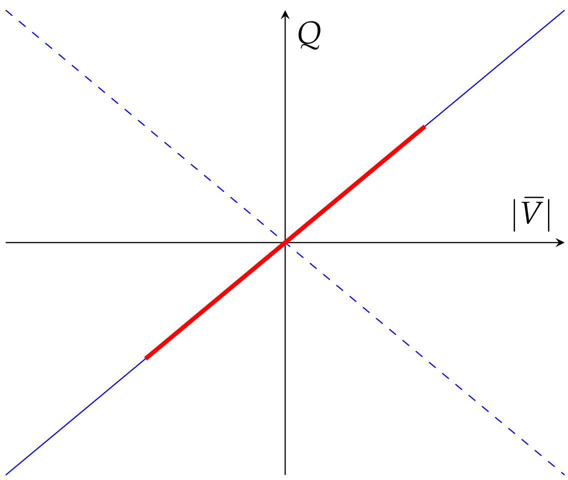

(b) Reactive power as a function of the voltage magnitude with constant current lagging behind the voltage (blue line) and with constant current leading the voltage (blue dashed). The red line shows the slope near a reasonable operating point for one of the cases.

Figure 4.7

Notice in Equation (4.67) how the sign of Q is entirely dependent on whether the current leads or lags the voltage, the slope is positive when the current lags and negative when it leads the voltage. Furthermore, notice how the slope of the active power as a function of voltage angle is negative if the current lags the voltage, and positive is the current leads, but is simply positive in the closed loop case. This means that the effect of this simple network actually changes the algebraic relationship between the inverter voltage and the power in such a way that the sign of the dependency of either the $V - Q$ or $P - \theta$ relation is switched. This is an issue, because the bus dynamics are not passive if the equilibrium defined by the closed loop system is not a stable equilibrium of the open loop bus dynamics in some neighborhood [1]. However, it seems that this condition cannot be satisfied with conventional $Q - V$, $P - \omega$ droop, when power transfer happens over an inductive line because of the way the algebraic relationship between voltage and power changes under the constant current condition.

4.7 Network as impedance

The issue of open loop stability can be fixed by changing the coordinates of the system such that the network is viewed as an impedance and the current becomes the output of the bus devices, and the bus voltage the input. However, for the interconnection to be passive both the inverters and the network must be passive. According to Dey *et al.* [19], the network, viewed as impedance, can be open loop stable and passive. Even though the bus devices are open loop stable in these new coordinates, it is still not possible to achieve passivity while controlling the power injected to the grid. Recall that from Definition 5.4 that a requirement for positive realness is that the quadratic form of the transfer matrix is positive definite in all frequencies ω for which $j\omega$ is not a pole of $G(s)$. It is investigated whether it is possible to achieve this at steady state when controlling the power. Since the network is an impedance, the output is the voltage and the controller must output a current. Thus any controller that have functional power control must output a current in accordance with the complex power equation at least within the control bandwidth. From the definition of the complex power, the injected current can be calculated from the voltage and the desired complex power:

$$\bar{I} = I_a + jI_b = \frac{2}{3}\left(\frac{\bar{S}}{\bar{V}}\right)^* = \frac{2}{3}\left(\frac{P + jQ}{V_a + jV_b}\right) = \frac{2}{3}\left(\frac{PV_a + QV_b}{V_a^2 + V_b^2} + j\frac{PV_b - QV_a}{V_a^2 + V_b^2}\right) \tag{4.68}$$

Assume that active and reactive powers (P and Q) reach some steady state due to these being the controlled variables. Linearizing Equation (4.68) in this steady state yields the necessary small signal relation from voltage to current needed to achieve the desired complex power. Note that this is not the entire bus dynamic. Rather, the control algorithm of the inverter will try to approach the relation in Equation (4.68) in a steady state. In order to check whether any controller that achieves the power set points in the steady state can be passive, the properties of the linearization of the map in Equation (4.68) is investigated:

$$\tilde{\bar{I}} = J_I(\hat{\bar{V}}, \hat{\bar{S}})\tilde{\bar{V}} \tag{4.69}$$

where:

J_I is the Jacobian of the current with respect to the voltage.

The Jacobian with regards to V_a and V_b is the following:

$$J_I = \begin{bmatrix} \frac{\partial I_a}{\partial V_a} & \frac{\partial I_a}{\partial V_b} \\ \frac{\partial I_b}{\partial V_a} & \frac{\partial I_b}{\partial V_b} \end{bmatrix} \tag{4.70}$$

The derivatives are found using the Symbolic Math Toolbox in Matlab to be:

$$J_{I,11} = \frac{\partial I_a}{\partial V_a} = -\frac{\partial I_b}{\partial V_b} = -\frac{2}{3}\frac{PV_a^2 + 2QV_aV_b - PV_b^2}{(V_a^2 + V_b^2)^2} \tag{4.71a}$$

$$J_{I,12} = \frac{\partial I_a}{\partial V_b} = \frac{\partial I_b}{\partial V_a} = -\frac{2}{3}\frac{-QV_a^2 + 2PV_aV_b + QV_b^2}{(V_a^2 + V_b^2)^2} \tag{4.71b}$$

The Jacobian thus becomes:

$$J_I = \begin{bmatrix} J_{I,11} & J_{I,12} \\ J_{I,12} & -J_{I,11} \end{bmatrix} \tag{4.72}$$

The unfortunate structure of this matrix means that it always has positive and negative eigenvalues as they can be found to be the following by solving the eigenvalue problem:

$$\lambda = \pm\sqrt{J_{I,11}^2 + J_{I,12}^2} \tag{4.73}$$

This means that the transfer matrix in a steady state, that is $j\omega = 0$, is not positive semi-definite, and therefore also not positive real. Hence the behavior of a bus device with functional P and Q control cannot be passive in these coordinates. Even though droop controllers does not exactly follow the set points, it is assumed that the voltage current relation approaches that of Equation (4.68).

Thus it can be concluded that the bus devices are not likely to be passive when viewing the network as either admittance or impedance. However, these are not the only possible options for coordinates to analyze the passivity in. One promising lead is to view the output of the bus devices as voltage magnitude and phase and the input as the active and reactive power. This possibility will be investigated in the next chapter.

5 Passivity in polar coordinates

The previous chapter described the network as an admittance and using the current and voltage at the bus connection as input and output respectively. It was found that the bus with droop control becomes open loop unstable at the equilibrium because the power droop fundamentally relies on the current reacting to changes in voltage. However, it might be possible to segment the system in a slightly different way such that both the bus and the network become passive. It was also found that viewing the network as an impedance did not fix the issue. Another possible alternative is to use a polar representation of the voltage phasor instead of the d and q components. The network has the voltage magnitude and phase as inputs and the active and reactive power as outputs in this case. This is promising, because the droop controlled bus becomes much simpler in this representation as the non-linear power calculation is moved into the network. First off, a feed forward damper is introduced in order to make the droop control passive. The passivity of the droop control is analyzed together with the closed loop stability of the grid using the circle criterion. Next, a simple example of two inverters connected through a purely inductive line is examined to show if such a system can be passive. The stability of interconnected inverters is shown under the assumptions that the network is lossless and the phase angle differences are small. The effects of the feed forward damper is further investigated. Lastly, the passivity of a more generalized interconnection of N inverters is shown to be passive under the mentioned assumptions.

5.1 Stability of droop control in polar coordinates

In polar coordinates achieving passivity of the grid requires more consideration [19], but before this, it is investigated whether power control can be passive with the power as input and voltage as output. In these coordinates, it is beneficial for the simplicity of the analysis to assume that the inverters point of coupling with the network is at the controlled voltage, and the line impedance of the inverter can simply be viewed as part of the network. In these coordinates, neither the power nor the voltage magnitude depends on the reference angle. Furthermore in the open loop the $Q - V$ and $P - \omega$ droops are entirely independent.

Under steady state conditions it can be assumed that the network frequency and the internal frequency of the power controller are the same. Since $Q - V$ droop is just a first order low-pass filter, it is strictly passive (See Appendix B). However, the $P - \omega$ droop is not passive because the relative degree of the system is 2 [14]. This is because of the series connection of an integrator and low-pass filter. By adding a feed forward term from the output of the low pass filter, directly to the output angle, bypassing the integrator, it is possible to passivate the control. This is illustrated in Figure 5.1. Note that this is equivalent to the selfsync algorithm presented in [20].

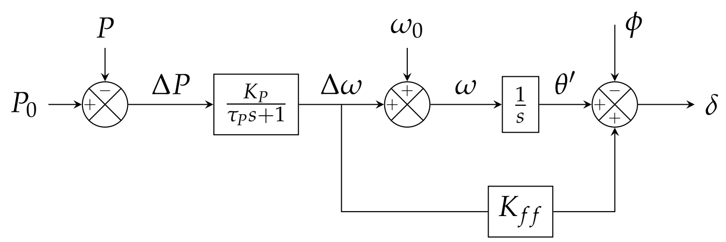

Figure 5.1: Droop control with a feed forward damper.

In a given steady state, it is assumed that the inverter is synchronized with the grid, and a network frequency ω_r is defined as the steady state frequency of the grid and the bus devices. The phase angle ϕ is the integral of this frequency. This is done such that the output of the bus devices represent compatible phasor angles and not absolute angles. The new output is then $\delta = \theta - \phi$. The state equations of this system can be written in the following manner, assuming ω_0 and P_0 are constant set points and that the feed forward term K_{ff} is a static gain.

$$\dot{\omega} = \frac{1}{\tau_P}\left(K_P(P_0 - P) - \omega + \omega_0\right) \tag{5.1a}$$

$$\dot{\delta}' = \omega - \omega_r \tag{5.1b}$$

$$\delta = \delta' + K_{ff}(\omega - \omega_0) \tag{5.1c}$$

The input is chosen as $-P$ because the active power enters the system with a minus in order to get negative feedback in the closed loop system. Figure 5.2 shows a block diagram of the system.

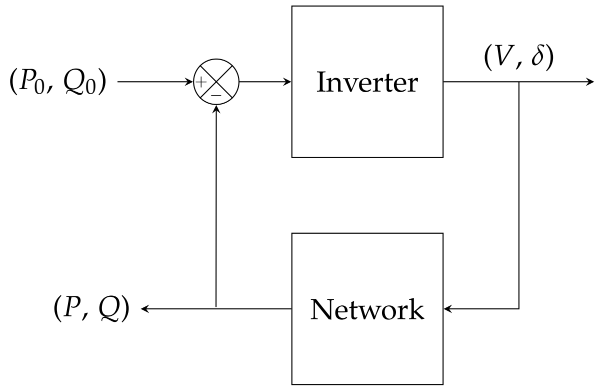

Figure 5.2: Feedback connection of inverter and network with polar voltage as input and power as output.

Indicated by the figure, the output of the network is P and Q, so in order for the feedback to be negative, the input to the inverter should be $-P$. This system is linearized in order to show that it is passive with changes in $-P$ as the input.

$$\begin{aligned} \begin{bmatrix} \dot{\widetilde{\omega}} \\ \dot{\widetilde{\delta}}' \end{bmatrix} &= \begin{bmatrix} \frac{-1}{\tau_P} & 0 \\ 1 & 0 \end{bmatrix} \begin{bmatrix} \widetilde{w} \\ \widetilde{\delta}' \end{bmatrix} + \begin{bmatrix} \frac{K_P}{\tau_P} \\ 0 \end{bmatrix} (-\widetilde{P}) \\ \widetilde{\delta} &= \begin{bmatrix} k_{ff} & 1 \end{bmatrix} \begin{bmatrix} \widetilde{\omega} \\ \widetilde{\delta}' \end{bmatrix} \end{aligned} \tag{5.2}$$

The equivalent transfer function from $-\widetilde{P}$ to $\widetilde{\delta}$ is shown in Equation (5.3).

$$\widetilde{\delta}(s) = \frac{K_P(k_{ff}s + 1)}{s(\tau_P s + 1)}(-\widetilde{P})(s) = G_P(s)(-\widetilde{P})(s) \tag{5.3}$$

The transfer function $G_P(s)$ has two poles, one in 0 and one in $-\frac{1}{\tau_P}$. According to the definition of positive realness, all poles must be in the closed left half plane, which they are.

For all other frequencies, $G_P(j\omega) + G_P^T(-j\omega)$ must be positive semi-definite. For SISO systems like this, $G_P(j\omega) + G_P^T(-j\omega)$ equals to $2Re[G_P(j\omega)]$ [14]. Thus the second condition for positive realness reduces to $Re[G_P(j\omega)] \geq 0$ for all $\omega \in [0, \infty)$ that are not poles of $G_P(s)$. Replacing s with $j\omega$

and removing the complex part of the denominator by expanding the fraction with the complex conjugate of the denominator gives:

$$G_P(j\omega) = K_P \frac{K_{ff}(j\omega)+1}{(j\omega)(\tau_P(j\omega)+1)} = K_P \frac{jK_{ff}\omega+1}{-\tau_P\omega^2+j\omega} = K_P \frac{(K_{ff}\omega^2-\tau_P\omega^2)-j(K_{ff}\tau_P\omega^3+\omega)}{\tau_P^2\omega^4+\omega^2} \tag{5.4}$$

The real part of $G_P(j\omega)$ is identified as:

$$Re[G_P(j\omega)] = K_P \frac{K_{ff}-\tau_P}{\tau_P^2\omega^2+1} \tag{5.5}$$

It can be seen that in order for this system to be positive real K_{ff} must be greater or equal to τ_P. Finally, the last condition for positive realness states that any pure imaginary pole of $G_P(s)$ must be a simple pole and the residue matrix $\lim_{s\to j\omega}(s-j\omega)G_P(s)$ must be positive semi-definite hermitian. Since there is a pole in 0, this condition must be checked. Since the imaginary pole is at 0, the residue becomes:

$$\lim_{s\to 0}(s-0)G_P(s) = \lim_{s\to 0} K_P \frac{K_{ff}s+1}{\tau_P s+1} = K_P \tag{5.6}$$

The Droop gain K_P is a real scalar and therefore hermitian. This means that as long as $K_P \geq 0$ and $K_{ff} \geq \tau_P$, $G_P(s)$ is positive real.

Thus it is concluded that the selfsync controller is passive but not strictly passive. In order to make the system strictly passive, another feedback from the phase angle δ would be required. As this phase angle is not measured, this output feedback is not possible. However, passivity ensures that there exists a Lyapunov function of the negative feedback connection of inverters and the grid. Because the dynamics of the grid are assumed to be much faster than that of the control, they can be viewed as a static non-linear map. One can then use the Circle Criterion to ensure absolute stability of the system, that is, the origin is globally uniformly asymptotically stable [14]. This is equivalent to the grid being the passivizing output feedback.

The multivariate circle criterion states that an observable and controllable system in negative feedback with a memoryless non-linearity ψ is absolutely stable if the following condition is fulfilled [14]:

$$\psi \in [K_1, \infty] \quad \text{and} \quad G(s)[I+K_1G(s)]^{-1} \quad \text{is strictly positive real} \tag{5.7}$$

The first condition $\psi \in [K_1, \infty]$ means that the feedback must belong to the sector $[K_1, \infty]$. For a memoryless function to belong to a sector one of the following must be true [14]:

Definition 5.1 *A memoryless function h(t,u) belongs to the sector*

- $[0, \infty]$ *if* $u^T h(t,u) \geq 0$.
- $[K_1, \infty]$ *if* $u^T[h(t,u) - K_1 u] \geq 0$.
- $[0, K_2]$ *with* $K_2 = K_2^T$ *if* $h^T(t,u)[h(t,u) - K_2 u] \leq 0$.
- $[K_1, K_2]$ *with* $K = K_2 - K_1 = K^T > 0$ *if* $[h(t,u) - K_1 u]^T[h(t,u) - K_2 u] \leq 0$

In all cases, the inequality should hold for all (t,u).

Let the state space representation of $G(s)$ be:

$$\begin{aligned} \dot{x} &= Ax + Bu \\ y &= Cx + Du \end{aligned} \tag{5.8}$$

The state space model for the $P - \omega$ droop is given in Equation (5.2). It is verified that the controller is controllable since the controlability matrix $\mathcal{C}$ has full rank:

$$\mathcal{C} = \begin{bmatrix} B & AB \end{bmatrix} = \begin{bmatrix} \frac{K_P}{\tau_P} & -\frac{K_P}{\tau_P^2} \\ 0 & \frac{K_P}{\tau_P} \end{bmatrix} \tag{5.9}$$

The observability matrix also has full rank due to the triangular structure:

$$\mathcal{O} = \begin{bmatrix} C \\ CA \end{bmatrix} = \begin{bmatrix} k_{ff} & 1 \\ 1 - \frac{k_{ff}}{\tau_P} & 0 \end{bmatrix} \tag{5.10}$$

Thus, the circle criterion in Equation (5.7) applies to the linearized droop controller. Next, the sector ψ belongs to is investigated. A transfer matrix of N droop controlled inverters will only have diagonal elements, since the $P - \omega$ and $Q - V$ droops are independent of each other, as are the inverters themselves. Thus, the requirements reduce to the negative feedback connection of the $P - \omega$ droop being positive real, and the same for the $Q - V$ droop for all the inverters individually. Since $G_P(s)$ is SISO, the closed loop transfer function from the circle criterion reduces to:

$$G_P(s)[I + K_1 G_P(s)]^{-1} = \frac{G_P(s)}{1 + K_1 G_P(s)} \tag{5.11}$$

It is assumed that ψ belongs to the sector $[\alpha I, \infty]$ with $\alpha > 0$ which is fulfilled when $\psi > \alpha$. The closed loop transfer function thus becomes:

$$\frac{G_P(s)}{1 + \alpha G_P(s)} = \frac{K_P(K_{ff}s + 1)}{s(\tau_P s + 1) + \alpha K_P(K_{ff}s + 1)} = \frac{K_P(K_{ff}s + 1)}{\tau_P s^2 + (\alpha K_P K_{ff} + 1)s + \alpha K_P} \tag{5.12}$$

To verify the strict positive realness of the closed loop transfer function, it first off needs to be Hurwitz. The poles of the feedback system are:

$$p_{G_P(s)} = \frac{-(\alpha K_P K_{ff} + 1) \pm \sqrt{(\alpha K_P K_{ff} + 1)^2 - 4\alpha \tau_P K_P}}{2\tau_P} \tag{5.13}$$

Since α, K_P, K_{ff}, and τ_P all are positive, the part left of the $\pm$-sign is always negative. In the case where the square root becomes complex, the poles are all negative. In the case where the square root is positive, it needs to be less than first part of the expression in order to produce negative poles:

$$\sqrt{(\alpha K_P K_{ff} + 1)^2 - 4\alpha \tau_P K_P} < (\alpha K_P K_{ff} + 1) \tag{5.14a}$$

$$(\alpha K_P K_{ff} + 1)^2 - 4\alpha K_P \tau_P < (\alpha K_P K_{ff} + 1)^2 \tag{5.14b}$$

$$-4\alpha K_P \tau_P < 0 \tag{5.14c}$$

Again, since α, K_P, and τ_P are positive the inequality holds true. The closed loop transfer function is therefore Hurwitz. The next condition is to check that the real part of the closed loop transfer function is positive definite for all frequencies that are not a pole:

$$\begin{aligned}\frac{G_P(j\omega)}{1+\alpha G_P(j\omega)} &= \frac{K_P(K_{ff}(j\omega)+1)}{\tau_P(j\omega^2)+(\alpha K_P K_{ff}+1)(j\omega)+\alpha K_P} = \frac{K_P + jK_P K_{ff}\omega}{\alpha K_P - \tau_P\omega^2 + j\omega(\alpha K_P K_{ff}+1)} \\ &= \frac{(K_P + jK_P K_{ff}\omega)(\alpha K_P - \tau_P\omega^2 - j\omega(\alpha K_P K_{ff}+1))}{(\alpha K_P - \tau_P\omega^2)^2 + \omega^2(\alpha K_P K_{ff}+1)^2}\end{aligned} \tag{5.15}$$

The real part of the closed loop transfer function thus becomes:

$$Re\left[\frac{G_P(j\omega)}{1+\alpha G_P(j\omega)}\right] = \frac{\alpha K_P^2 + \alpha K_P^2 K_{ff}^2\omega^2 + K_P\omega^2(K_{ff}-\tau_P)}{(\alpha K_P - \tau_P\omega^2)^2 + \omega^2(\alpha K_P K_{ff}+1)^2} \tag{5.16}$$

All parts of the expression above are either squared or positive with the exception being the difference term at the end. The positive realness of $G_P(s)$ requires $K_{ff} \geq \tau_P$ and thus $K_{ff} - \tau_P \geq 0$, confirming the positive definiteness of the closed loop transfer function.

The last condition for strict positive realness of SISO transfer functions requires that either the transfer function is positive definite at infinity, or that it is zero at infinity and $\lim_{\omega\to\infty}\omega^2 Re[G(j\omega)] > 0$. The transfer function evaluated at infinity is:

$$\frac{G_P(\infty)}{1+\alpha G_P(\infty)} = \lim_{s\to\infty}\frac{G_P(s)}{1+\alpha G_P(s)} = \lim_{s\to\infty}\frac{\frac{K_P K_{ff}}{s} + \frac{K_P}{s^2}}{\tau_P + \frac{\alpha K_P K_{ff}+1}{s} + \frac{\alpha K_P}{s^2}} = 0 \tag{5.17}$$

Since the closed loop transfer function at infinity is zero, the other limit needs to be checked as well:

$$\begin{aligned}\lim_{\omega\to\infty}\omega^2 Re\left[\frac{G_P(j\omega)}{1+\alpha G_P(j\omega)}\right] &= \lim_{\omega\to\infty}\omega^2\frac{\alpha K_P^2 + \alpha K_P^2 K_{ff}^2\omega^2 + K_P\omega^2(K_{ff}-\tau_P)}{(\alpha K_P - \tau_P\omega^2)^2 + \omega^2(\alpha K_P K_{ff}+1)^2} \\ &= \lim_{\omega\to\infty}\frac{\frac{\alpha K_P^2}{\omega^2} + \alpha K_P^2 K_{ff}^2 + K_P(K_{ff}-\tau_P)}{\tau_P^2 + \frac{\alpha^2 K_P^2}{\omega^2} - \frac{2\alpha K_P\tau_P}{\omega^2} + \frac{(\alpha K_P K_{ff}+1}{\omega^2}} \\ &= \frac{\alpha K_P^2 K_{ff}^2 + K_P(K_{ff}-\tau_P)}{\tau_P^2} > 0\end{aligned} \tag{5.18}$$

Thus, it is shown that the $P-\omega$ droop in the closed loop is absolutely stable according to the circle criterion.

In order to confirm absolute stability for the entire closed loop system, the $Q-V$ droop in closed loop also needs to be strict positive real. The closed loop transfer function from the circle criterion for the $Q-V$ droop, which only consists of a first order low-pass filter, is the following:

$$\frac{G_Q(s)}{1+\alpha G_Q(s)} = \frac{K_Q}{\tau_Q s + \alpha K_Q + 1} = \frac{K_Q}{\alpha K_Q + 1}\frac{1}{s\frac{\tau_Q}{\alpha K_Q+1}+1} \tag{5.19}$$

As was seen before, a first order low pass filter is always strict positive real as long as the gain and time constant are strict positive (see Appendix B). For the closed loop $Q-V$ droop the gain is positive as long as $K_Q > 0$ and $\alpha K_Q > -1$. Furthermore, the time constant must be positive, which is the case when $\tau_Q > 0$ and $\alpha K_Q > -1$. Hence, the closed loop $Q-V$ system is absolutely stable under these requirements.

To recap, both the $P-\omega$ and $Q-V$ droop are absolute stable as long as $K_P > 0$, $K_Q > 0$, $K_{ff} \geq \tau_P$, $\psi \in [\alpha I, \infty]$ with $\alpha > 0$, and $\alpha K_Q > -1$. The second to last requirement says that the quadratic form of the memoryless feedback must be positive definite which sets a requirement on the network. However, the quadratic form of the network is not guaranteed to have positive eigenvalues. To see how this might be the case, the next section explores a simple example grid.

5.2 Passivity of example network

In this section the passivity of an example network of two inverters connected in series is investigated. The goal is to determine if such a grid lives up to the requirements set in the previous section. The network system is shown in Figure 5.3.

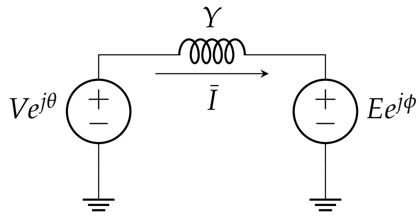

Figure 5.3: Network example with two buses and a line admittance.

In the new coordinates the network has the voltage phases θ and ϕ and magnitudes V and E as inputs and the active and reactive powers at the buses, P_V, P_E, Q_V, and Q_E as outputs. Recall that the complex power was given in Equations (4.28) as:

$$P = \frac{3}{2}(V_d I_d + V_q I_q) \tag{5.20a}$$
$$Q = \frac{3}{2}(V_q I_d - V_d I_q) \tag{5.20b}$$

From Figure 5.3 the current can be expressed from the admittance and voltages as:

$$\bar{I} = Y(\bar{V} - \bar{E}) \tag{5.21}$$

Given the admittance $Y = G + jB$, the relationship between the current and voltages becomes:

$$\begin{aligned} I_d + jI_q &= (G + jB)\left[(V_d + jV_q) - (E_d + jE_q)\right] \\ &= (GV_d - BV_q - GE_d + BE_q) + j(BV_d + GV_q - BE_d - GE_q) \end{aligned} \tag{5.22}$$

Using this expression for the current, the active and reactive powers at the V-bus are written as a function of only the voltages and admittance:

$$\begin{aligned} P_V &= \frac{3}{2}\left[V_d\left(GV_d - BV_q - GE_d + BE_q\right) + V_q\left(BV_d + GV_q - BE_d - GE_q\right)\right] \\ &= \frac{3}{2}\left[G(V_d^2 + V_q^2) - G(V_d E_d + V_q E_q) + B(V_d E_q - V_q E_d)\right] \end{aligned} \tag{5.23a}$$
$$\begin{aligned} Q_V &= \frac{3}{2}\left[V_q\left(GV_d - BV_q - GE_d + BE_q\right) - V_d\left(BV_d + GV_q - BE_d - GE_q\right)\right] \\ &= \frac{3}{2}\left[-B(V_d^2 + V_q^2) + G(V_d E_q - V_q E_d) + B(V_d E_d + V_q E_q)\right] \end{aligned} \tag{5.23b}$$

When calculating the power at the E-bus, the current magnitude is the same but the sign is reversed:

$$P_E = \frac{3}{2}(E_d(-I_d) + E_q(-I_q)) \tag{5.24a}$$

$$Q_E = \frac{3}{2}(E_q(-I_d) - E_d(-I_q)) \tag{5.24b}$$

Substituting the current gives:

$$\begin{aligned} P_E &= -\frac{3}{2}\left[E_d(GV_d - BV_q - GE_d + BE_q) + E_q(BV_d + GV_q - BE_d - GE_q)\right] \\ &= \frac{3}{2}\left[G(E_d^2 + E_q^2) - G(V_dE_d + V_qE_q) - B(V_dE_q - V_qE_d)\right] \end{aligned} \tag{5.25a}$$

$$\begin{aligned} Q_E &= -\frac{3}{2}\left[E_q(GV_d - BV_q - GE_d + BE_q) - E_d(BV_d + GV_q - BE_d - GE_q)\right] \\ &= \frac{3}{2}\left[-B(E_d^2 + E_q^2) - G(V_dE_q - V_qE_d) + B(V_dE_d + V_qE_q)\right] \end{aligned} \tag{5.25b}$$

Next, the voltage representation is changed into polar coordinates using the following relations:

$$\begin{aligned} V_d &= V\cos(\theta) \qquad & E_d &= E\cos(\phi) \\ V_q &= V\sin(\theta) \qquad & E_q &= E\sin(\phi) \end{aligned} \tag{5.26}$$

Replacing the voltages in Equations (5.23) and Equations (5.25) yields:

$$\begin{aligned} P_V = \frac{3}{2}[&G(V^2\cos^2\theta + V^2\sin^2\theta) - G(V\cos\theta E\cos\phi + V\sin\theta E\sin\phi) \\ &+ B(V\cos\theta E\sin\phi - V\sin\theta E\cos\phi)] \end{aligned} \tag{5.27a}$$

$$\begin{aligned} Q_V = \frac{3}{2}[&-B(V^2\cos^2\theta + V^2\sin^2\theta) + G(V\cos\theta E\sin\phi - V\sin\theta E\cos\phi) \\ &+ B(V\cos\theta E\cos\phi + V\sin\theta E\sin\phi)] \end{aligned} \tag{5.27b}$$

$$\begin{aligned} P_E = \frac{3}{2}[&G(E^2\cos^2\phi + E^2\sin^2\phi) - G(V\cos\theta E\cos\phi + V\sin\theta E\sin\phi) \\ &- B(V\cos\theta E\sin\phi - V\sin\theta E\cos\phi)] \end{aligned} \tag{5.27c}$$

$$\begin{aligned} Q_E = \frac{3}{2}[&-B(E^2\cos^2\phi + E^2\sin^2\phi) - G(V\cos\theta E\sin\phi - V\sin\theta E\cos\phi) \\ &+ B(V\cos\theta E\cos\phi + V\sin\theta E\sin\phi)] \end{aligned} \tag{5.27d}$$

The addition and subtraction formulas for sine and cosine are needed from here:

$$\cos^2\alpha + \sin^2\alpha = 1 \tag{5.28a}$$

$$\cos(\alpha - \beta) = \cos\alpha\cos\beta + \sin\alpha\sin\beta \tag{5.28b}$$

$$\sin(\alpha - \beta) = \sin\alpha\cos\beta - \cos\alpha\sin\beta \tag{5.28c}$$

Using these trigonometric identities be power expression can be reduced to:

$$P_V = \frac{3}{2}\left[GV^2 - GVE\cos(\theta - \phi) - BVE\sin(\theta - \phi)\right] \tag{5.29a}$$

$$Q_V = \frac{3}{2}\left[-BV^2 - GVE\sin(\theta - \phi) + BVE\cos(\theta - \phi)\right] \tag{5.29b}$$

$$P_E = \frac{3}{2}\left[GE^2 - GVE\cos(\theta - \phi) + BVE\sin(\theta - \phi)\right] \tag{5.29c}$$

$$Q_E = \frac{3}{2}\left[-BE^2 + GVE\sin(\theta - \phi) + BVE\cos(\theta - \phi)\right] \tag{5.29d}$$

The powers are linearized in the magnitudes and phases of the inverters.

$$\begin{bmatrix} \widetilde{P}_V \\ \widetilde{P}_E \\ \widetilde{Q}_V \\ \widetilde{Q}_E \end{bmatrix} = J_{P,Q}(\hat{\theta},\hat{\phi},\hat{V},\hat{E}) \begin{bmatrix} \widetilde{\theta} \\ \widetilde{\phi} \\ \widetilde{V} \\ \widetilde{E} \end{bmatrix} = \left.\begin{bmatrix} \frac{\partial P_V}{\partial \theta} & \frac{\partial P_V}{\partial \phi} & \frac{\partial P_V}{\partial V} & \frac{\partial P_V}{\partial E} \\ \frac{\partial P_E}{\partial \theta} & \frac{\partial P_E}{\partial \phi} & \frac{\partial P_E}{\partial V} & \frac{\partial P_E}{\partial E} \\ \frac{\partial Q_V}{\partial \theta} & \frac{\partial Q_V}{\partial \phi} & \frac{\partial Q_V}{\partial V} & \frac{\partial Q_V}{\partial E} \\ \frac{\partial Q_E}{\partial \theta} & \frac{\partial Q_E}{\partial \phi} & \frac{\partial Q_E}{\partial V} & \frac{\partial Q_E}{\partial E} \end{bmatrix}\right|_{\hat{\theta},\hat{\phi},\hat{V},\hat{E}} \begin{bmatrix} \widetilde{\theta} \\ \widetilde{\phi} \\ \widetilde{V} \\ \widetilde{E} \end{bmatrix} \tag{5.30}$$

where:

$\widetilde{P}_E, \widetilde{P}_E, \widetilde{Q}_V, \widetilde{Q}_E$	are the small signal active and reactive powers
$\widetilde{\theta}, \widetilde{\phi}, \widetilde{V}, \widetilde{E}$	are the small signal phase angles and magnitudes
$J_{P,Q}(\hat{\theta},\hat{\phi},\hat{V},\hat{E})$	is the Jacobian of the active and reactive power evaluated at the operating point.

The partial derivatives in the Jacobian can be calculated from Equations (5.29), but are not shown symbolically here. Rather, the Jacobian is evaluated in a steady state. This steady state is found by simulating two controlled inverters using a similar simulator to the one in Section 4.4:

$$\begin{bmatrix} \widetilde{P}_V \\ \widetilde{P}_E \\ \widetilde{Q}_V \\ \widetilde{Q}_E \end{bmatrix} = K \begin{bmatrix} \widetilde{\theta} \\ \widetilde{\phi} \\ \widetilde{V} \\ \widetilde{E} \end{bmatrix} = \begin{bmatrix} 46.4090 & -46.4090 & 2.6073 & -1.5838 \\ -46.3656 & 46.3656 & -2.5961 & 1.5730 \\ -1.5374 & 1.5374 & 47.8928 & -47.8069 \\ 2.5268 & -2.5268 & -47.6373 & 47.5622 \end{bmatrix} \begin{bmatrix} \widetilde{\theta} \\ \widetilde{\phi} \\ \widetilde{V} \\ \widetilde{E} \end{bmatrix} \tag{5.31}$$

Recall that in order for the closed loop system to be strict positive real, the memoryless feedback K needed to belong to the sector $K \in [\alpha I, \infty]$ with $\alpha > 0$. A memoryless function belongs to the sector $[K_1, \infty]$ if [14]:

$$u^T[h(u) - K_1 u] \geq 0 \tag{5.32}$$

For the linearized network to belong to the sector $[\alpha I, \infty]$ the following must be true:

$$u^T(Ku - \alpha u) \geq 0 \tag{5.33}$$

The input u inside the parenthesis in Equation (5.33) can be factored outside of the parenthesis:

$$u^T(K - \alpha I)u \geq 0 \tag{5.34}$$

Thus, the eigenvalues of the quadratic form of $K - \alpha I$ must be positive. This means that, because $\alpha > 0$, the eigenvalues of $\frac{1}{2}(K + K^T)$ must be positive and bigger than α. The eigenvalues of $\frac{1}{2}(K + K^T)$ are:

$$\lambda_K = \begin{bmatrix} -0.0058 \\ 0 \\ 92.7842 \\ 95.4512 \end{bmatrix} \tag{5.35}$$

Sadly, there is not only an eigenvalue in zero, but also one that is negative. In fact, one of the eigenvalues will always be zero because of the symmetry of the example. The power over an inductor depends mostly on the angle difference between the voltages on either side. Because there are only two angles, the angle difference from one side will always be minus the difference from the other side. Thus in the linearization, the first and second column in K will be the negative of each other, making the matrix column rank deficient, guaranteeing an eigenvalue in zero. Since the eigenvalues of $\frac{1}{2}(K + K^T)$ are not positive, the closed loop system is not strict positive real either and thus the circle criterion cannot guarantee absolute stability of the closed loop system. Having an eigenvalue in zero is not necessarily a big issue as the network can still be passive, but not strictly passive. However, it requires a bit more work to guarantee asymptotic stability of the closed loop system in this case. The negative eigenvalue means that the system is not passive at all. The negative eigenvalue is very close to being zero, and it is of interest to investigate what assumptions must be made in order for the network to become passive, and whether asymptotic stability can be guaranteed with those assumptions.

5.3 Stability of interconnected inverters using the invariance principle

In this section it is illustrated by a simple example how the invariance principle may be used to show the stability of multiple interconnected droop controlled inverters around an operating point. The system investigated in the following is the same as in Section 5.2. For simplicity it is assumed that the inverters are connected through lossless transmission lines and the difference in phase angle is small. Changes in power are therefore proportional to changes in phase angle [21]. How these assumptions simplify the system can be seen by investigating the Jacobian in Equation (5.30). Lossless transmission lines mean that the conductivity G of the lines are zero. The active power injected by two inverters connected via a lossless inductive transmission line is found to be:

$$P_{12} = \frac{3}{2}(-BV_1V_2\sin(\phi_1 - \phi_2)) \tag{5.36a}$$

$$P_{21} = \frac{3}{2}(BV_1V_2\sin(\phi_1 - \phi_2)) \tag{5.36b}$$

where:

P_{ij} is the power transmitted from inverter i to inverter j.

The linearization of the active powers in this case is:

$$\begin{bmatrix} \widetilde{P}_{12} \\ \widetilde{P}_{21} \end{bmatrix} = B \begin{bmatrix} -\hat{V}_1\hat{V}_2\cos(\hat{\phi}_1 - \hat{\phi}_2) & \hat{V}_1\hat{V}_2\cos(\hat{\phi}_1 - \hat{\phi}_2) & -\hat{V}_2\sin(\hat{\phi}_1 - \hat{\phi}_2) & -\hat{V}_1\sin(\hat{\phi}_1 - \hat{\phi}_2) \\ \hat{V}_1\hat{V}_2\cos(\hat{\phi}_1 - \hat{\phi}_2) & -\hat{V}_1\hat{V}_2\cos(\hat{\phi}_1 - \hat{\phi}_2) & \hat{V}_2\sin(\hat{\phi}_1 - \hat{\phi}_2) & \hat{V}_1\sin(\hat{\phi}_1 - \hat{\phi}_2) \end{bmatrix} \begin{bmatrix} \widetilde{\phi}_1 \\ \widetilde{\phi}_2 \\ \widetilde{V}_1 \\ \widetilde{V}_2 \end{bmatrix} \tag{5.37}$$

Note that B has a negative value when transmission lines are inductive. Since the angle difference is small, the cosine term in the angle derivatives are close to one. The sine term in the voltage derivatives becomes very small. The active power is thus almost independent of changes in voltages. Under these assumptions, the linearization becomes:

$$\begin{bmatrix} \widetilde{P}_{12} \\ \widetilde{P}_{21} \end{bmatrix} = -B\hat{V}_1\hat{V}_2 \begin{bmatrix} 1 & -1 \\ -1 & 1 \end{bmatrix} \begin{bmatrix} \widetilde{\phi}_1 \\ \widetilde{\phi}_2 \end{bmatrix} \tag{5.38}$$

Similarly, the reactive powers only depend linearly on the voltages and are almost independent of the phase angles. It is therefore sufficient to show passivity of the $P - \omega$ and the $Q - V$ part of the network individually under these assumptions. The structure of the feedback connection of the inverters and the network is shown in Figure 5.4. This structure is different from the previous example in that the inverter only includes one integrator for the $P - \omega$ part, namely the one from the low pass filter. The other integrator, which calculates the phase angle is moved into the network, which no longer is memoryless as a result. The $Q - V$ part of the interconnection is unchanged.

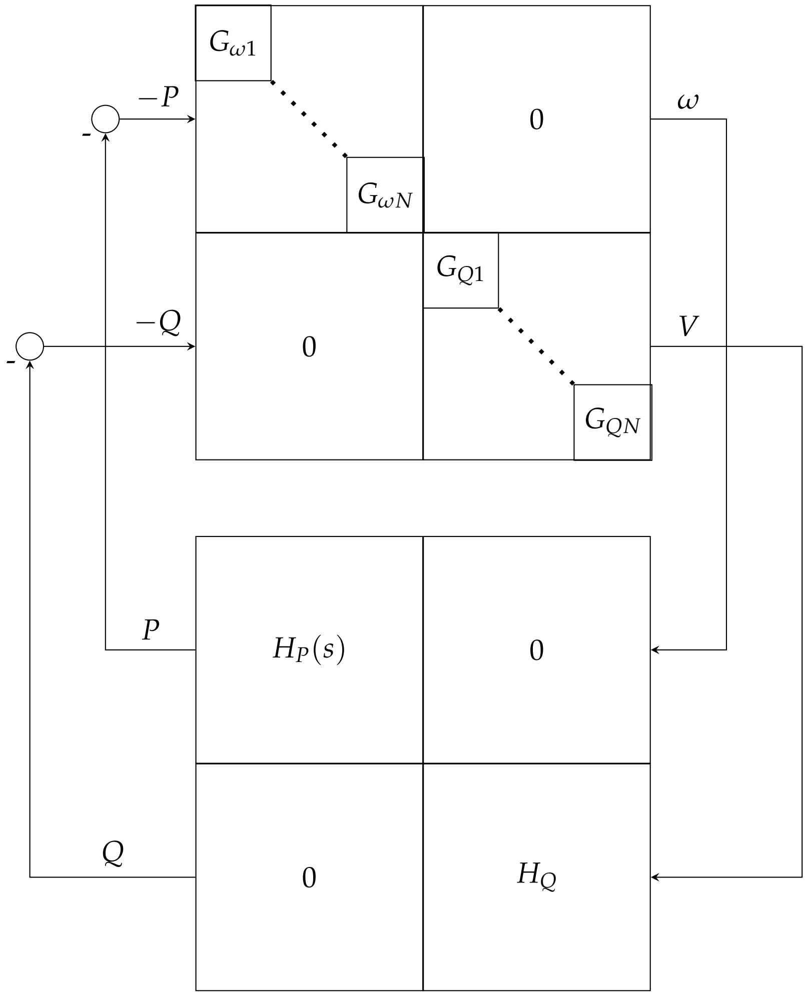

Figure 5.4: Illustration of feedback connections of droop controlled inverters and the network.

First, the $P - \omega$ part of the system is investigated. The $Q - V$ droop is treated in a later section. Starting with the $P - \omega$ part of the network, the derivative of the difference in phase angles can be written as:

$$\frac{d}{dt}\begin{bmatrix}\widetilde{\delta}_{12}\\ \widetilde{\delta}_{21}\end{bmatrix} = \begin{bmatrix}1 & -1\\ -1 & 1\end{bmatrix}\begin{bmatrix}\widetilde{\omega}_1\\ \widetilde{\omega}_2\end{bmatrix} \tag{5.39}$$

where:

$\widetilde{\delta}_{ij}$ is the change in phase angle difference between inverter i and j.
$\widetilde{\omega}_i$ is the change in frequency of the i'th inverter.

Because of the assumptions, the changes in active power only depend on the changes in phase angle differences. But the changes in active power in Equation (5.38) are not written as a function of the phase angle differences. By multiplying the matrix in front of the phase angles in Equation (5.38) with the phase angles, the linearization becomes:

$$\begin{bmatrix}\widetilde{P}_{12}\\ \widetilde{P}_{21}\end{bmatrix} = -B\hat{V}_1\hat{V}_2\begin{bmatrix}\widetilde{\phi}_1 - \widetilde{\phi}_2\\ \widetilde{\phi}_2 - \widetilde{\phi}_1\end{bmatrix} = \begin{bmatrix}\Gamma_{12} & 0\\ 0 & \Gamma_{21}\end{bmatrix}\begin{bmatrix}\widetilde{\delta}_{12}\\ \widetilde{\delta}_{21}\end{bmatrix} \tag{5.40}$$

where:

Γ_{ij} is the proportionality constant for the power transfer between inverters i and j.

It is important to note that $\Gamma_{12} = \Gamma_{21}$ because of the symmetry in the example. In order to not lose generality, the subscripts are kept throughout this section. The transfer function from changes in frequency $\widetilde{\omega}$ to the changes in active power $\widetilde{P}$ can be found by combining Equation (5.39) and Equation (5.40):

$$\begin{bmatrix} \widetilde{P}_{12}(s) \\ \widetilde{P}_{21}(s) \end{bmatrix} = \frac{1}{s} \begin{bmatrix} \Gamma_{12} & -\Gamma_{12} \\ -\Gamma_{21} & \Gamma_{21} \end{bmatrix} \begin{bmatrix} \widetilde{\omega}_1(s) \\ \widetilde{\omega}_2(s) \end{bmatrix} = H_P(s) \begin{bmatrix} \widetilde{\omega}_1(s) \\ \widetilde{\omega}_2(s) \end{bmatrix} \tag{5.41}$$

Passivity may be shown by investigating the positive realness of the transfer function $H_P(s)$ [14]. The first requirement is that the real part of all poles of all elements of a transfer matrix are in the closed left half plane. The poles of $H_P(s)$ are all 0 because of the $\frac{1}{s}$ term in $H_P(s)$. The second requirement is that the transfer function plus its conjugate transpose is positive semi definite:

$$H_P(j\omega) + H_P^T(-j\omega)^T = \frac{1}{j\omega} \begin{bmatrix} \Gamma_{12} & -\Gamma_{12} \\ -\Gamma_{21} & \Gamma_{21} \end{bmatrix} + \frac{1}{-jw} \begin{bmatrix} \Gamma_{12} & -\Gamma_{12} \\ -\Gamma_{21} & \Gamma_{21} \end{bmatrix}^T = 0 \tag{5.42}$$

Since $H_P(j\omega) + H_P^T(-j\omega) = 0$ it is also positive semi-definite. Lastly the residue matrix at any simple pure imaginary pole must be positive semi-definite hermitian. The residue of the transfer matrix for the poles in zero is:

$$\lim_{s \to j0} \frac{(s - j0)}{s} \begin{bmatrix} \Gamma_{12} & -\Gamma_{12} \\ -\Gamma_{21} & \Gamma_{21} \end{bmatrix} = \begin{bmatrix} \Gamma_{12} & -\Gamma_{12} \\ -\Gamma_{21} & \Gamma_{21} \end{bmatrix} \tag{5.43}$$

All elements in the residue matrix have the same absolute value, hence the eigenvalues of the matrix are in 0 and $2\Gamma_{12} > 0$. Furthermore, since the residue matrix is real symmetric, it is also hermitian. Thus the transfer matrix $H_P(s)$ is positive real. This means that the $P - \omega$ part of the network with the frequencies as input and the active power as output is passive and there exists some storage function $V_P(\widetilde{\delta}) > 0 \quad \forall \widetilde{\delta} \neq 0$ with $V_P(0) = 0$ such that $\widetilde{P}^T \widetilde{\omega} \geq \dot{V}_P(\widetilde{\delta})$.

In addition to the network, the passivity of the inverter dynamics is also investigated. The dynamics of the frequency droop may be written as follows:

$$\frac{d}{dt} \begin{bmatrix} \widetilde{\omega}_1 \\ \widetilde{\omega}_2 \end{bmatrix} = \begin{bmatrix} -\frac{1}{\tau_{P,1}} & 0 \\ 0 & -\frac{1}{\tau_{P,2}} \end{bmatrix} \begin{bmatrix} \widetilde{\omega}_1 \\ \widetilde{\omega}_2 \end{bmatrix} + \begin{bmatrix} \frac{K_{P,1}}{\tau_{P,1}} & 0 \\ 0 & \frac{K_{P,2}}{\tau_{P,2}} \end{bmatrix} \begin{bmatrix} -\widetilde{P}_{12} \\ -\widetilde{P}_{21} \end{bmatrix} \tag{5.44}$$

This system is diagonal, with a low pass filter on each diagonal. A first order low pass filter is always output strictly passive (see Appendix B). Notice how if one adds the positive feedback with gain $\frac{1}{K_P}$ to either one of the systems it degenerates into a pure integrator, which is lossless. This also means that the inverters excess Output Feedback Passivity (OFP) is inversely proportional with the droop gain. Because the system is output strictly passive it has a storage function $V_\omega(\widetilde{\omega})$ with $\widetilde{\omega}^T(-\widetilde{P}) \geq \dot{V}_\omega(\widetilde{\omega}) + \widetilde{\omega}\rho(\widetilde{\omega}), \quad \widetilde{\omega}\rho(\widetilde{\omega}) > 0 \, \forall \, \widetilde{\omega} \neq 0$.

In order to investigate stability the sum of storage functions is investigated as a Lyapunov function candidate for the closed loop system.

$$\dot{V}_\omega(\widetilde{\omega}) + \dot{V}_P(\widetilde{\delta}) \leq \widetilde{\omega}^T \widetilde{P} + \widetilde{\omega}^T(-\widetilde{P}) - \widetilde{\omega}\rho(\widetilde{\omega}) \leq -\widetilde{\omega}\rho(\widetilde{\omega}) \tag{5.45}$$

Notice that the derivative of this Lyapunov function is negative definite everywhere except when $\widetilde{\omega} = 0$. However, the system can only stay identically in $\widetilde{\omega} = 0$ when $\dot{\widetilde{\omega}} = 0$ which is only the case when $\widetilde{P} = 0$ and $\widetilde{\omega} = 0$. Thus the origin is the only invariant set, and the origin is asymptotically stable according to the invariance principle [14].

When moving the integrator to the network, passivity and stability is shown even without the feed forward damper in this example. Therefore, it is investigated how the feed forward damper influences the passivity of this example.

5.4 Effects of the feed forward damper

The feed forward damper that is necessary to passivate the transfer function from active power to voltage angle as seen in Section 5.1 is not a prerequisite for asymptotic stability. To see how the feed forward damper increases the passivity margins of the transfer function from frequency to power, a storage function candidate for the system is investigated. Recall that the phase angle difference between two inverters was defined as:

$$\widetilde{\delta}_{ij} = \widetilde{\phi}_i - \widetilde{\phi}_j \tag{5.46}$$

A damper is added to each phase angle, bypassing the integrator:

$$\widetilde{\phi}_i = \widetilde{\phi}'_i + K_{ff,i}\widetilde{\omega}_i \tag{5.47}$$

Note that $\widetilde{\phi}'_i$ is the internal phase angle of the inverter calculated by the integrator without the damper. Substituting the new phase angle with the damper into Equation (5.46) gives:

$$\begin{aligned} \widetilde{\delta}_{ij} = \widetilde{\phi}_i - \widetilde{\phi}_j &= (\widetilde{\phi}'_i + K_{ff,i}\widetilde{\omega}_i) - (\widetilde{\phi}'_j + K_{ff,j}\widetilde{\omega}_j) \\ &= (\widetilde{\phi}'_i - \widetilde{\phi}'_j) + (K_{ff,i}\widetilde{\omega}_i - K_{ff,j}\widetilde{\omega}_j) \\ &= \widetilde{\delta}'_{ij} + \begin{bmatrix} K_{ff,i} & -K_{ff,j} \end{bmatrix} \begin{bmatrix} \widetilde{\omega}_i \\ \widetilde{\omega}_j \end{bmatrix} \end{aligned} \tag{5.48}$$

where:

$\widetilde{\delta}'_{ij}$ is the change in phase angle difference between the internal inverters phase angles from their integrators without the dampers.

The dynamics of the internal phase angle differences are still the same:

$$\frac{d}{dt}\begin{bmatrix} \widetilde{\delta}'_{12} \\ \widetilde{\delta}'_{21} \end{bmatrix} = \begin{bmatrix} 1 & -1 \\ -1 & 1 \end{bmatrix} \begin{bmatrix} \widetilde{\omega}_1 \\ \widetilde{\omega}_2 \end{bmatrix} \tag{5.49}$$

The main difference comes in the output map of the system. The active powers with the dampers are given as:

$$\begin{bmatrix} \widetilde{P}_{12} \\ \widetilde{P}_{21} \end{bmatrix} = \begin{bmatrix} \Gamma_{12} & 0 \\ 0 & \Gamma_{21} \end{bmatrix} \begin{bmatrix} \widetilde{\delta}'_{12} \\ \widetilde{\delta}'_{21} \end{bmatrix} + \begin{bmatrix} \Gamma_{12} & 0 \\ 0 & \Gamma_{21} \end{bmatrix} \begin{bmatrix} K_{ff,1} & -K_{ff,2} \\ -K_{ff,1} & K_{ff,2} \end{bmatrix} \begin{bmatrix} \widetilde{\omega}_1 \\ \widetilde{\omega}_2 \end{bmatrix} \tag{5.50}$$

A storage function candidate for this system could be:

$$V(\widetilde{\delta}') = \frac{\Gamma_{12}}{4}\left(\widetilde{\delta}'^2_{12} + \widetilde{\delta}'^2_{21}\right) \tag{5.51}$$

where:

$\widetilde{\delta}'$ is the vector containing all phase angle differences.

Note again, that Γ_{12} and Γ_{21} are the same value. Taking the time derivative of the storage function candidate yields:

$$
\begin{aligned}
\dot{V}(\widetilde{\delta}') &= \frac{\Gamma_{12}}{2}\left(\widetilde{\delta}'_{12}\frac{d\widetilde{\delta}'_{12}}{dt} + \widetilde{\delta}'_{21}\frac{d\widetilde{\delta}'_{21}}{dt}\right) = \frac{\Gamma_{12}}{2}\begin{bmatrix}\widetilde{\delta}'_{12} & \widetilde{\delta}'_{21}\end{bmatrix}\frac{d}{dt}\begin{bmatrix}\widetilde{\delta}'_{12}\\ \widetilde{\delta}'_{21}\end{bmatrix} \\
&= \frac{\Gamma_{12}}{2}\begin{bmatrix}\widetilde{\delta}'_{12} & \widetilde{\delta}'_{21}\end{bmatrix}\begin{bmatrix}1 & -1\\ -1 & 1\end{bmatrix}\begin{bmatrix}\widetilde{\omega}_1\\ \widetilde{\omega}_2\end{bmatrix} = \Gamma_{12}\begin{bmatrix}\widetilde{\delta}'_{12} & \widetilde{\delta}'_{21}\end{bmatrix}\begin{bmatrix}\widetilde{\omega}_1\\ \widetilde{\omega}_2\end{bmatrix} \\
&= \Gamma_{12}\left(\widetilde{\delta}'_{12}\widetilde{\omega}_1 + \widetilde{\delta}'_{21}\widetilde{\omega}_2\right)
\end{aligned} \tag{5.52}
$$

Given the expression for the active powers in Equation (5.50), the supply rate is given as:

$$
\begin{aligned}
\widetilde{P}^T\widetilde{\omega} &= \widetilde{P}_{12}\widetilde{\omega}_1 + \widetilde{P}_{21}\widetilde{\omega}_2 \\
&= (\Gamma_{12}\widetilde{\delta}'_{12} + \Gamma_{12}K_{ff,1}\widetilde{\omega}_1 - \Gamma_{12}K_{ff,2}\widetilde{\omega}_2)\widetilde{\omega}_1 + (\Gamma_{12}\widetilde{\delta}'_{21} + \Gamma_{12}K_{ff,2}\widetilde{\omega}_2 - \Gamma_{12}K_{ff,1}\widetilde{\omega}_1)\widetilde{\omega}_2 \\
&= \Gamma_{12}\widetilde{\delta}'_{12}\widetilde{\omega}_1 + \Gamma_{12}\widetilde{\delta}'_{21}\widetilde{\omega}_2 + \Gamma_{12}K_{ff,1}\widetilde{\omega}_1^2 + \Gamma_{12}K_{ff,2}\widetilde{\omega}_2^2 - \Gamma_{12}(K_{ff,2} + K_{ff,1})\widetilde{\omega}_1\widetilde{\omega}_2
\end{aligned} \tag{5.53}
$$

The first two terms can be identified to be the time derivative of the storage function candidate:

$$
\widetilde{P}^T\widetilde{\omega} = \dot{V}(\widetilde{\delta}') + \Gamma_{12}k_{ff1}\widetilde{\omega}_1^2 + \Gamma_{12}k_{ff2}\widetilde{\omega}_2^2 - \Gamma_{12}(k_{ff2} + k_{ff1})\widetilde{\omega}_1\widetilde{\omega}_2 \tag{5.54}
$$

The polynomial added to the derivative of the storage function to make it equal to the supply rate can be rewritten to a quadratic form in order to show if it is positive semi-definite:

$$
\dot{V}(\widetilde{\delta}') + \widetilde{\omega}^T\Gamma_{12}\begin{bmatrix}K_{ff,1} & -\frac{K_{ff,1}+K_{ff,2}}{2}\\ -\frac{K_{ff,1}+K_{ff,2}}{2} & K_{ff,2}\end{bmatrix}\widetilde{\omega} = \widetilde{P}^T\widetilde{\omega} \tag{5.55}
$$

The characteristic polynomial of the quadratic form is:

$$
\begin{aligned}
\det\left|\begin{bmatrix}K_{ff,1}-\lambda & -\frac{K_{ff,1}+K_{ff,2}}{2}\\ -\frac{K_{ff,1}+K_{ff,2}}{2} & K_{ff,2}-\lambda\end{bmatrix}\right| &= (K_{ff,1}-\lambda)(K_{ff,2}-\lambda) - \frac{(K_{ff,1}+K_{ff,2})^2}{4} \\
&= \lambda^2 - (K_{ff,1}+K_{ff,2})\lambda + K_{ff,1}k_{ff2} - \frac{1}{4}(K_{ff,1}+K_{ff,2})^2
\end{aligned} \tag{5.56}
$$

The eigenvalues are the solutions to this characteristic polynomial:

$$
\begin{aligned}
\lambda &= \frac{K_{ff,1}+K_{ff,2} \pm \sqrt{(K_{ff,1}+K_{ff,2})^2 - 4\left(K_{ff,1}K_{ff,2} - \frac{(K_{ff,1}+K_{ff,2})^2}{4}\right)}}{2} \\
&= \frac{K_{ff,1}+K_{ff,2} \pm \sqrt{2(K_{ff,1}^2+K_{ff,2}^2)}}{2}
\end{aligned} \tag{5.57}
$$

In order for the quadratic form matrix to be positive semi-definite, the eigenvalues must be positive. For the eigenvalue with the negative square root term to be positive semi-definite the following inequality must be true:

$$
0 \le K_{ff,1} + K_{ff,2} - \sqrt{2(K_{ff,1}^2+K_{ff,2}^2)} \tag{5.58a}
$$

$$
\sqrt{2(K_{ff,1}^2+K_{ff,2}^2)} \le K_{ff,1} + K_{ff,2} \tag{5.58b}
$$

From here it is necessary to require that $K_{ff,1} + K_{ff,2} \geq 0$. With this requirement, both sides of the inequality can be squared:

$$2(K_{ff,1}^2 + K_{ff,2}^2) \leq K_{ff,1}^2 + K_{ff,2}^2 + 2K_{ff,1}K_{ff,2} \tag{5.59a}$$
$$K_{ff,1}^2 + K_{ff,2}^2 \leq 2K_{ff,1}K_{ff,2} \tag{5.59b}$$
$$(K_{ff,1} - K_{ff,2})^2 \leq 0 \tag{5.59c}$$

For the last inequality to hold true $K_{ff,1}$ must be equal to $K_{ff,2}$.

For the other eigenvalue to be positive semi-definite the following must hold true:

$$K_{ff,1} + K_{ff,2} + \sqrt{(2(K_{ff,1}^2 + K_{ff,2}^2)} \geq 0 \tag{5.60}$$

The square root part is again always positive and $K_{ff,1} + K_{ff,2}$ was required to be positive from before. Thus both eigenvalues of the quadratic form are positive or zero as long as $K_{ff,1} + K_{ff,2} \geq 0$ and $K_{ff,1} = K_{ff,2}$.

Since $K_{ff,1} = K_{ff,2}$, one of the damper gains can be replaced with the other in Equation (5.55):

$$\widetilde{P}^T\widetilde{\omega} = \dot{V}(\widetilde{\delta}') + \widetilde{\omega}^T\Gamma_{12}K_{ff,1}\begin{bmatrix} 1 & -1 \\ -1 & 1 \end{bmatrix}\widetilde{\omega} \tag{5.61}$$

The eigenvalues of the quadratic term are zero and $2\Gamma_{12}K_{ff,1}$. The corresponding eigenvectors are $\widetilde{\omega}_1 = \widetilde{\omega}_2$ for the eigenvalue in zero and $\widetilde{\omega}_1 = -\widetilde{\omega}_2$ for the other eigenvalue. This means that the feed forward damper adds output feedback passivity to the network part of the $P - \omega$ droop interconnection in all directions except $\widetilde{\omega}_1 = \widetilde{\omega}_2$, as the eigenvalue in this direction is zero. This likely improves the performance of the overall control scheme. It might also be possible to loosen the equality constraint of the feed forward damper gains by taking into account the output strict passivity of the frequency droop filter.

A simulation example of the linearized system is made in order to show the effect of the damper. The frequency in each inverter is shown with and without the damper in Figure 5.5.

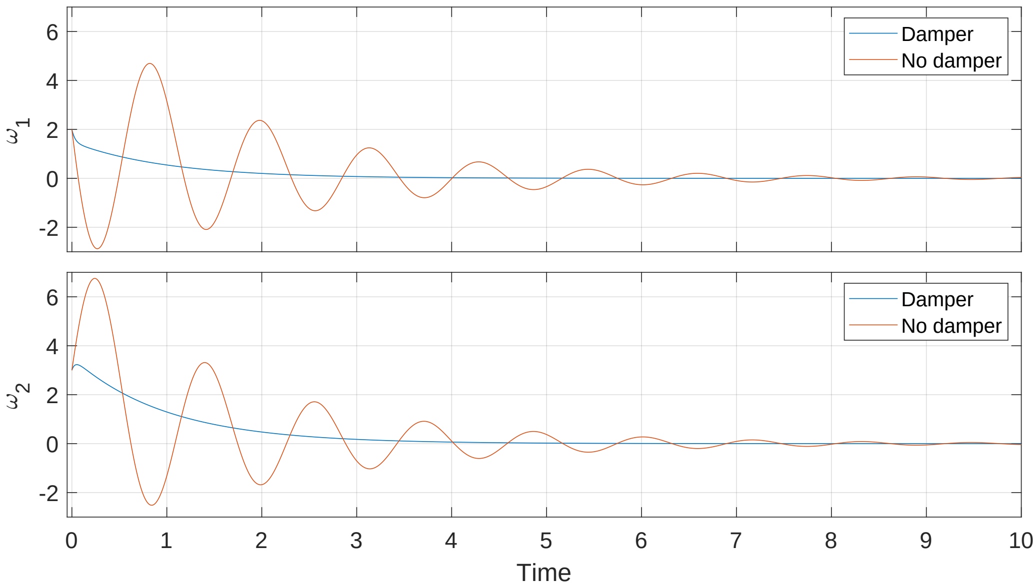

Figure 5.5: Simulation of a linearized grid with two droop controlled inverters with and without dampers. The simulation parameters are: $\tau_P = 1$, $K_P = 10$, $\Gamma = 1$, and $K_{ff,1} = K_{ff,2} = 1$.

As can be seen on the figure, the damper drastically reduces frequency oscillations when the system finds a steady state.

It has thus been shown, that the feed forward damper increases the passivity margins of the $P - \omega$ part of the network. Passivity can be achieved with two interconnected inverters under the assumptions that the transmission lines are lossless and the phase angle differences between inverters are small and the feed forward damper affects the passivity of the $P - \omega$ loop positively. In the next section, the analysis is extended to include N interconnected inverters instead of only two.

5.5 N interconnected inverters

In order to show the stability in the case of N interconnected inverters a transfer function description is constructed in the same manner as for the case of two inverters and the positive realness is investigated. Denote with $\widetilde{P}_1, \widetilde{P}_2, \cdots, \widetilde{P}_N$ the active powers injected into the grid from the inverters. The active power an inverter supplies to the grid is proportional to the change in phase angle difference, under the assumptions of Section 5.3:

$$\widetilde{P}_i = \sum_{\substack{j=1 \\ j \neq i}}^{N} \Gamma_{ij} \widetilde{\delta}_{ij} \tag{5.62}$$

where:

$\Gamma_{ij} = \frac{\partial P_i}{\partial \delta_{ij}}$ is the proportionality constant between the active power and the phase angle difference.

The changes in all active powers in the network can therefore be written in matrix form as follows:

$$\begin{bmatrix} \widetilde{P}_1 \\ \widetilde{P}_2 \\ \vdots \\ \widetilde{P}_N \end{bmatrix} = \begin{bmatrix} \Gamma_{12} & \Gamma_{13} & \cdots & \Gamma_{1N} & & & & & & & & \\ & & & & \Gamma_{21} & \Gamma_{23} & \cdots & \Gamma_{2N} & & & & \\ & & & & & & & & \ddots & & & \\ & & & & & & & & & \Gamma_{N1} & \Gamma_{N2} & \cdots & \Gamma_{NN-1} \end{bmatrix} \begin{bmatrix} \widetilde{\delta}_{12} \\ \widetilde{\delta}_{13} \\ \vdots \\ \widetilde{\delta}_{1N} \\ \widetilde{\delta}_{21} \\ \widetilde{\delta}_{23} \\ \vdots \\ \widetilde{\delta}_{2N} \\ \widetilde{\delta}_{N1} \\ \widetilde{\delta}_{N2} \\ \vdots \\ \widetilde{\delta}_{NN-1} \end{bmatrix} \tag{5.63}$$

Furthermore, the changes in phase angle difference are given as the integral of the difference in the changes in inverter frequencies:

$$\widetilde{\delta}_{ij} = \frac{1}{s}(\widetilde{\omega}_i - \widetilde{\omega}_j) \tag{5.64}$$

This can also be written in matrix form, which gives:

$$\begin{bmatrix} \widetilde{\delta}_{12} \\ \widetilde{\delta}_{13} \\ \vdots \\ \widetilde{\delta}_{1N} \\ \widetilde{\delta}_{21} \\ \widetilde{\delta}_{23} \\ \vdots \\ \widetilde{\delta}_{2N} \\ \widetilde{\delta}_{N1} \\ \widetilde{\delta}_{N2} \\ \vdots \\ \widetilde{\delta}_{NN-1} \end{bmatrix} = \frac{1}{s} \begin{bmatrix} 1 & -1 & & & \\ 1 & & -1 & & \\ \vdots & & & \ddots & \\ 1 & & & & -1 \\ -1 & 1 & & & \\ & 1 & -1 & & \\ & \vdots & & \ddots & \\ & 1 & & & -1 \\ -1 & & & & 1 \\ & -1 & & & 1 \\ & & \ddots & & \vdots \\ & & & -1 & 1 \end{bmatrix} \begin{bmatrix} \widetilde{\omega}_1 \\ \widetilde{\omega}_2 \\ \vdots \\ \widetilde{\omega}_N \end{bmatrix} \tag{5.65}$$

Combining Equation (5.62) and Equation (5.64) yields the following equation:

$$\widetilde{P}_i = \sum_{\substack{j=1 \\ j\neq i}}^{N} \Gamma_{ij} \frac{1}{s} (\widetilde{\omega}_i - \widetilde{\omega}_j) = \frac{1}{s} \left[\sum_{\substack{j=1 \\ j\neq i}}^{N} \Gamma_{ij} \widetilde{\omega}_i - \sum_{\substack{j=1 \\ j\neq i}}^{N} \Gamma_{ij} \widetilde{\omega}_j \right] \tag{5.66}$$

The first sum of proportionality constants, pertaining to $\widetilde{\omega}_i$ is collected into one constant:

$$\Xi_i = \sum_{\substack{j=1 \\ j\neq i}}^{N} \Gamma_{ij} \tag{5.67}$$

With this change, the change in active power for the i'th inverter becomes:

$$\widetilde{P}_i = \frac{1}{s} \left[\Xi_i \widetilde{\omega}_i - \sum_{\substack{j=1 \\ j\neq i}}^{N} \Gamma_{ij} \widetilde{\omega}_j \right] \tag{5.68}$$

Equation (5.68) can be written in matrix form as follows:

$$\begin{bmatrix} \widetilde{P}_1 \\ \widetilde{P}_2 \\ \widetilde{P}_3 \\ \vdots \\ \widetilde{P}_N \end{bmatrix} = \frac{1}{s} \begin{bmatrix} \Xi_1 & -\Gamma_{12} & -\Gamma_{13} & \cdots & -\Gamma_{1N} \\ -\Gamma_{21} & \Xi_2 & -\Gamma_{23} & \cdots & -\Gamma_{2N} \\ -\Gamma_{31} & -\Gamma_{32} & \Xi_3 & \ddots & \vdots \\ \vdots & \vdots & \ddots & \ddots & -\Gamma_{(N-1)N} \\ -\Gamma_{N1} & -\Gamma_{N2} & \cdots & -\Gamma_{N(N-1)} & \Xi_N \end{bmatrix} \begin{bmatrix} \widetilde{\omega}_1 \\ \widetilde{\omega}_2 \\ \widetilde{\omega}_3 \\ \vdots \\ \widetilde{\omega}_N \end{bmatrix} \tag{5.69}$$

In order to show passivity via. positive realness the poles of the transfer matrix in Equation (5.69) need to be less or equal to zero. Because of the $\frac{1}{s}$ term, all poles are equal to zero. For all other frequencies, the transfer matrix must be positive semi definite and hermitian. It is seen that the transfer matrix is *Diagonally Dominant*, that is, the diagonal entries Ξ_i are greater than or equal to the sum of the absolute values of the off diagonal entries Γ_{ij} [22]:

$$\Xi_i \geq \sum_{j\neq i} |\Gamma_{ij}| \tag{5.70}$$

Symmetric diagonally dominant matrices are always positive semi definite. Because the proportionality constants Γ_{ij} are symmetric in the sense that $\Gamma_{ij} = \Gamma_{ji}$, it can be concluded that the matrix is symmetric and therefore also positive semi definite. For all poles on the imaginary axis, the residue matrix must be positive semi definite as well. Because the positive semi definiteness of the transfer matrix is independent of the pole in zero, it is still positive semi definite if the pole is removed. Thus, the transfer matrix is positive real. This means that there exist a storage function for which $\dot{V}_{H_P} \leq \widetilde{P}^T \widetilde{\omega}$. Thus, the strict positive realness of the individual transfer matrices $G_{\omega,i}$ guarantees stability via the invariance principle just like it did in the case of two inverters.

It can be concluded that the sharing of active power between inverters is stable when they are connected through inductive lines and the angle differences between the inverters are small. Furthermore, the margin of passivity is inversely proportional to K_P. The feed forward dampers can potentially be used to further improve the passivity of the inverters and the dynamic response. In order to ensure the stability of the entire grid, the voltage control also needs to be stable. The next section therefore investigates the passivity of the $Q - V$ part of the interconnection.

5.6 Stability of the reactive power regulation

In Section 5.2 the reactive powers for a system of two connected inverters were found. Assuming that the transmission lines are lossless, the reactive powers of two connected inverters are:

$$Q_1 = \frac{3}{2}[-BV_1^2 + BV_1V_2\cos(\phi_1 - \phi_2)] \tag{5.71a}$$

$$Q_2 = \frac{3}{2}[-BV_2^2 + BV_1V_2\cos(\phi_1 - \phi_2)] \tag{5.71b}$$

It was mentioned earlier, that the reactive power is almost independent of the phase angle difference, as long as the difference is small. The linearization of the reactive power with respect to the voltages is:

$$\begin{bmatrix} \widetilde{Q}_1 \\ \widetilde{Q}_2 \end{bmatrix} = \frac{3}{2} \begin{bmatrix} -2B\hat{V}_1 + B\hat{V}_2 & B\hat{V}_1 \\ B\hat{V}_2 & -2B\hat{V}_2 + B\hat{V}_1 \end{bmatrix} \begin{bmatrix} \widetilde{V}_1 \\ \widetilde{V}_2 \end{bmatrix} \tag{5.72}$$

Note, when $\hat{V}_1 = \hat{V}_2$ the matrix becomes diagonally dominant and symmetric, meaning it is positive semi-definite, because B is negative. However, when this is not the case the matrix can have negative eigenvalues, and passivity of the inverters are not sufficient to show stability.

Consider now the case of N interconnected inverters. Each inverter supplies a reactive power. In contrast to the active power, the reactive power transfer in the interconnection is not lossless. Assume that each inverter is connected to each other inverter through an equivalent inductive line as shown in Figure 5.6.

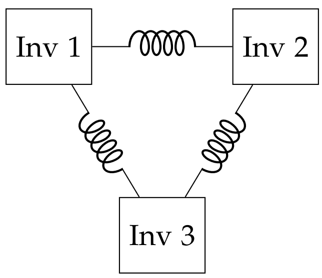

Figure 5.6: Equivalent network of three inverters connected through inductive transmission lines.

A linearization of the reactive powers of two inverters connected via a single inductive line is given in Equation (5.72). The reactive power that one inverter injects into the network in total is equal to the sum of reactive powers that inverter injects into all its equivalent connections. More specifically, the reactive power inverter i injects into the equivalent connection with inverter j is given as:

$$\widetilde{Q}_{ij} = \begin{bmatrix} -2B_{ij}\hat{V}_i + B_{ij}\hat{V}_j & B_{ij}\hat{V}_i \end{bmatrix} \begin{bmatrix} \widetilde{V}_i \\ \widetilde{V}_j \end{bmatrix} \tag{5.73}$$

where:

B_{ij} is the susceptance of the equivalent inductive connection between inverters i and j.

Note that the $\frac{3}{2}$ is hidden away in the B's. The total reactive power from the i'th inverter is then:

$$\widetilde{Q}_i = \sum_{\substack{j=1 \\ j\neq i}}^{N} \widetilde{Q}_{ij} = \left[\sum_{\substack{j=1 \\ j\neq i}}^{N} -2B_{ij}\hat{V}_i + B_{ij}\hat{V}_j \right] \widetilde{V}_i + \left[\sum_{\substack{j=1 \\ j\neq i}}^{N} B_{ij}\hat{V}_i\widetilde{V}_j \right] \tag{5.74}$$

The sum in front of $\widetilde{V}_i$ is collected into:

$$\mathcal{K}_i = \sum_{\substack{j=1 \\ j\neq i}}^{N} -2B_{ij}\hat{V}_i + B_{ij}\hat{V}_j \tag{5.75}$$

Substituting $\mathcal{K}_i$ into the total reactive power yields:

$$\widetilde{Q}_i = \mathcal{K}_i\widetilde{V}_i + \sum_{\substack{j=1 \\ j\neq i}}^{N} B_{ij}\hat{V}_i\widetilde{V}_j \tag{5.76}$$

This can also be expressed in matrix form:

$$\begin{bmatrix} \widetilde{Q}_1 \\ \widetilde{Q}_2 \\ \widetilde{Q}_3 \\ \vdots \\ \widetilde{Q}_N \end{bmatrix} = \begin{bmatrix} \mathcal{K}_1 & B_{12}\hat{V}_1 & B_{13}\hat{V}_1 & \cdots & B_{1N}\hat{V}_1 \\ B_{21}\hat{V}_2 & \mathcal{K}_2 & B\hat{V}_2 & \cdots & B_{2N}\hat{V}_2 \\ B_{31}\hat{V}_3 & B_{32} & \mathcal{K}_3 & \ddots & \vdots \\ \vdots & \vdots & \ddots & \ddots & B_{(N-1)N}\hat{V}_{N-1} \\ B_{N1}\hat{V}_N & B_{N2}\hat{V}_N & \cdots & B_{N(N-1)}\hat{V}_N & \mathcal{K}_N \end{bmatrix} \begin{bmatrix} \widetilde{V}_1 \\ \widetilde{V}_2 \\ \widetilde{V}_3 \\ \vdots \\ \widetilde{V}_N \end{bmatrix} \tag{5.77}$$

It is seen that when every voltage is equal the matrix is positive semi definite, as it is diagonally dominant and symmetric. But when this is not the case it is not positive nor symmetric. However, it is reasonable to assume that the voltage differences between the inverters are small and it can be assumed that in a given steady state the network can belong to some sector which may be lower bounded by the sector $[-\alpha I, \infty]$. The network belongs to this sector if [14]:

$$x^T(H_Q + \alpha I)x \geq 0 \qquad \forall x \neq 0 \tag{5.78}$$

where:

H_Q is the transfer matrix from the voltages to the reactive powers.

The circle criterion states that for the system to be stable $G_Q(s)(1 - \alpha G_Q(s))^{-1}$ must be strictly positive real [14]. Due to the diagonal structure of $G_Q(s)$ and the lower bound of the sector it is enough if every diagonal system is strictly positive real, that is Equation (5.79) must be strictly positive real for every inverter.

$$G_{Q,i}(s)(1-\alpha G_{Q,i}(s))^{-1} = \frac{K_{Q,i}}{s\tau_{Q,i}+1}\frac{1}{1-\alpha\frac{K_{Q,i}}{s\tau_{Q,i}+1}} = \frac{K_{Q,i}}{1-\alpha K_{Q,i}}\frac{1}{s\frac{\tau_{Q,i}}{1-\alpha K_{Q,i}}+1} \tag{5.79}$$

Equation (5.79) is strictly positive real whenever the time constant $\frac{\tau_{Q,i}}{1-\alpha K_{Q,i}}$ is positive as it is a first order low pass filter with positive gain (See Appendix B). Therefore $\alpha K_{Q,i} < 1$ and $K_{Q,i} > 0$ is sufficient for stability given the assumptions. Note that this condition is conservative as it might be possible to lower bound the sector which the network belongs to with a matrix that does not have the same diagonal elements instead of $-\alpha I$. This would mean that some inverters may be allowed a high K_Q, which means better control of the reactive power delivered by those inverters. However, if one is mostly interested in regulating the voltage, letting $K_{Q,i}$ be small is much more likely to fulfill the stability conditions.

Another observation to be aware of is that capacitive loads are a source of reactive power. This means that they absorb negative reactive power proportional to the voltage over them. The inverters must therefore provide less reactive power to compensate. Capacitors could thereby work towards making the network more negative i.e lowering the smallest eigenvalue of $\frac{1}{2}(H_Q + H_Q^T)$. This means α must be larger to provide a lower bound for the sector the network belongs to, limiting the range of viable droop gains guaranteeing stability via the circle criterion.

It is seen that both the $P-\omega$ and $Q-V$ parts of the network are asymptotically stable under some rather limiting assumptions of the network and the steady state. Therefore, it is of interest to investigate, by some more general simulation examples, what happens when those assumptions are not met. This is because one cannot expect the assumptions made in this chapter to hold for any real configuration of a grid.

6 The effects of loads and losses

In the previous chapter assumptions about the network were made in order to simplify the analysis and showcase the basic relations in inverter based networks. This was done to show that there is some feasibility to the notion of guaranteeing stability based only on the parameters of the inverters and some basic assumptions of the power grid. However, in a real network there will be loses and loads that also impact the stability of the network, and it is important to investigate the validity of the previous results under less ideal conditions. First, a simulation model of the *Two Area Network* from Kundur *et al.* [2] is build using graph theory. The simulation is used to investigate whether the system is stable when using only droop controlled inverters, as well as the effect that certain controller parameters have on the behavior of the system. Later on, a simulation of the IEEE 24 Bus *Reliability Test System* is made and investigated using the same methods.

6.1 Two Area Network

As a first approach a simulation model of four inverters supplying a two load network consisting of mainly inductive, but slightly resistive lines is investigated. Such a network is shown in Figure 6.1 and is based on the Two Area Network example from Kundur *et al.* [2, page 813].

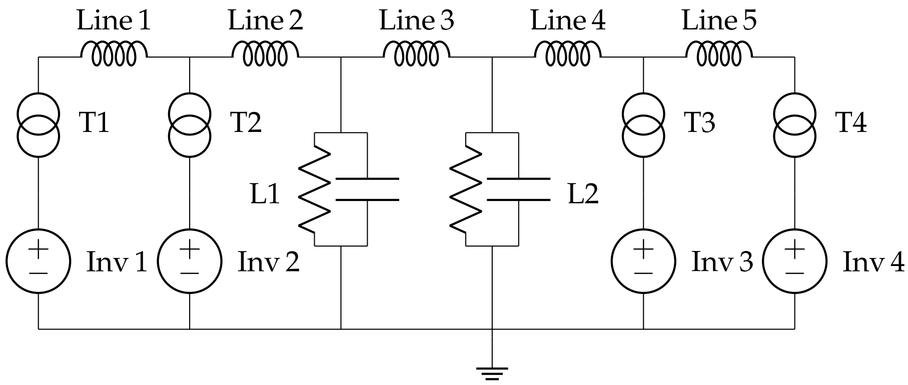

Figure 6.1: Simple network for investigation of inverter behavior with lossy lines and capacitive loads, **T** are transformers, **Inv** are inverters, **L** are loads, and **Line** are transmission lines.

The inverters are connected to the transmission lines via transformers, denoted T1 through T4. It assumed that the turn ratio of the transformers are equal to the ratio of base units on each side of the transformer. In this case the transformer can be viewed as a simple impedance [2]. The transmission lines themselves are shown as an inductance, but also include a series resistance, as mentioned earlier. The loads denoted L1 and L2 are resistive loads with a shunt capacitance.

In order to solve the network in the simulation, graph theory is used. A directed graph of the network in Figure 6.1 is constructed and shown in Figure 6.2.

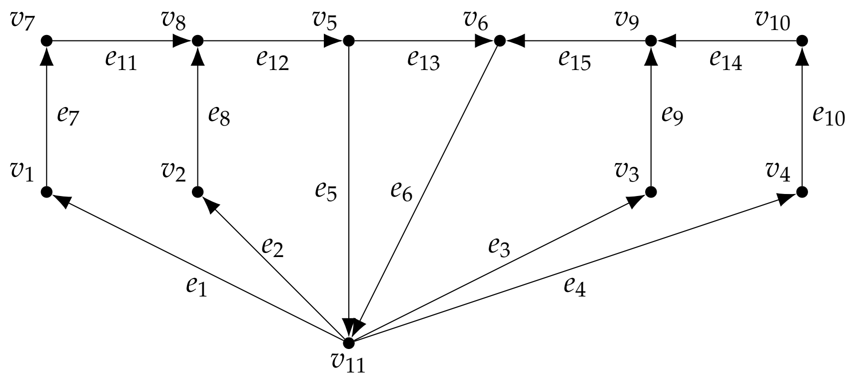

Figure 6.2: Directed graph of the Two Area Network from Kundur in Figure 6.1.

Each vertex represents a voltage in the network, with v_{11} representing the common ground. Each edge represents a component. The edges are organized in such a way that the first 4 correspond to the inverters, 5 and 6 correspond to the loads, 7 through 10 correspond to the transformers, and the rest are transmission lines. The direction of the edges are chosen in the direction of the expected power flow. The incidence matrix of the graph shown in Figure 6.2 is constructed by looking at the direction of the edges leaving and arriving at each vertex. An edge leaving a vertex places a +1 in the incidence matrix, while an edge arriving places a -1:

$$A = \begin{bmatrix} -1 & 0 & 0 & 0 & 0 & 0 & 1 & 0 & 0 & 0 & 0 & 0 & 0 & 0 & 0 \\ 0 & -1 & 0 & 0 & 0 & 0 & 0 & 1 & 0 & 0 & 0 & 0 & 0 & 0 & 0 \\ 0 & 0 & -1 & 0 & 0 & 0 & 0 & 0 & 1 & 0 & 0 & 0 & 0 & 0 & 0 \\ 0 & 0 & 0 & -1 & 0 & 0 & 0 & 0 & 0 & 1 & 0 & 0 & 0 & 0 & 0 \\ 0 & 0 & 0 & 0 & 1 & 0 & 0 & 0 & 0 & 0 & 0 & -1 & 1 & 0 & 0 \\ 0 & 0 & 0 & 0 & 0 & 1 & 0 & 0 & 0 & 0 & 0 & 0 & -1 & -1 & 0 \\ 0 & 0 & 0 & 0 & 0 & 0 & -1 & 0 & 0 & 0 & 1 & 0 & 0 & 0 & 0 \\ 0 & 0 & 0 & 0 & 0 & 0 & 0 & -1 & 0 & 0 & -1 & 1 & 0 & 0 & 0 \\ 0 & 0 & 0 & 0 & 0 & 0 & 0 & 0 & -1 & 0 & 0 & 0 & 0 & 1 & -1 \\ 0 & 0 & 0 & 0 & 0 & 0 & 0 & 0 & 0 & -1 & 0 & 0 & 0 & 0 & 1 \\ 1 & 1 & 1 & 1 & -1 & -1 & 0 & 0 & 0 & 0 & 0 & 0 & 0 & 0 & 0 \end{bmatrix} \tag{6.1}$$

The columns of A represent the edges and are ordered the same way as the edges in the graph, meaning that the first 6 columns correspond to the inverters and loads. In order to obtain the reduced incidence matrix $\overline{A}$, the last row of A is removed. To calculate the cycle matrix B, the reduced incidence matrix needs to be partitioned into two parts: One containing a set of chords, and one containing the remaining spanning tree. Cutting all but one connection from the inverters and loads to ground (v_{11}) creates a spanning tree. The set of the first 5 columns in A are therefore a valid choice of chords. Denote the chord partition $\overline{A}_C$ and the tree partition $\overline{A}_T$, then $\overline{A} = \begin{bmatrix} \overline{A}_C & \overline{A}_T \end{bmatrix}$, where $\overline{A}_C$ is the first 5 columns of $\overline{A}$ and $\overline{A}_T$ are the remaining columns. The cycle matrix B is then given as [23]:

$$B = \begin{bmatrix} I & -\overline{A}_C(\overline{A}_T^T)^{-1} \end{bmatrix} = \begin{bmatrix} 1 & 0 & 0 & 0 & 0 & 1 & 1 & 0 & 0 & 0 & 1 & 1 & 1 & 0 & 0 \\ 0 & 1 & 0 & 0 & 0 & 1 & 0 & 1 & 0 & 0 & 0 & 1 & 1 & 0 & 0 \\ 0 & 0 & 1 & 0 & 0 & 1 & 0 & 0 & 1 & 0 & 0 & 0 & 0 & 1 & 0 \\ 0 & 0 & 0 & 1 & 0 & 1 & 0 & 0 & 0 & 1 & 0 & 0 & 0 & 1 & 1 \\ 0 & 0 & 0 & 0 & 1 & -1 & 0 & 0 & 0 & 0 & 0 & 0 & -1 & 0 & 0 \end{bmatrix} \tag{6.2}$$

With the cycle matrix established, the next step is to calculate the edge currents. To do this, the edge current and voltage vectors are ordered in such a way that the edges corresponding to controlled voltage sources are placed first:

$$i = \begin{bmatrix} i_v \\ i_R \end{bmatrix} \qquad \Delta v = \begin{bmatrix} \Delta v_v \\ \Delta v_R \end{bmatrix} \tag{6.3}$$

Furthermore, the cycle matrix is re-ordered the same way:

$$B = \begin{bmatrix} B_v & B_R \end{bmatrix} \tag{6.4}$$

The cycle currents i_C are then given as [23]:

$$i_C = -(B_R Z B_R^T)^{-1} B_v \Delta v_v \tag{6.5}$$

where:

Z is a diagonal matrix containing the impedances of non voltage controlled source edges in the correct order.

The controlled voltage source edges Δv_v depend on the inverter voltage phasors $\overline{V}$, which are states of the ODE simulation, and the reduced incidence matrix, which indicates the sign of the voltage drop across these edges:

$$\Delta v_v = \overline{A}_v' \overline{V} \tag{6.6}$$

where:

$\overline{A}_v'$ is a square matrix containing the voltage source edges and corresponding vertices of the reduced incidence matrix.

Finally, the edge currents i are given from the cycle currents as follows [23]:

$$i = B^T i_C = -B^T (B_R Z B_R^T)^{-1} B_v \overline{A}_v' \overline{V} \tag{6.7}$$

With all edge currents known, the non voltage source edge voltages can be obtained from the cycle currents using Ohm's law [23]:

$$\Delta v_R = Z i_R = Z B_R^T i_C \tag{6.8}$$

With the network solved, the rest of the simulation is an ODE similar to the one set up in previous simulations. As mention before, the inverter voltage phasors are states in the ODE. More specifically, the voltage magnitudes V_i and phase angles ϕ_i are states in addition to the inverter frequencies ω_i. The complex power of each inverter S_i is calculated from the inverter voltage phasor and the calculated edge current pertaining to the inverter $i_{v,i}$:

$$S_i = P_i + jQ_i = \frac{3}{2}(V_i e^{j\phi_i})(i_{v,i})^* \tag{6.9}$$

The frequency, voltage magnitude, and phase dynamics are the same as in earlier chapters:

$$\frac{d}{dt}\begin{bmatrix} \omega_i \\ V_i \\ \phi_i' \end{bmatrix} = \begin{bmatrix} \frac{K_{P,i}}{\tau_{P,i}}(P_{0,i} - P_i) - \frac{\omega_i - \omega_{0,i}}{\tau_{P,i}} \\ \frac{K_{Q,i}}{\tau_{Q,i}}(Q_{0,i} - Q_i) - \frac{V_i - V_{0,i}}{\tau_{Q,i}} \\ \omega_i \end{bmatrix} \tag{6.10a}$$

$$\phi_i = \phi_i' + K_{ff,i}(\omega_i - \omega_{0,i}) \tag{6.10b}$$

These dynamics are implemented for all four inverters. The only thing missing now are network and controller parameters. The network parameters are the impedances of all the non voltage source edges and the controller parameters are the droop gains and time constants as well as frequency, voltage magnitude, and power set points.

6.2 Model parameters

In order to select values such that impedances of the transmission lines and the loads are sensible given the simulation voltages, the Two Area Network example from Kundur *et al.* [2, page 813] is used as a baseline. These values are then scaled such that the nominal value of voltages of all inverters and loads are 1 unit. In the example the base power for the transformers are 900 MVA and for the simulation all powers are scaled down by this amount, meaning all currents and impedances are scaled. The base unit of the currents and impedances are:

$$I_{base} = \frac{S_{base}}{V_{base}} \qquad \text{and} \qquad Z_{base} = \frac{V_{base}}{I_{base}} \tag{6.11}$$

Load 1 is supposed to draw $(967 - j100)$ MVA given with a nominal voltage of 230 kV line to line rms. Recall that the per phase complex power in terms of voltage and impedance is given as:

$$S = V_{rms} I_{rms}^* = V_{rms} \left(\frac{V_{rms}}{Z} \right)^* = \frac{V_{rms}^2}{Z^*} \tag{6.12}$$

Thus the per phase impedance of L1 is the following:

$$\begin{aligned} Z_{L1,pu} &= \frac{Z_{L1}}{Z_{base}} = \frac{1}{Z_{base}} \frac{V_{L1}^2}{S_{L1}^*} = \frac{I_{base}}{V_{base}} \frac{V_{L1}^2}{S_{L1}^*} = \frac{S_{base}}{V_{base}^2} \frac{V_{L1}^2}{S_{L1}^*} \\ &= \frac{900\,\text{MVA}}{(230\,\text{kV})^2} \frac{(230\,\text{kV})^2}{(967 + j100)\,\text{MVA}} = (0.92 - j0.095)\,\text{pu} \end{aligned} \tag{6.13}$$

The unit impedances are found for every other device in the same manner and shown in Table 6.1.

Table 6.1: Network parameters for simulation

Device	unit impedance
L1	$0.92 - j0.095$
L2	$0.5 - j0.043$
T1	$j0.15$
T2	$j0.15$
T3	$j0.15$
T4	$j0.15$
Line 1	$0.023 + j0.23$
Line 2	$0.009 + j0.09$
Line 3	$0.2 + j2$
Line 4	$0.009 + j0.09$
Line 5	$0.023 + j0.23$

Next, the controller parameters and set points need to be chosen. Typically, the droop gain is chosen such that a 5 % change in frequency or voltage corresponds to a 100 % change in P and Q respectively [2]. This means that the droop gains should be $K_P = K_Q = 0.05$ for all inverters. Because the $P - \omega$ droop equation in Equation (6.10a) is not in per unit, the frequency droop gain needs to be scaled to $K_P = 2\pi 50 \cdot 0.05 \approx 15.7$. Because the time varying phasor modeling relies on the dynamics of electrical components being much faster than the dynamics of the inverter, the time constants of the droop control need to be sufficiently slow. The network in Figure 6.1 consists of some series connected impedances and resistances. The time constant of an R-L circuit is $\tau = \frac{L}{R}$, where L is the inductance and R is the resistance of the equivalent circuit. The loop in Figure 6.1 with the highest inductance to resistance ratio is from inverter 1 through load 2 passing through lines 1 to 3. The corresponding impedances can be found in Table 6.1. This loop has an equivalent impedance in per unit of:

$$\begin{aligned} Z_\tau &= Z_{\text{T1}} + Z_{\text{Line1}} + Z_{\text{Line2}} + Z_{\text{Line3}} + Z_{\text{L2}} \\ &= j0.15 + 0.023 + j0.23 + 0.009 + j0.09 + 0.2 + j2 + 0.5 - j0.043 \\ &= 0.7320 + j2.4270\,\text{pu} \end{aligned} \tag{6.14}$$

Note that the impedance still has a unit similar to Ω, but with the base unit of Z_{base} instead of $1\,\Omega$. The equivalent inductance is found by dividing the reactance by the nominal frequency $\omega_0 = 2\pi 50\,\frac{\text{rad}}{\text{s}}$:

$$L_\tau = \frac{Im[Z_\tau]}{\omega_0} = \frac{2.4270\,\text{pu}}{2\pi 50\,\frac{\text{rad}}{\text{s}}} = 0.0077\,\frac{\text{pu}\cdot\text{s}}{\text{rad}} \tag{6.15}$$

The approximate time constant of the network is thus:

$$\tau = \frac{L_\tau}{R_\tau} = \frac{0.0077\,\frac{\text{pu}\cdot\text{s}}{\text{rad}}}{0.7320\,\text{pu}} \approx 0.01\,\frac{\text{s}}{\text{rad}} \tag{6.16}$$

Multiplying τ with $2\pi\,\text{rad}$ gives the approximate rise time of any step dynamics:

$$T = 2\pi\,\text{rad} \cdot \tau \approx 0.0628\,\text{s} \tag{6.17}$$

Hence, the time constants τ_P and τ_Q have to be at least 10 times bigger than $\tau \approx 0.0628\,\text{s}$ to ensure that the network is decoupled from the outer power control. They are chosen to be both $\tau_P = \tau_Q = 0.7$. The feed forward damper gain K_{ff} is chosen to be slightly larger than τ_P at $K_{ff} = 0.75$.

The droop controller set points generally need to be set according to the loads on the network. The target frequency ω_0 is almost always going to be the rated frequency $\omega_0 = 2\pi 50\,\frac{\text{rad}}{\text{s}}$. The active and reactive power set points P_0 and Q_0 depend on what the expected power requirements of the loads are. In this example, it was determined by simulating a steady state, that when all inverters share power, the active power set points should all be $P_0 = 0.8\,\text{pu}$, while the reactive power set points should be $Q_{0,1} = Q_{0,4} = 0.23\,\text{pu}$ and $Q_{0,2} = Q_{0,3} = 0.43\,\text{pu}$. Lastly, the voltage set point V_0 is used to control the voltage at the loads. In order to set the voltage at the loads accurately, another outer control loop would be needed. Instead, an appropriate voltage set point of $V_0 = 1.045\,\text{pu}$, which gives voltages across the loads which are approximately 1 pu.

The simulation is implemented with `ode15s()` in Matlab and run for 10 seconds with a relative tolerance of 10^{-5}. The states for all 4 inverters during this simulation are shown in Figure 6.3.

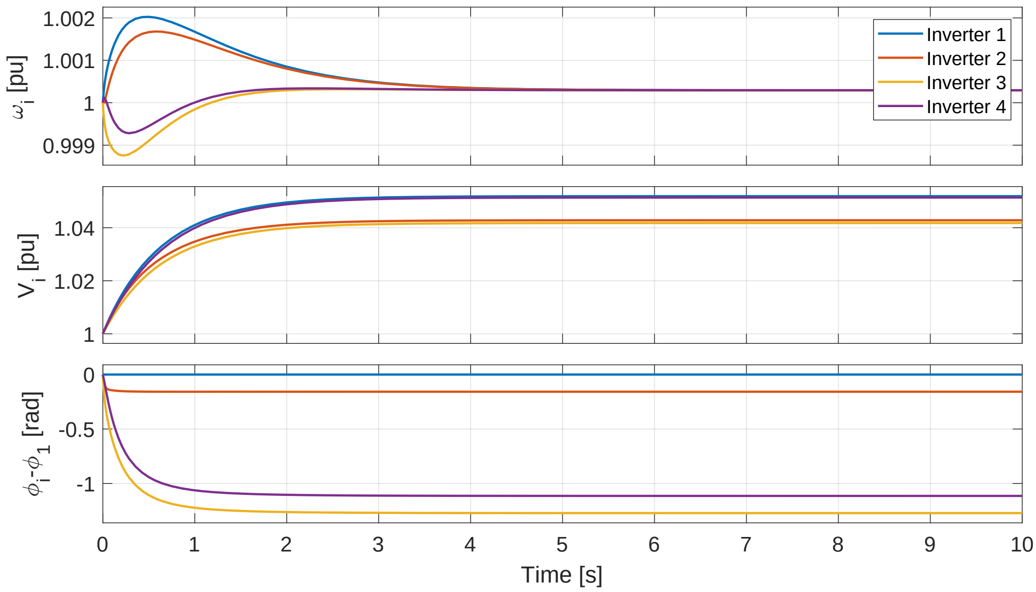

Figure 6.3: Inverter states from simulation of the system in Figure 6.1. The states from top to bottom are: Frequency ω_i, Voltage magnitude V_i, and voltage phase angle differences $\phi_i - \phi_1$.

Because of the choices of set points in the controller the steady state values for the frequencies are close to 1 pu. The power sharing seems to work as intended, since the frequencies are a bit higher, indicating that the load is smaller than the set point. The voltage amplitudes are split into two groups according to the reactive power set points, which is expected, since the two loads are different. Furthermore, they appear to be close to the set point value of 1.045 pu. The phase angles are shown relative to the phase angle of inverter 1. This is done to show how the angles are behaving relative to each other. The absolute phase angles increase at almost the same rates, making it difficult to identify the phase angle differences.

To verify that the power sharing is working as intended, the active and reactive power injected by the inverters is plotted. These can be seen in Figure 6.4.

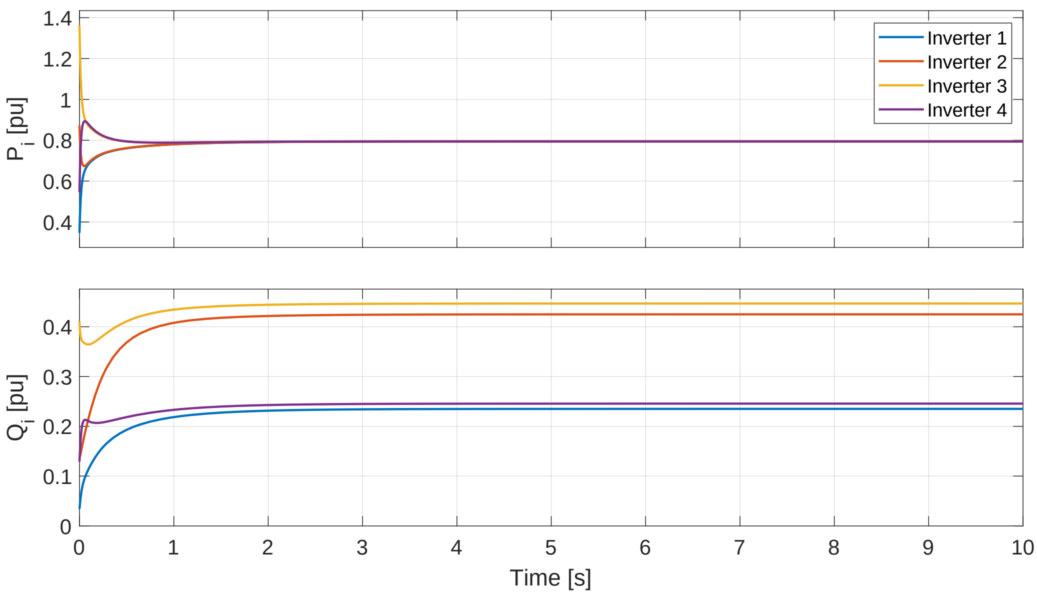

Figure 6.4: Active and reactive power injected into the grid from the inverters. The powers are given as a fraction of their rated output.

As can be seen from Figure 6.4, the active power is shared equally between all inverters. This is expected since the active power droop gains and set points for all inverters are equal as well. The reactive powers are also somewhat following their set points. It is important to note, that the inverters do not arrive at their power set points by themselves, because they have to supply whatever power is drawn by the loads. There is no control loop that ensures frequency reference tracking. Instead, the droop gains and power set points control how much each inverter contributes to the required power draw. However, if the power set points are chosen wisely, the steady state is very close to the set points, which produces only a small deviation from the rated frequency and voltage.

With the network simulation functioning as expected and the control parameters chosen, it is investigated how the network in steady state compares to the previous analysis. Also, it is of interest to push the simulation into areas where the system becomes unstable to investigate what might cause instability.

6.3 Network behavior

In order to investigate how the behavior of the two area system compares to that of the passivity analysis in Section 5.3 the linearized relation from the simulation between power and inverter voltage is calculated in a steady state of the simulation of the previous section, and shown in Equation (6.18).

$$
\begin{aligned}
K &= \left[\begin{array}{c|c} K_{11} & K_{12} \\ \hline K_{21} & K_{22} \end{array}\right] = \left[\begin{array}{c|c} \frac{\partial P}{\partial \phi} & \frac{\partial P}{\partial V} \\ \hline \frac{\partial Q}{\partial \phi} & \frac{\partial Q}{\partial V} \end{array}\right] \\
&= \left[\begin{array}{cc|cc|cc|cc}
2.0818 & -2.0904 & 0.0121 & -0.0034 & 0.8989 & 0.43 & 0.0863 & 0.0341 \\
-2.1328 & 2.1431 & 0.0073 & -0.0177 & -0.1834 & 1.3384 & 0.2188 & 0.0848 \\
\hline
-0.0629 & -0.1931 & 2.3337 & -2.0777 & -0.0644 & -0.1283 & 1.686 & -0.0334 \\
-0.0276 & -0.0818 & -1.9865 & 2.0959 & -0.0233 & -0.0439 & 0.5605 & 0.957 \\
\hline
0.6001 & -0.4686 & -0.094 & -0.0375 & 2.3214 & -1.9183 & 0.0111 & -0.0031 \\
0.2017 & 0.1297 & -0.2382 & -0.0931 & -1.9402 & 2.7464 & 0.0067 & -0.0161 \\
\hline
0.0708 & 0.1398 & -0.2473 & 0.0367 & -0.0572 & -0.1772 & 2.9642 & -1.891 \\
0.0256 & 0.0479 & -0.6102 & 0.5367 & -0.0251 & -0.0751 & -1.8247 & 2.3546
\end{array}\right]
\end{aligned}
\tag{6.18}
$$

In this example there exist two weakly coupled areas separated by the dashed lines in the in the Jacobian K in Equation (6.18). It shows a strong coupling between the inverters in each area but a weak coupling between the areas. This is seen by investigating each row of K and observing which angles influence the power in each inverter. Looking at the first row, the power in inverter 1 is highly dependent on the angle in inverter 1 and 2 but has little influence from 3 and 4. It is also seen that the coupling from voltage to active power is not close to zero in this case. In general it is seen that the assumptions made in Section 5.3 are far from the situation in this example network. The angle differences between the two areas are quite large because of the weak coupling. Also, the resistive loads make the active power transfer voltage dependent. However, the network is stable and behaves nicely with the power control parameters based only on rules of thumb and the findings of the passivity analysis of a simplified network. This result could be a coincidence, but it suggest that there might exist a set of broad conditions for a given network for which the power control of grid forming inverters is guaranteed to be stable, requiring only simple rules for the power control parameters.

The analysis in Section 5.3 suggested that a high capacitance in the network could destabilize the system. Therefore, the load's shunt capacitances are increased until the system becomes unstable. Increasing the capacitance to 4 times the normal value yields the results shown in Figure 6.5 and Figure 6.6. However, the mechanism of the instability is due to the non-linearity of the system.

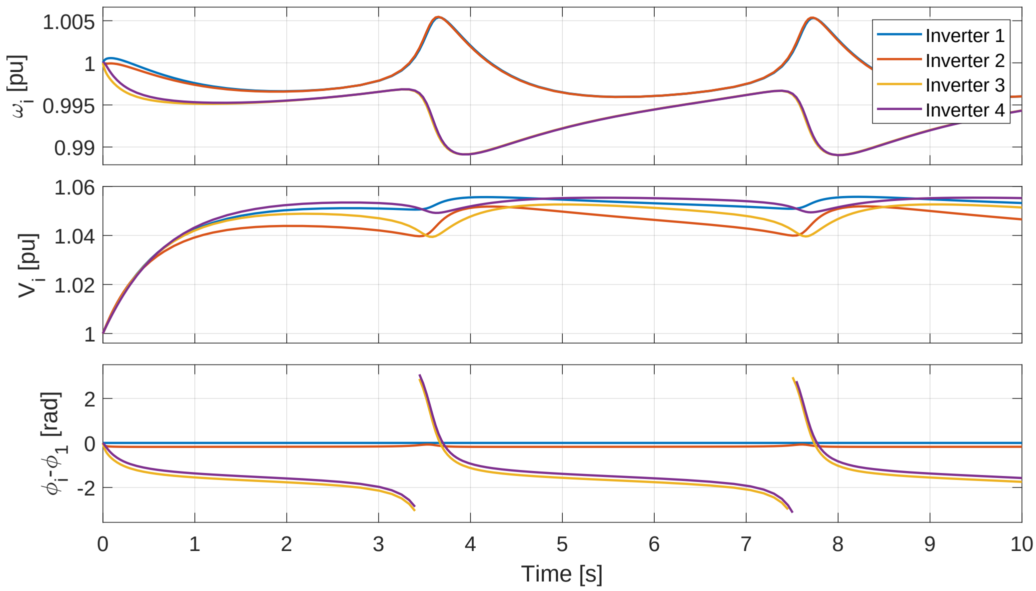

Figure 6.5: Inverter states of the two area Kundur simulation with 4 times increased capacitance.

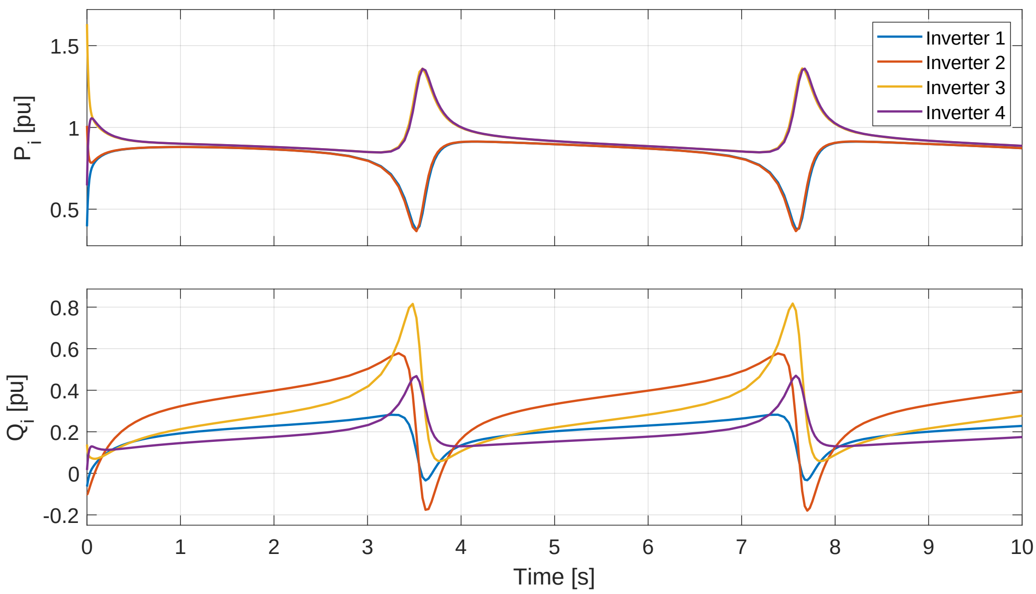

Figure 6.6: Inverter power of the two area Kundur simulation with 4 times increased capacitance.

From Figure 6.6 and Figure 6.5 it is seen that there are power oscillations between the two areas. The problem is the droop control set points. The system attempts to transfer more active power between the areas than is possible with the voltages in the system and the droop control never manages to find an equilibrium. However, changing the set points such that inverter 3 and 4 attempt to deliver more power and 1 and 2 less, makes the system stable again. Figure 6.7 and Figure 6.8 show how the change in set points influences the inverters.

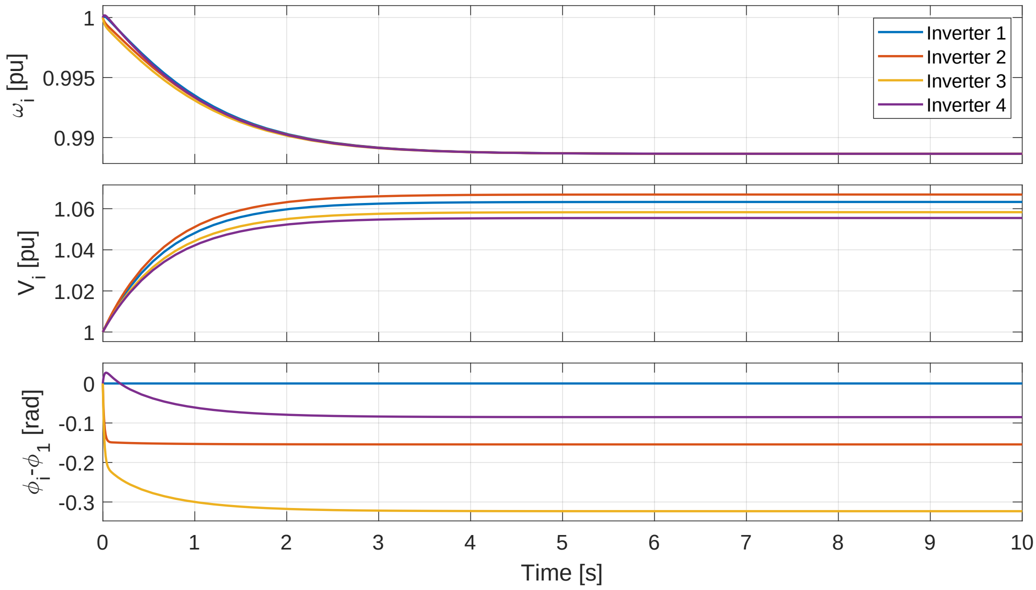

Figure 6.7: Inverter states of the two area Kundur simulation with 4 times increased capacitance and the following active power set points $P_0 = \begin{bmatrix} 0.6 & 0.6 & 1 & 1 \end{bmatrix}$.

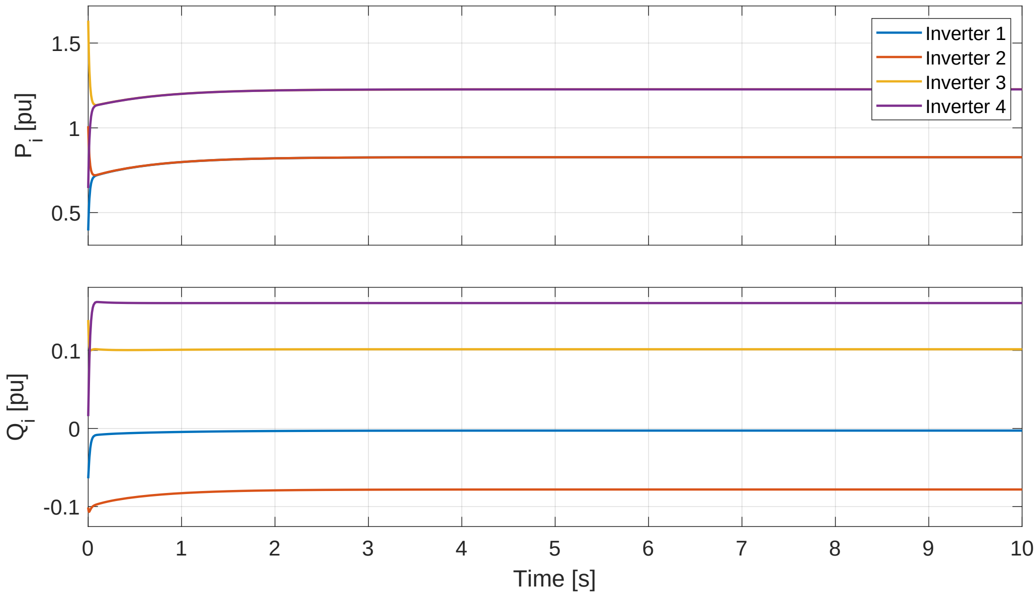

Figure 6.8: Inverter power of the two area Kundur simulation with 4 times increased capacitance and the following active power set points $P_0 = \begin{bmatrix} 0.6 & 0.6 & 1 & 1 \end{bmatrix}$.

This is a non-linear behavior that is not captured in any of the linearized models. This result highlights that it is important that the set points are reasonable given the network, especially when some areas of the network are weakly coupled. Given that it was possible to reach a steady state, it is interesting to see if the eigenvalues of K_{22} are reduced as is expected with an increase in capacitive load. The linearized network matrix is shown for this network in the steady state:

$$K_{HC} = \left[\begin{array}{cc:cc|cc:cc} 2.3425 & -2.2261 & -0.0778 & -0.0386 & 0.9314 & 0.4635 & 0.0731 & 0.0194 \\ -2.2779 & 2.5975 & -0.2166 & -0.1029 & -0.1653 & 1.4405 & 0.1687 & 0.0408 \\ \hdashline -0.1108 & -0.2662 & 2.5789 & -2.2018 & 0.0159 & 0.0934 & 2.2518 & -0.1435 \\ -0.0416 & -0.0957 & -2.0293 & 2.1667 & 0.0131 & 0.0527 & 0.7856 & 1.3706 \\ \hline 0.619 & -0.5167 & -0.0809 & -0.0214 & 2.1033 & -1.9967 & -0.0704 & -0.035 \\ 0.1837 & 0.0479 & -0.1865 & -0.045 & -2.0501 & 2.1897 & -0.1958 & -0.0933 \\ \hdashline -0.0177 & -0.1041 & -0.0365 & 0.1583 & -0.0998 & -0.2388 & 2.5152 & -1.9962 \\ -0.0145 & -0.0588 & -0.8689 & 0.9422 & -0.0375 & -0.0859 & -1.8349 & 2.2554 \end{array}\right] \tag{6.19}$$

The eigenvalues of the lower right quadrant of K_{HC} are compared to the eigenvalues of the same quadrant of K:

$$\operatorname{eig}\left(\frac{1}{2}(K_{HC,22} + K_{HC,22}^T)\right) = \begin{bmatrix}0.0208 & 0.5626 & 4.1598 & 4.3204\end{bmatrix} \tag{6.20a}$$

$$\operatorname{eig}\left(\frac{1}{2}(K_{22} + K_{22}^T)\right) = \begin{bmatrix}0.5633 & 0.8055 & 4.4696 & 4.5482\end{bmatrix} \tag{6.20b}$$

As it is seen from Equations (6.20) the eigenvalues are indeed reduced, but not to the point of becoming negative. In an attempt to make a more general passivity based stability criterion that includes this network, the output strict passivity of the $Q - V$ droop is used.

Consider a block diagonal system of a passive and an output strictly passive system, $G_1(s) = \frac{y_1(s)}{-u_1(s)}$ and $G_2(s) = \frac{y_2(s)}{-u_2(s)}$ respectively, connected in negative feedback by the matrix K such that:

$$\begin{bmatrix}u_1 \\ u_2\end{bmatrix} = K \begin{bmatrix}y_1 \\ y_2\end{bmatrix} = \begin{bmatrix}K_{11} & K_{12} \\ K_{21} & K_{22}\end{bmatrix} \begin{bmatrix}y_1 \\ y_2\end{bmatrix} \tag{6.21}$$

Note that G_1 and G_2 have $-u_1$ and $-u_2$ as inputs, such that the negative feedback is defined algebraically. Because G_1 is passive and G_2 is output strictly passive, there exist storage functions V_1 and V_2 for each block. The sum of the time derivatives of these storage functions is then:

$$\dot{V}_1 + \dot{V}_2 \leq -y_1^T u_1 - y_2^T u_2 - y_2^T \psi y_2 \tag{6.22}$$

where:

ψ is a positive definite matrix

Inserting Equation (6.21) into the previous equation yields the following:

$$\dot{V}_1 + \dot{V}_2 \leq -y_1^T \begin{bmatrix}K_{11} & K_{12}\end{bmatrix} \begin{bmatrix}y_1 \\ y_2\end{bmatrix} - y_2^T \begin{bmatrix}K_{21} & K_{22}\end{bmatrix} \begin{bmatrix}y_1 \\ y_2\end{bmatrix} - y_2^T \psi y_2 \tag{6.23a}$$

$$\dot{V}_1 + \dot{V}_2 \leq -\begin{bmatrix}y_1^T & y_2^T\end{bmatrix} \begin{bmatrix}K_{11} & K_{12} \\ K_{21} & K_{22} + \psi\end{bmatrix} \begin{bmatrix}y_1 \\ y_2\end{bmatrix} \tag{6.23b}$$

Thus the system is guaranteed to be Lyapunov stable whenever:

$$\begin{bmatrix}K_{11} & K_{12} \\ K_{21} & K_{22} + \psi\end{bmatrix} \geq 0 \tag{6.24}$$

In order to find out what ψ is, the storage function of the $Q - V$ droop is investigated. Consider the dynamics of the $Q - V$ droop with $x = V$ and $u = -Q$:

$$\begin{aligned} \dot{x} &= -\frac{1}{\tau_Q}x + \frac{K_Q}{\tau_Q}u \\ y &= x \end{aligned} \tag{6.25}$$

A storage function candidate for this system could be:

$$V_Q(x) = \frac{\tau_Q}{2K_Q}x^2 \tag{6.26}$$

Using the definintion of $\dot{x}$, the time derivative of the storage function candidate becomes:

$$\dot{V}_Q(x) = \frac{\tau_Q}{K_Q}x\left(-\frac{1}{\tau_Q}x + \frac{K_Q}{\tau_Q}u\right) = -\frac{1}{K_Q}x^2 + xu \tag{6.27}$$

Because the output of the system is the state ($y = x$), the state in the previous equation can be replaced:

$$\dot{V}_Q(x) = -\frac{1}{K_Q}y^2 + yu \tag{6.28a}$$

$$yu = \dot{V}_Q(x) + \frac{1}{K_Q}y^2 \tag{6.28b}$$

It can therefore be concluded, that $\psi = \frac{1}{K_Q}I$. Adding this to K_{22} means that the quadratic form of K has the following eigenvalues:

$$\begin{aligned} &\operatorname{eig}\left(\frac{1}{2}\begin{bmatrix} K_{11} & K_{12} \\ K_{21} & K_{22} + \frac{1}{K_Q}I \end{bmatrix} + \begin{bmatrix} K_{11} & K_{12} \\ K_{21} & K_{22} + \frac{1}{K_Q}I \end{bmatrix}^T\right) = \\ &\begin{bmatrix} -0.0691 & 0.1857 & 4.1806 & 4.2259 & 20.5986 & 20.8392 & 24.5012 & 24.5791 \end{bmatrix} \end{aligned} \tag{6.29}$$

It is seen that the quadratic form is not positive semi definite and therefore the passivity of the inverters themselves are not enough to guarantee small signal stability. It is possible to make K_Q smaller, however no level of K_Q can make this particular eigenvalue zero. The eigenvalue seems to stem from the asymmetry in the phase dependency. Recall from Section 5.3 that the symmetry of the transfer function from frequency to power, and by extension from phase to power, is required to be symmetric for the diagonal dominance to show that it is positive semi definite. In this system the sum of each entry in every row of K_{11} is zero and the diagonal entries are positive. However, it is not symmetric and hence the quadratic form of K_{11} has a negative eigenvalue. Thus, it has not been shown that the passivity of the inverter control is enough to guarantee small signal stability in networks with loads and losses. It seems like designing the inverters to be passive could easily result in stable networks as it did in this case, however one has to verify the stability by different means. It is of interest to simulate how the droop controlled inverters reacts to load changes as these are common disturbances on the grid.

6.4 Load step and parameter ranges

Another interesting behavior of the system is the response to increases and decreases in load. For this purpose, the impedance of Load 1 is increased by 25 % at 5 seconds into the simulation. Also, there exist a large range of controller parameters for which the inverters are passive. First off, it was shown in Section 5.1 that the droop gain K_P must be positive for the inverter system to be passive. Choosing a negative droop gain would change the negative power feedback into a positive feedback and the system will become unstable. Increasing the droop gain has the effect, that the frequency changes more with changes in power. It is therefore of interest to keep the droop gain as small as possible. On the other hand, a small droop gain also means that the control bandwidth is drastically reduced, which affects the time it takes for the inverters in the network to share the new load. The time constant τ_P only affects the control bandwidth and thus varying the time constant only makes the control faster or slower. In reality, the dynamic phasor approximation becomes less accurate for smaller time constant, but this would not be seen in the simulation results. The one parameter of the inverter control that does have an interesting effect on the system is the feed forward gain K_{ff}. Therefore, it is also of interest to investigate different values of the feed forward damper, both inside and outside the passive range. A simulation is run for three different feed forward gains $K_{ff} = \tau_P$, $K_{ff} = 0.2\tau_P$, and $K_{ff} = 4\tau_P$. For reference, the passivity criteria required the feed forward gain to be greater or equal to the time constant. The state trajectories of these simulations are shown in Figure 6.9 and the active and reactive power as well as the power shared across the inter area transmission line are shown in Figure 6.10.

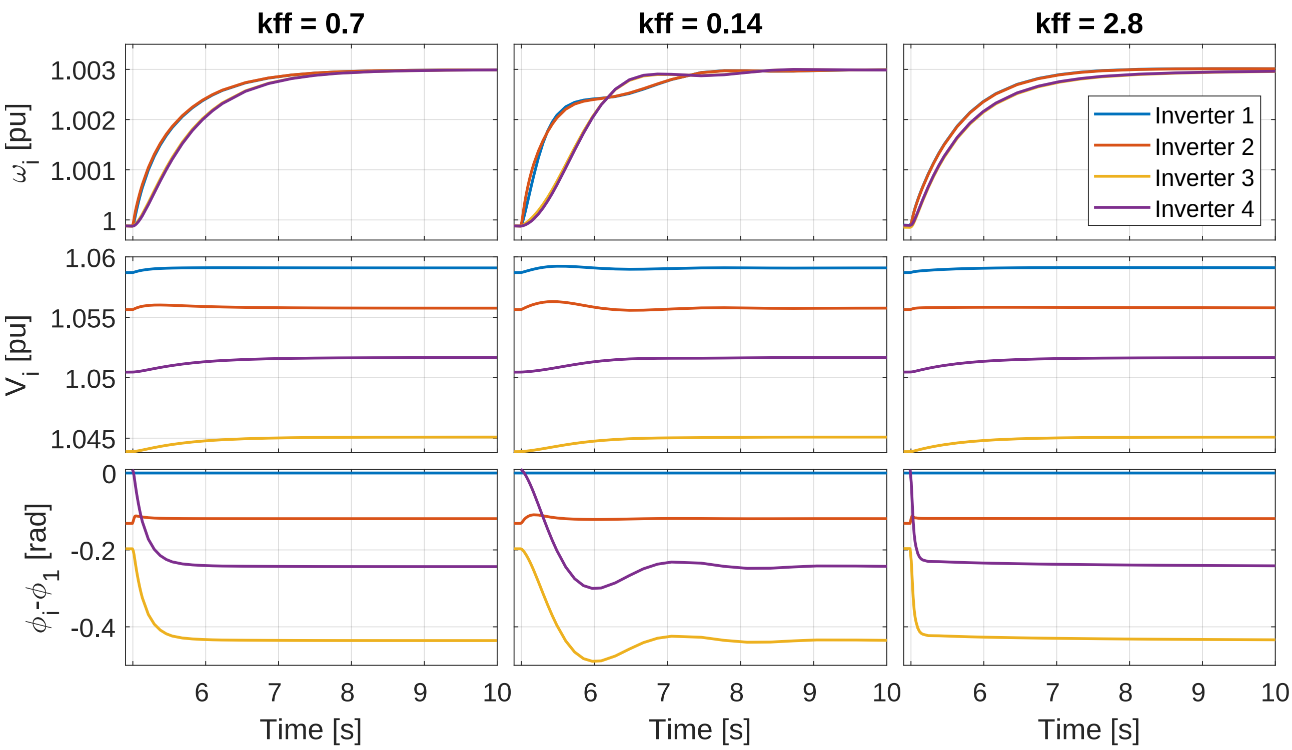

Figure 6.9: Response to a 25% increase in impedance in area 1 of droop controlled inverters with different levels of feed forward dampening.

It is seen from the figure that decreasing the dampening below the time constant results in slight oscillations, and that increasing the feed forward dampening leads to a faster response of the angles, however it takes longer for the internal frequencies to synchronize.

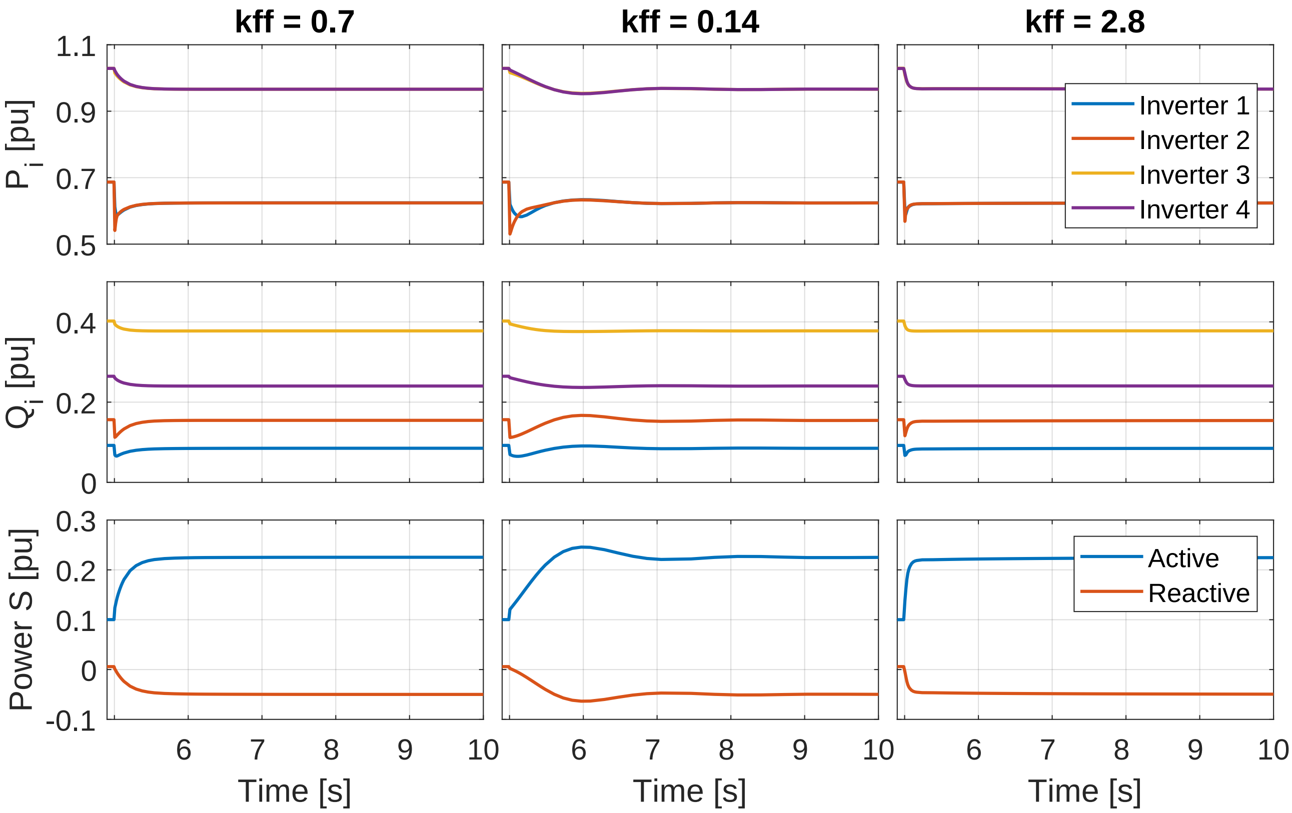

Figure 6.10: Response to 25% increase in impedance in area 1 of droop controlled inverters with different levels of feed forward dampening. The last row is the power transfer from area 1 to area 2

From Figure 6.10 it is seen that when the load of area 1 decreases the power transfer to area 2 is increased. An important thing to keep in mind is that the transmission line between the two areas can only transfer a limited amount of power. If the power transfer between the two areas saturates, the synchronization mechanism breaks down. This is because at some point, the phase angle difference becomes larger than 90° and the angle-power relationship changes sign, meaning that further increases in phase angle difference reduce the power transfer rather than increase it. It is therefore very important that the set points are set according to the carrying capacity of weak links in the network. To illustrate this the same step is performed, however the power set points are set so the power transfer to area 2 is almost saturated from the beginning. The results of these simulations are shown in Figure 6.11 and Figure 6.12.

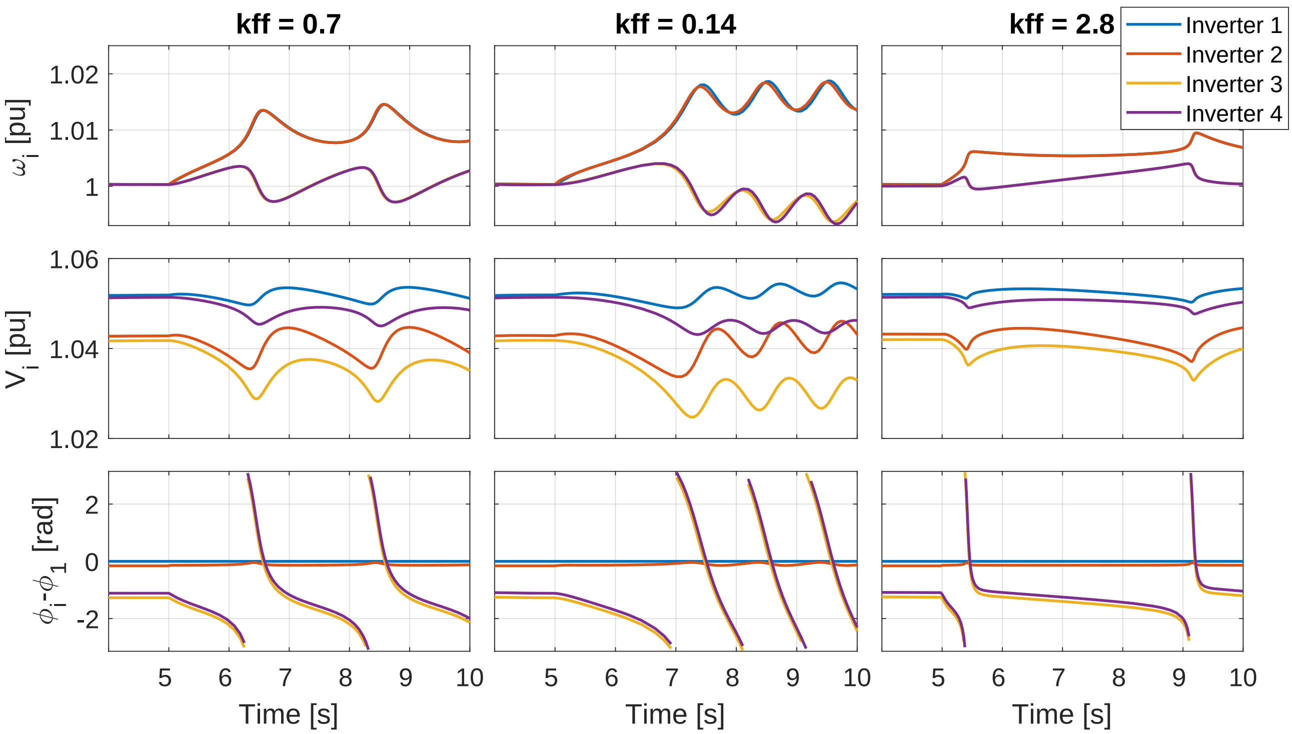

Figure 6.11: Response to 25% increase in impedance in area 1 of droop controlled inverters with different levels of feed forward dampening. The initial active power set points of the two areas are equal to enforce larger power transfer in the steady state.

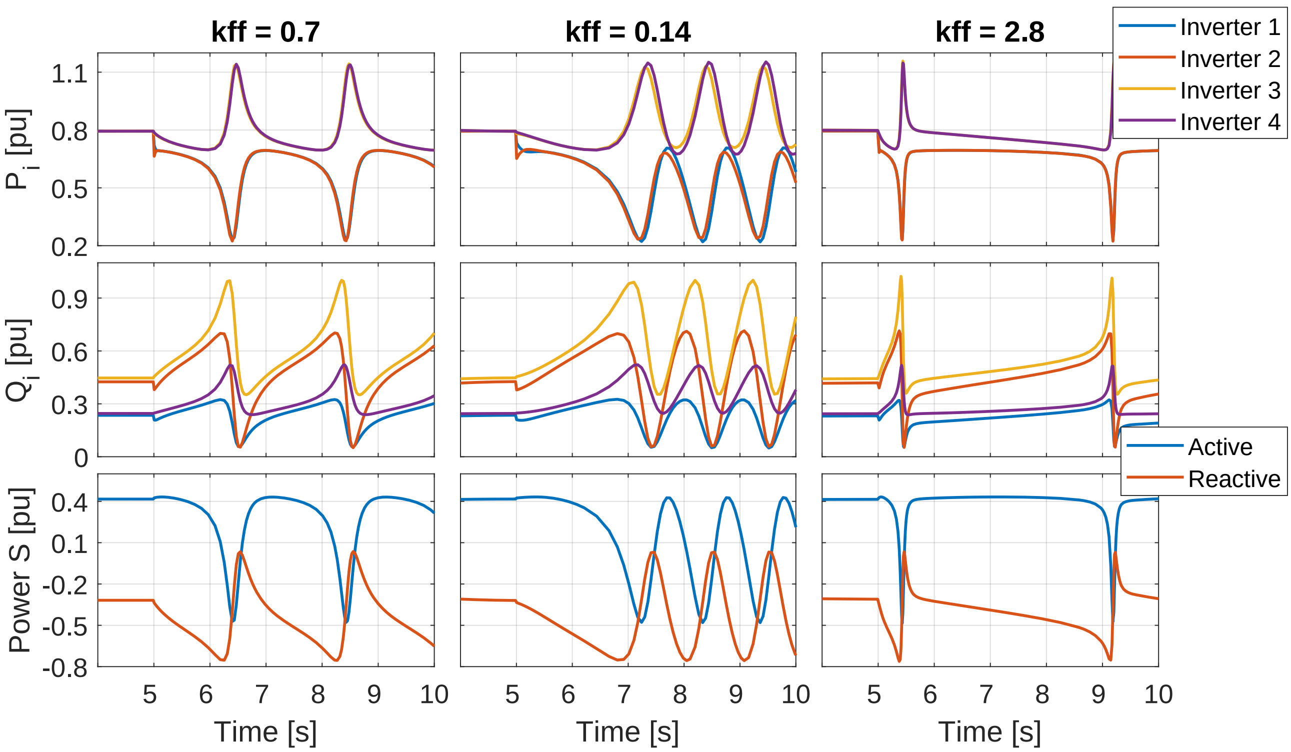

Figure 6.12: Response to 25% increase in impedance in area 1 of droop controlled inverters with different levels of feed forward dampening. The last row is the power transfer from area 1 to area 2. The initial active power set points of the two areas are equal to enforce larger power transfer in the steady state.

It is seen that when the load in area 1 is reduced, the power transfer to area 2 increases slightly. Since the power transfer through the cable is already very close to being saturated, increasing the frequency in area 1 does not result in greater power transfer, as it otherwise would and the two areas desynchronize. This means that some level of coordination between areas of droop controlled inverters is a necessity. It seems that, as long as the set points to the system are set within the carrying capacities of the cables, at least for this example network the system is capable of synchronizing. In the next section a more complex network configuration is investigated in order to show that the control works for most kinds of interconnections.

6.5 IEEE 24 Bus Network

In order to see if a different network configuration yields different results a setup with more inverters and lines is simulated. The simulation setup is based on the IEEE 24 bus reliability test system [3]. The line diagram of this system can be seen in Figure 6.13.

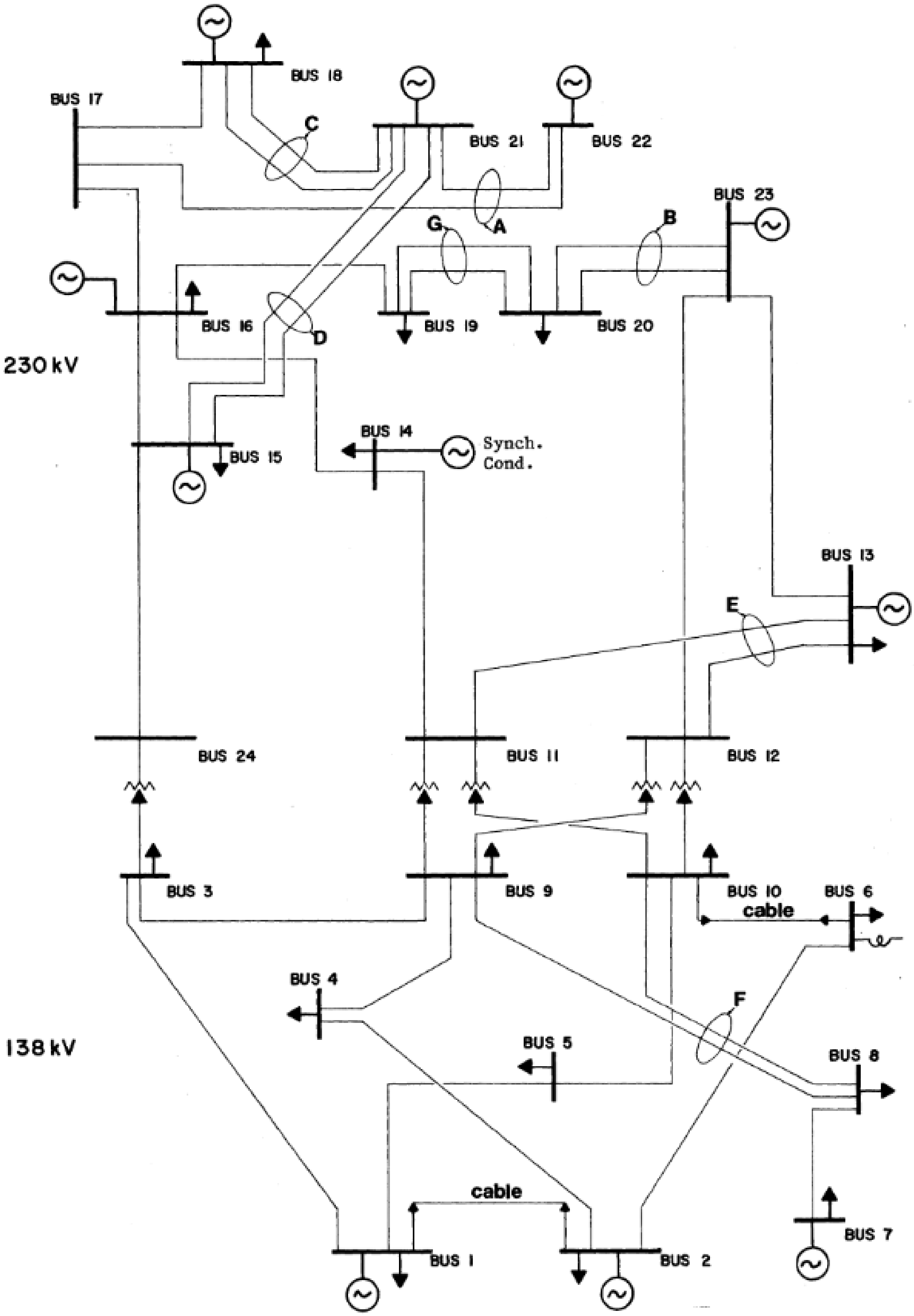

Figure 6.13: Copyright © 1979, IEEE. Line diagram of the 24 bus IEEE Reliability Test System [3].

This setup has 10 generators, that are replaced by voltage source inverters in order to investigate how droop controlled inverters interact. The power draw of the loads is given in the network specification. These are then modeled as impedances the same way as in Section 6.2. Transmission lines are modeled with their equivalent π-circuits and transformers are modeled with their equivalent impedance. The per unit values for these are found in the IEEE paper [3]. The synchronous condenser at bus 14 and the reactor at bus 6 are omitted from the simulation. With loads modeled as impedances and generation units as controlled voltage sources a graph of the network is constructed and solved with graph theory in the same manner as described previously in this chapter. The reactive power set points of all inverters are set to 0, and the active power set points and droop gains are set according to their ratings in such a way that the steady state frequency before the step is close to 1 per unit. The voltage set points are chosen such that the voltage across the loads is approximately 1 per unit as well. Some buses have multiple generating units. In that case they have been lumped into one and their power rating is accumulated. In order to perturb the network, a load step is applied at $t = 5\,\mathrm{s}$, where the impedance of half of the loads is decreased by 25 % (bus 1-9). The feed forward damping gain K_{ff} is again changed in order to observe its effects on the system. The results of this simulation is shown in Figure 6.14

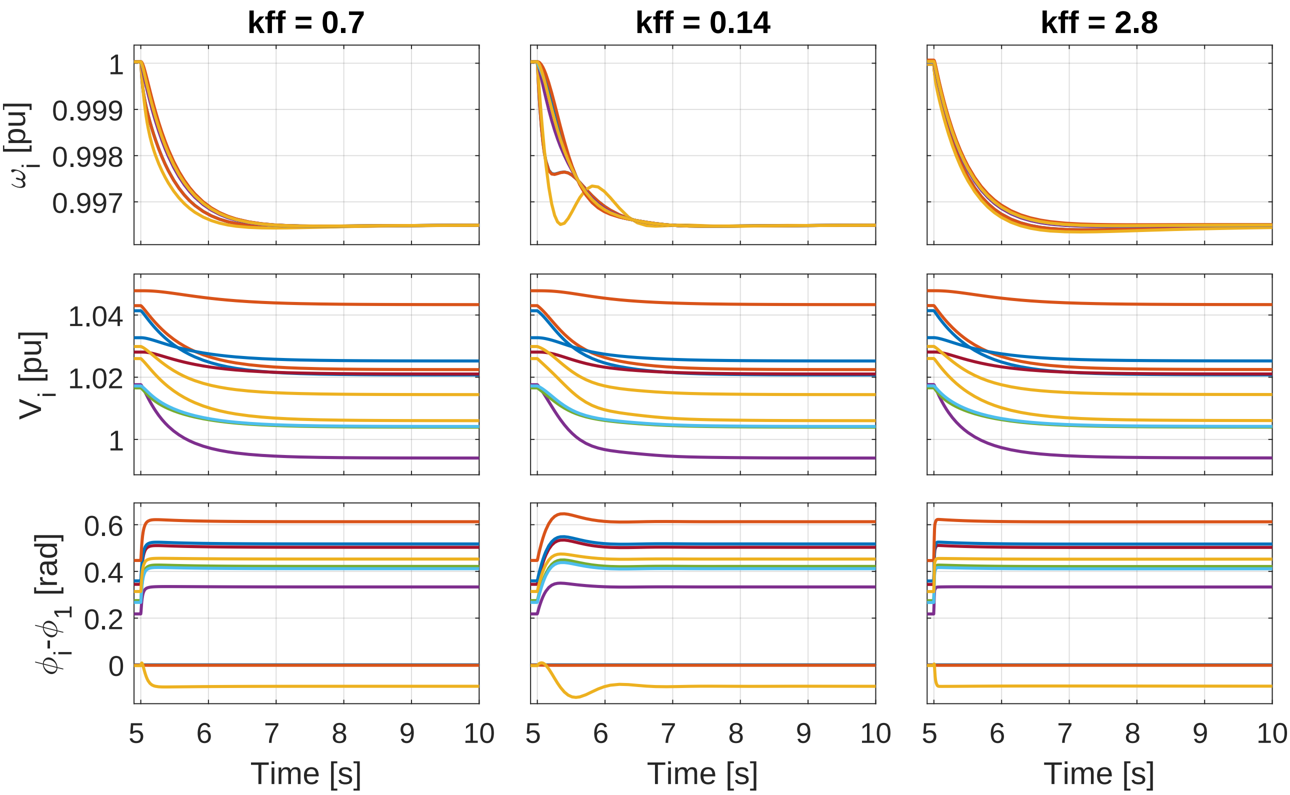

Figure 6.14: State trajectories of the 10 inverters in the IEEE Reliability Test system after a step reducing the impedance of half of the loads by 25 % for three different feed forward dampening gains.

Once again, with the feed forward dampening in the passive range the system is very well behaved. This network seems to be even less problematic than the Two Area Kundur example. It requires more perturbation to reach an unstable configuration of set points and loads because of the generally stronger connections between the inverters. It is seen that designing the inverters so that the transfer function from power to phase angle is passive yields very well behaved responses to changes in loads. This reinforces the statement that networks with a large amount of droop controlled inverters are very likely to synchronize nicely even though stability cannot be guaranteed through any of the passivity arguments investigated. However, there are still many nuances that are omitted from the analysis. Some of these are discussed further in the next chapter.

7 Discussion

Throughout the report some interesting questions have come up that are not investigated fully. This chapter discusses some things that are potentially interesting to include in some future work. The biggest problem with the passivity of the grid forming droop control is that the network transfer matrix is not positive definite without strict assumptions. A passivating feedback from the phase angle to the active power set point could be a solution to this problem. The inverters are modeled as controlled voltage sources in this report. In practice however, the current of grid forming inverters has to be limited in order to protect the hardware. The effects of this current limiting is also discussed. The capacity of the energy storage of the inverter is also discussed, as it is needed to supply the inertia that is required from them. Lastly, the effect of measurement noise on the system is discussed, in order to get a better understanding of the sensitivity of the control.

7.1 Feedback passivation with coordinated control

It was seen in Chapter 6 that the networks transfer matrix was very close to being positive definite and therefore passive. Thus, it does not require a large increase of the diagonal elements of this matrix in order to make it passive. However, this increase must come from the inverter control. It is possible in theory to reference every inverter to a global grid frequency and phase. With this reference phase, a feedback can be made from the phase angle of each inverter to their power set point compensating for negative eigenvalues in the grid. This is illustrated in figure Figure 7.1.

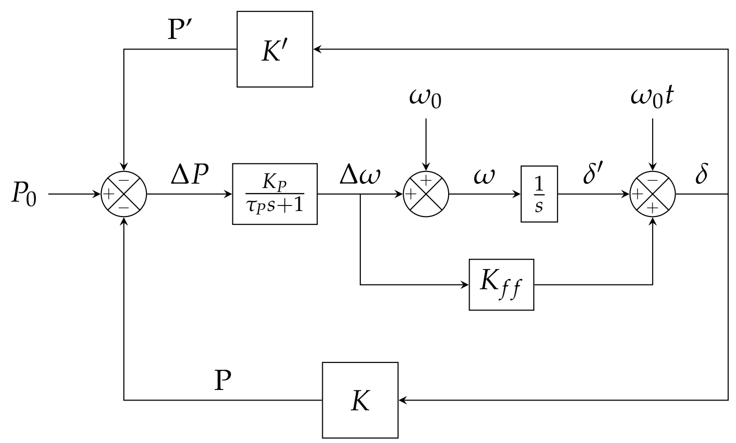

Figure 7.1: Closed loop $P - \omega$ system of a single inverter with feed forward damper and feed back passivation K'.

Notice that the feedback from inverter angle to power is equivalent to a positive feedforward over the network matrix K. This feedback has some interesting effects. It essentially counteracts power sharing across weak links as it gives the inverters an inherent reluctance to allow large angle differences. The small signal model can be passivated by increasing the gain of this feedback, depending on how negative the network is. In order to show how this works, the exact same simulation as the one shown in Figure 6.12 of the Two Area Network by Kundur is performed. However, this time with the feedback passivation gain as the tested variable and $K_{ff} = 0.7$. The state trajectories for $K' = 0$, $K' = 0.1$, and $K' = 0.2$ are shown in Figure 7.2. The active and reactive powers and the inter area power transfer is shown in Figure 7.3.

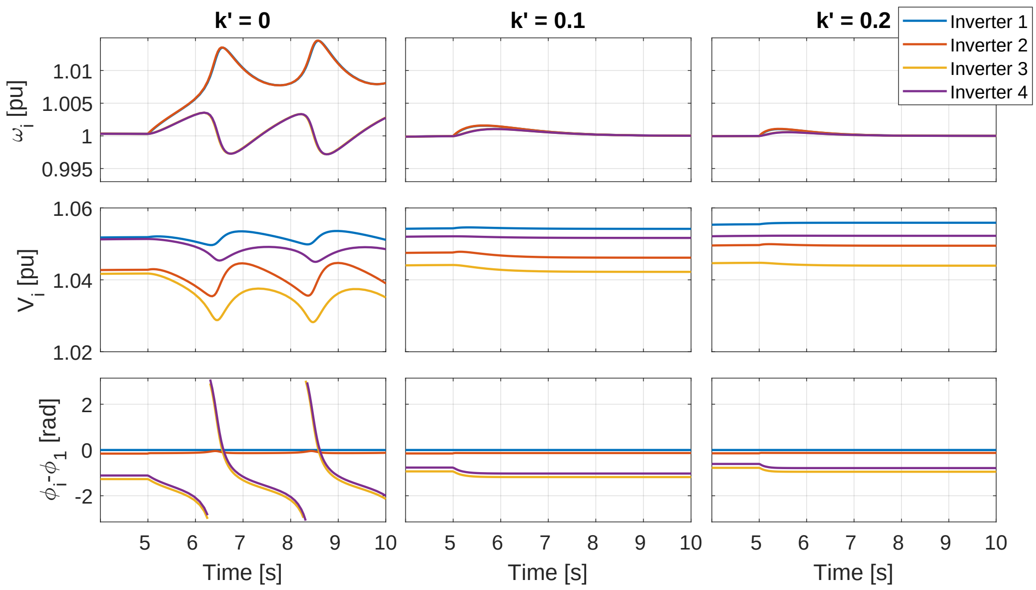

Figure 7.2: State trajectories following a 25 % increased impendace in area 1 of the Two Area Network by Kundur for three different feedback passivation gains.

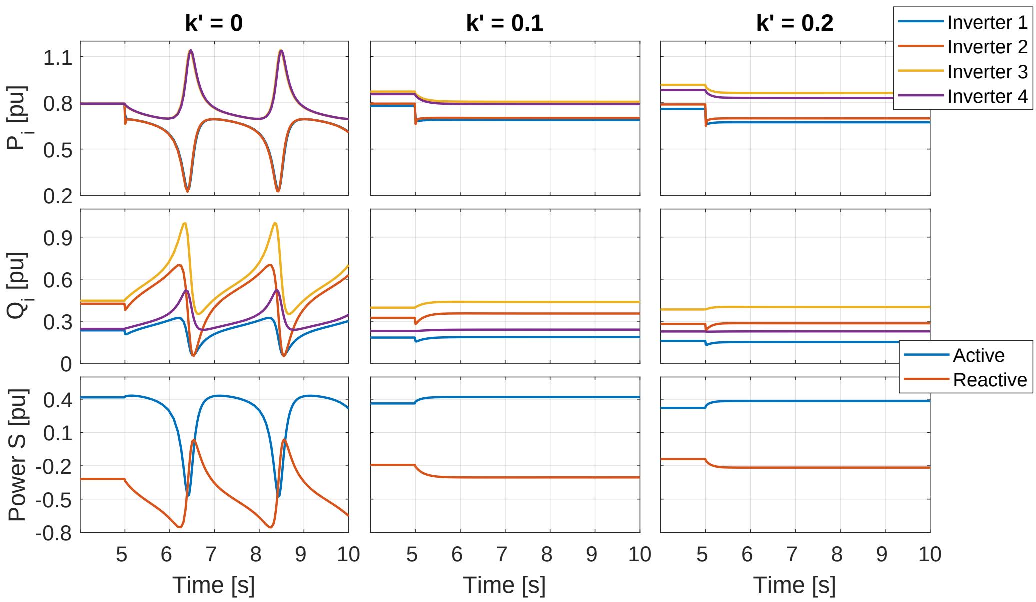

Figure 7.3: Active and reactive power as well as inter area power transfer following a 25 % increased impedance in area 1 of the Two Area Network by Kundur for three different feedback passivation gains.

It is seen that with the coordinated passivation the system is now able to stay synchronized even though the weak link is very close to saturation. Another effect of this feedback is that the steady state frequency is always precisely the agreed upon frequency. Therefore it seems that if it is possible to synchronize the inverters like this it gives a tool to increase the robustness of both small and large signal stability of the network. Unfortunately synchronizing the time at every inverter with an accuracy much smaller than a single period of the reference frequency might require an expensive solution. As it was seen in Chapter 6 the network can also be stable without this passivation granted sensibly chosen set points. In many cases it may be more sensible to analyze the stability by other means than passivity and design the network accordingly.

7.2 Current limiting

Many inverters have to protect themselves from over current, one such current limitation algorithm is the virtual impedance. This works by reducing the setpoint to the inner voltage controller according to a virtual output impedance. This virtual impedance can also be increased and reduced according to how close the inverter is to the current limit. This has the effect that the inverter does not follow exactly the setpoints of the outer controller when the current is limited [16]. Therefore, it is also important to investigate how the inner control of the inverter affects its ability to stay synchronized with the grid given large load changes and other disturbances. However, doing this requires a model that is valid in a wider bandwidth than the phasor model applied to the analysis of the outer control.

7.3 Capacity for virtual inertia

In order to provide the virtual inertia as determined by the low pass filter of the frequency droop control, it is necessary that the devices in question has the capacity to provide it. That is, they need some sort of energy storage. In windturbines some of this energy could be extracted from the rotating mass, though this may limit the turbine controls capability to efficiently track maximum wind power and in general the interaction with the turbine control should be considered [24]. In solar farms a storage solution would be necessary in order to draw the energy required to provide inertia. However, this may not be a limiting factor as the cost of utility scale energy storage is expected to decline further as battery technology and manufacturing improves [25]. Furthermore, energy storage may be necessary regardless in order to replace the demand response capability of convectional fossil fuel based generation.

7.4 Disturbances and noise

In order to assess the effects of measurement noise and disturbances on the control performance, the possible sources of disturbances and signal noise have to be identified. The most relevant disturbance in the system is the load impedances, as they are the most likely to change unpredictably during normal operation of the system. In Section 6.4 this disturbance is tested by applying a 25 % step to the load impedance. As was seen in that section, the system does not become unstable with such a disturbance, even for feed forward damper gains outside of the range that makes the droop control passive. The other concern with regards to robustness of the control is the measurement noise on the power. Since the droop controller needs to calculate the power by measuring the voltage and current there will be some measurement noise associated to the power. However, the first thing this signal encounters in the control is a low-pass filter. Therefore, it is expected that the measurement noise does not significantly affect the droop control. Another source of noise in the system is the harmonic distortion coming from the modulation algorithm generating the AC voltage in the inverter [26]. Although there are regulations for the amount of harmonic noise that is allowed to be injected into the grid [27], it is unlikely that this distortion would have much effect on the control performance even without the regulation, because of the aforementioned low-pass filter. Because of the phasor model that is used in this report, the effects of noise and harmonic distortion is difficult to determine. Most of the noise will likely not make it through the low pass filter anyway.

8 Conclusion

While passivity is a good tool for ensuring stability of large interconnected non-linear systems, it does have its limitations. A low frequency time varying phasor model is used for investigating the passivity of the primary control of droop controlled inverters. This model does not account for the inner control loops of the inverters nor the dynamics of components on the network. It is concluded that modeling the network as an admittance in rectangular coordinates like Spanias *et al.* [1] yielded issues with open loop stability of the inverter dynamics. It is also shown that modeling the network as an impedance means the required voltage-current relationship to achieve close to constant power cannot be passive.

In polar coordinates with power as input and voltage as output the behavior of the inverter can be passive. This requires the application of a feed forward damper to bypass the integrator that calculates the phase angle from the frequency. This is because the relative degree of the inverter control must be one or zero for it to be passive. With this feed forward damper in place, the inverter dynamics are passive as long as the droop gain $K_P > 0$ and the feed forward damper gain K_{ff} is greater or equal to the time constant of the low pass filter τ_P ($K_{ff} \geq \tau_P$). Making use of the circle criterion, it is shown that an interconnection of inverters can be absolutely stable as long as the network is strictly passive. This requires that the reactive power droop gain K_Q is greater than zero. However, power networks are in general not passive and cannot be strictly passive in these coordinates due to rank deficiency in the network representation. Using the invariance principle and moving the frequency integration to the network, it is possible to show stability of the network. This requires the assumptions that the network is lossless and the phase angle differences between inverters are small, suggesting that strongly coupled networks are well behaved.

Using simulation models based on the Two Area Network example by Kundur and the IEEE 24 Bus Reliability Test System, it is shown that a passivizing feed forward damper yields damped responses of the inverters to load variations. Graph theory is used to solve the electrical network that the inverters are connected through, and Matlabs ODE solver to solve the dynamics of the inverters. It is seen that weakly coupled areas can easily de-synchronize as only small changes in loads can be enough to saturate the power transfer of the connecting cable. Otherwise, the simulated networks are stable and well behaved.

While it is not possible to guarantee stability with conventional droop control using the passivity arguments investigated in this report, it is discussed that the networks investigated requires only a small passivizing feedback from the phase angles back to the power setpoints to ensure small signal stability and extend the region of large signal stability. While such a feedback is simple in theory, it would require coordination of the phase angle between the inverters needing accurate timing.

In conclusion passivity is not directly applicable as a tool to ensure stability of a grid of droop controlled inverters in any of the coordinates presented. However, stability can be guaranteed with the addition of a passivizing feedback. Even though stability in general can not be guaranteed, the control performance is improved by the addition of a feed forward damper in the active power control.

Bibliography

[1] C. Spanias and I. Lestas, "A system reference frame approach for stability analysis and control of power grids", *IEEE Transactions on Power Systems*, vol. 34, no. 2, pp. 1105–1115, 2019. DOI: 10.1109/TPWRS.2018.2872549.

[2] P. Kundur and N. Balu, *Power System Stability and Control* (EPRI power system engineering series). McGraw-Hill, 1994, ISBN: 9780780334632.

[3] P. M. Subcommittee, "IEEE Reliability Test System", *IEEE Transactions on Power Apparatus and Systems*, vol. PAS-98, no. 6, pp. 2047–2054, 1979. DOI: 10.1109/TPAS.1979.319398.

[4] "Regulation (EU) 2021/1119 of the European Parliament and the council of 30 June 2021 establishing the framework for achieving climate neutrality and amending Regulations (EC) No 401/2009 and (EU) 2018/1999 ('European Climate Law')", *OJ L243*, pp. 1–17,

[5] Eurostat, *Electricity production capacities by main fuel groups and operator*. [Online]. Available: https://ec.europa.eu/eurostat/databrowser/view/NRG_INF_EPC__custom_5139615/default/line?lang=en.

[6] R. H. Lasseter, Z. Chen, and D. Pattabiraman, "Grid-forming inverters: A critical asset for the power grid", *IEEE Journal of Emerging and Selected Topics in Power Electronics*, vol. 8, no. 2, pp. 925–935, 2020. DOI: 10.1109/JESTPE.2019.2959271.

[7] K. Daware, *Electrical power grid - structure and working*. [Online]. Available: https://www.electricaleasy.com/2016/01/electrical-power-grid-structure-working.html (visited on Mar. 1, 2023).

[8] S. Riepl, *Grobes und prinzipielles Schema der Stromversorgung in Deutschland*, Oct. 2007. [Online]. Available: https://de.wikipedia.org/wiki/Datei:Stromversorgung.png (visited on Mar. 1, 2023).

[9] F. Bianchi, H. De Battista, and R. J. Mantz, *Wind Turbine Control Systems: Principles, Modelling and Gain Scheduling Design*. Jan. 2007.

[10] "Commission Regulation (EU) 2017/1485 of 2 August 2017 establishing a guideline on electricity transmission system operation", *OJ L220*, pp. 1–120,

[11] "Commission Regulation (EU) 2016/631 of 14 April 2016 establishing a network code on requirements for grid connection of generators", *OJ L112*, pp. 1–68,

[12] D. Pattabiraman, R. H. Lasseter., and T. M. Jahns, "Comparison of grid following and grid forming control for a high inverter penetration power system", in *2018 IEEE Power & Energy Society General Meeting (PESGM)*, 2018, pp. 1–5. DOI: 10.1109/PESGM.2018.8586162.

[13] D. B. Rathnayake, M. Akrami, C. Phurailatpam, *et al.*, "Grid forming inverter modeling, control, and applications", *IEEE Access*, vol. 9, pp. 114 781–114 807, 2021. DOI: 10.1109/ACCESS.2021.3104617.

[14] H. Khalil, *Nonlinear Control* (Always Learning). Pearson Education Limited, 2014, ISBN: 9781292060507. [Online]. Available: https://books.google.dk/books?id=-WbjoAEACAAJ.

[15] M. Xia, P. J. Antsaklis, and V. Gupta, "Passivity indices and passivation of systems with application to systems with input/output delay", in *53rd IEEE Conference on Decision and Control*, IEEE, 2014, pp. 783–788, ISBN: 9781479977468.

[16] A. D. Paquette and D. M. Divan, "Virtual impedance current limiting for inverters in microgrids with synchronous generators", *IEEE Transactions on Industry Applications*, vol. 51, no. 2, pp. 1630–1638, 2015. DOI: 10.1109/TIA.2014.2345877.

[17] Y. Levron, J. Belikov, and D. Baimel, "A tutorial on dynamics and control of power systems with distributed and renewable energy sources based on the dq0 transformation", *Applied Sciences*, vol. 8, p. 1661, Sep. 2018. DOI: 10.3390/app8091661.

[18] J. D. Irwin, R. Nelms, and A. Patnaik, *Engineering Circuit Analysis*. Wiley, 2015, ISBN: 9781118960639.

[19] K. Dey and A. M. Kulkarni, *Passivity of electrical transmission networks modelled using rectangular and polar d-q variables*, 2021. arXiv: 2111.15377 [eess.SY].

[20] P. Unruh, M. Nuschke, P. Strauß, and F. Welck, "Overview on grid-forming inverter control methods", *Energies*, vol. 13, no. 10, 2020, ISSN: 1996-1073. DOI: 10.3390/en13102589. [Online]. Available: https://www.mdpi.com/1996-1073/13/10/2589.

[21] J. D. Watson and I. Lestas, "Control of interlinking converters in hybrid ac/dc grids: Network stability and scalability", *IEEE Transactions on Power Systems*, vol. 36, no. 1, pp. 769–780, 2021. DOI: 10.1109/TPWRS.2020.3032471.

[22] K. Briggs, *"diagonally dominant matrix." from mathworld–a wolfram web resource, created by eric w. weisstein*, visited: 19-04-2023. [Online]. Available: https://mathworld.wolfram.com/DiagonallyDominantMatrix.html.

[23] N. Deo, *Graph Theory with Applications to Engineering and Computer Science* (Prentice-Hall series in automatic computation). Prentice-Hall of India, 1974, ISBN: 9788120301450. [Online]. Available: https://books.google.dk/books?id=ToHHwAEACAAJ.

[24] L. Lu and N. A. Cutululis, "Virtual synchronous machine control for wind turbines: A review", *Journal of Physics: Conference Series*, vol. 1356, no. 1, p. 012 028, Oct. 2019. DOI: 10.1088/1742-6596/1356/1/012028. [Online]. Available: https://dx.doi.org/10.1088/1742-6596/1356/1/012028.

[25] NREL, *Utility-scale battery storage*, 2022. [Online]. Available: https://atb.nrel.gov/electricity/2022/utility-scale_battery_storage (visited on May 22, 2023).

[26] A. Oliva, S. Ang, J. Balda, and H. Chiacchiarini, "Harmonic distortion reduction in power inverters", in *2004 IEEE 35th Annual Power Electronics Specialists Conference (IEEE Cat. No.04CH37551)*, vol. 2, 2004, 1226–1231 Vol.2. DOI: 10.1109/PESC.2004.1355597.

[27] E. C. for Electrotechnical Standardization, *Ds/en 50160:2022, Voltage characteristics of electricity supplied by public electricity networks*. [Online]. Available: https://webshop.ds.dk/standard/M352587/ds-en-50160-2022.

Appendix

A Comparison of simulation to the linearization

In order to compare the behavior of the linearization to the non-linear simulation, two additional inputs are defined: The active and reactive power set points, P_0 and Q_0 respectively. The additions to the Jacobians are calculated. The first addition is to the B matrix in the linearization. Two more columns are added, one for the derivative of the state dynamics with respect to the active power, and one for the reactive power. Since only the frequency dynamics depend on the active power set point, and only the voltage dynamics depend on the reactive power set point, the addition to the B matrix becomes:

$$B' = \left[B \;\middle|\; \begin{bmatrix} \frac{\partial f_\omega}{\partial P_0} & \frac{\partial f_\omega}{\partial Q_0} \\ \frac{\partial f_{V_d}}{\partial P_0} & \frac{\partial f_{V_d}}{\partial Q_0} \\ \frac{\partial f_\delta}{\partial P_0} & \frac{\partial f_\delta}{\partial Q_0} \end{bmatrix} \right] = \left[B \;\middle|\; \begin{bmatrix} \frac{K_P}{\tau_P} & 0 \\ 0 & \frac{K_Q}{\tau_Q} \\ 0 & 0 \end{bmatrix} \right] = \left[\begin{array}{cc|cc} -462.1052 & -50.3091 & 300 & 0 \\ -13.6792 & 153.7486 & 0 & 100 \\ 0 & 0 & 0 & 0 \end{array} \right] \tag{A.1}$$

Similarly, two columns are added to the D matrix as well:

$$D' = \left[D \;\middle|\; \begin{bmatrix} \frac{\partial h}{\partial P_0} & \frac{\partial h}{\partial Q_0} \end{bmatrix} \right] = \left[D \;\middle|\; \begin{bmatrix} 0 & 0 \\ 0 & 0 \end{bmatrix} \right] = \left[\begin{array}{cc|cc} 0 & 0.0314 & 0 & 0 \\ -0.0314 & 0 & 0 & 0 \end{array} \right] \tag{A.2}$$

The new system P' with the additional inputs and outputs becomes:

$$P' : \quad \begin{aligned} \dot{\tilde{x}} &= A\tilde{x} + B'\tilde{u}' \\ \tilde{y} &= C\tilde{x} + D'\tilde{u}' \end{aligned} \tag{A.3}$$

where:

$\tilde{u}' = \begin{bmatrix} \tilde{I}_a & \tilde{I}_b & \tilde{P}_0 & \tilde{Q}_0 \end{bmatrix}^T$ is the augmented input.

Now, when closing the loop there are two inputs, which are the changes in active and reactive power set points. The new interconnection is shown in Figure A.1.

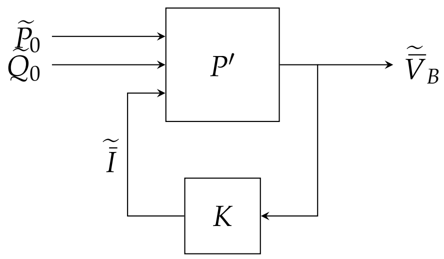

Figure A.1: Augmented system of the linearized inverter dynamics P and the network K.

Using Matlab, the step response of the MIMO system P' is calculated using the `step()`-function. The function returns the state trajectories as well as the output. Ohm's law is used to calculate the current in the network from the internal and bus voltage like in Equation (4.14):

$$\overline{I} = Y_L(\overline{V} - \overline{V}_B) \tag{A.4}$$

The injected power from the inverter can now be calculated using the power calculation in Equation (4.26):

$$\tilde{\overline{S}} = \tilde{P} + j\tilde{Q} = \frac{3}{2}\tilde{\overline{V}}_B \tilde{\overline{I}}^* \tag{A.5}$$

The steady state simulation is run again with the same parameters as before. At $t = 5\,\mathrm{s}$ a step of $5\,\%$ is applied to the active power. The same step is applied to the linear system and the power is calculated using Equation (A.5). The general shape of the step response of the linearization looks similar to the results from Section 4.4. Therefore the residuals between the simulation and the linearization is plotted instead. The residual of the step response is shown in Figure A.2

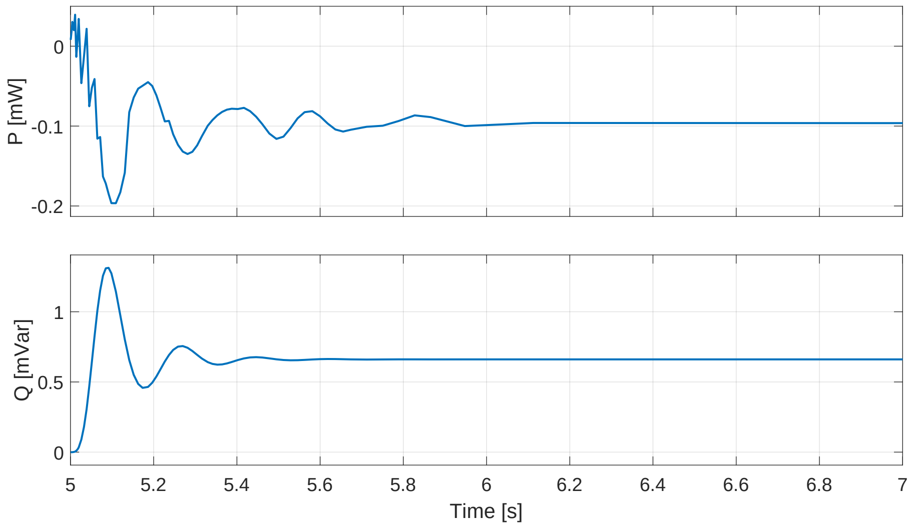

Figure A.2: Residual of the active and reactive power between the simulation and linearization during a $5\,\%$ step on the active power. For comparison, the peak variations in P and Q due to the step are the following: $P : 35\,\mathrm{mW}$, $Q : 0.09\,\mathrm{mVAr}$.

Note that the units on Figure A.2 is in mW and mVAr, meaning the residual of the active power is between two to three orders of magnitudes smaller than the step size. Even though the variation in reactive power is small, the residual is larger. This suggest some non-linear relationship between the active and reactive power for which the linearized model is less suited. The state trajectories and outputs show a similar magnitude of linearization error. These can be seen in Figure A.3 and Figure A.4.

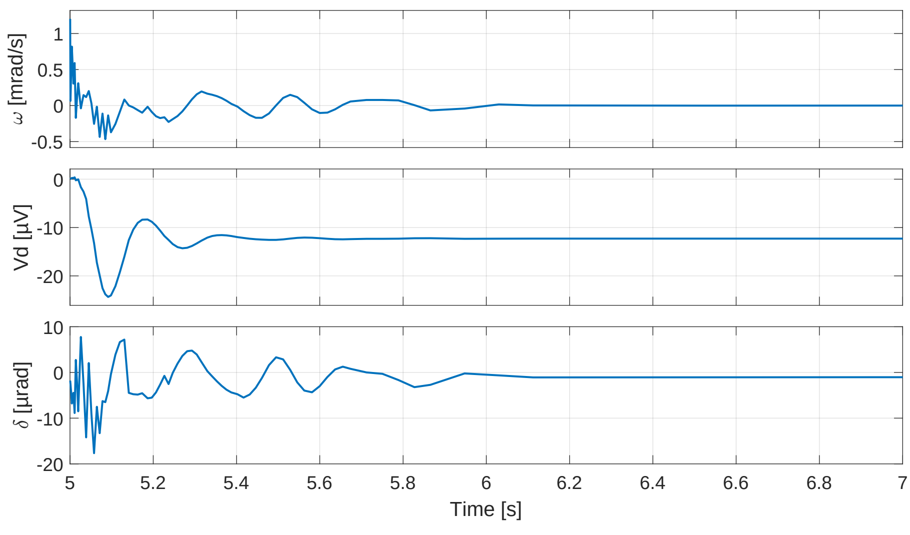

Figure A.3: Residual of the state trajectories between the simulation and linearization during a $5\,\%$ step on the active power. For comparison, the peak variations due to the step are the following: $\omega : 141\,\frac{\mathrm{mrad}}{\mathrm{s}}$, $V_d : 393\,\mu\mathrm{V}$, $\delta : 7846\,\mu\mathrm{rad}$.

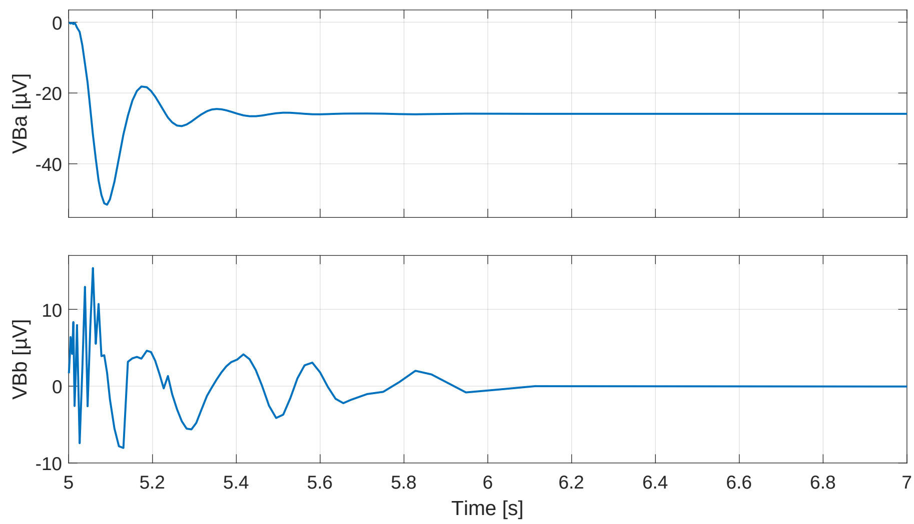

Figure A.4: Residual of the bus voltage between the simulation and linearization during a 5 % step on the active power. For comparison, the peak variations due to the step are the following: $V_{B,a}$: 369 µV, $V_{B,b}$: 7384 µV.

Note again the units on the figures. Because the error is small enough, results obtained from the linearization are deemed to apply to the non-linear system as well, at least in some region around the steady state of 5 % active power. Therefore, the passivity properties can be investigated on the linear system.

B Positive realness of a first order low pass filter

The transfer function for a first order low pass filter is as follows:

$$G(s) = \frac{K}{s\tau + 1} \tag{B.1}$$

A definition of positive realness of a transfer function matrix is given in Lemma 5.1 in Khalil [14].

Lemma B.1 *Let $G(s)$ be an $m \times m$ proper rational transfer function matrix, and suppose* $\det[G(s) + G^T(-s)]$ *is not identically zero. Then, $G(s)$ is strictly positive real if and only if:*

1. *$G(s)$ is Hurwitz; that is, poles of all elements of $G(s)$ have negative real parts,*
2. *$G(j\omega) + G^T(-j\omega)$ is positive definite for all $\omega \in R$, and*
3. *either $G(\infty) + G^T(\infty)$ is positive definite or it is positive semidefinite and* $\lim_{\omega\to\infty} \omega^{2(m-q)} \det[G(j\omega) + G^T(-j\omega)] > 0$*, where $q = rank[G(\infty) + G^T(\infty)]$.*

Furthermore Khalil [14] mentions that:
"In the case of $m = 1$, the frequency-domain condition of the lemma reduces to $Re[G(j\omega)] > 0$ for all $\omega \in [0, \infty)$ and either $G(\infty) > 0$ or $G(\infty) = 0$ and $\lim_{\omega\to\infty} \omega^2 Re[G(j\omega)] > 0$."

A simple first order low-pass filter has a transfer function matrix of order $m = 1$. The pole of $G(s)$ is in $-\frac{1}{\tau}$. Thus as long as $\tau > 0$ the first condition is fulfilled. For the second condition, the real part of the transfer function matrix $G(j\omega)$ is needed. The transfer function matrix in $j\omega$ is:

$$G(j\omega) = \frac{K}{j\omega\tau + 1} = \frac{K(1 - j\omega\tau)}{\omega^2\tau^2 + 1} \tag{B.2}$$

The real part of this transfer function is:

$$Re[G(j\omega)] = \frac{K}{\omega^2\tau^2 + 1} \tag{B.3}$$

It is seen that $Re[G(j\omega)] > 0$ and thus positive definite when $K > 0$. For the last condition, it is seen that:

$$\lim_{s\to\infty} \frac{K}{s\tau + 1} = \lim_{s\to\infty} \frac{\frac{K}{s}}{\tau + \frac{1}{s}} = 0 \tag{B.4}$$

It is therefore necesary to determine if the following limit is greater than zero:

$$\lim_{\omega\to\infty} \omega^2 Re[G(j\omega)] = \lim_{\omega\to\infty} \omega^2 \frac{K}{\omega^2\tau^2 + 1} = \lim_{\omega\to\infty} \frac{K}{\tau^2 + \frac{1}{\omega^2}} = \frac{K}{\tau^2} \tag{B.5}$$

Thus, it is seen that a first order low-pass filter is strictly positive real whenever the gain and the time constant are strictly positive.